



**US Army Corps
of Engineers®**
Engineer Research and
Development Center

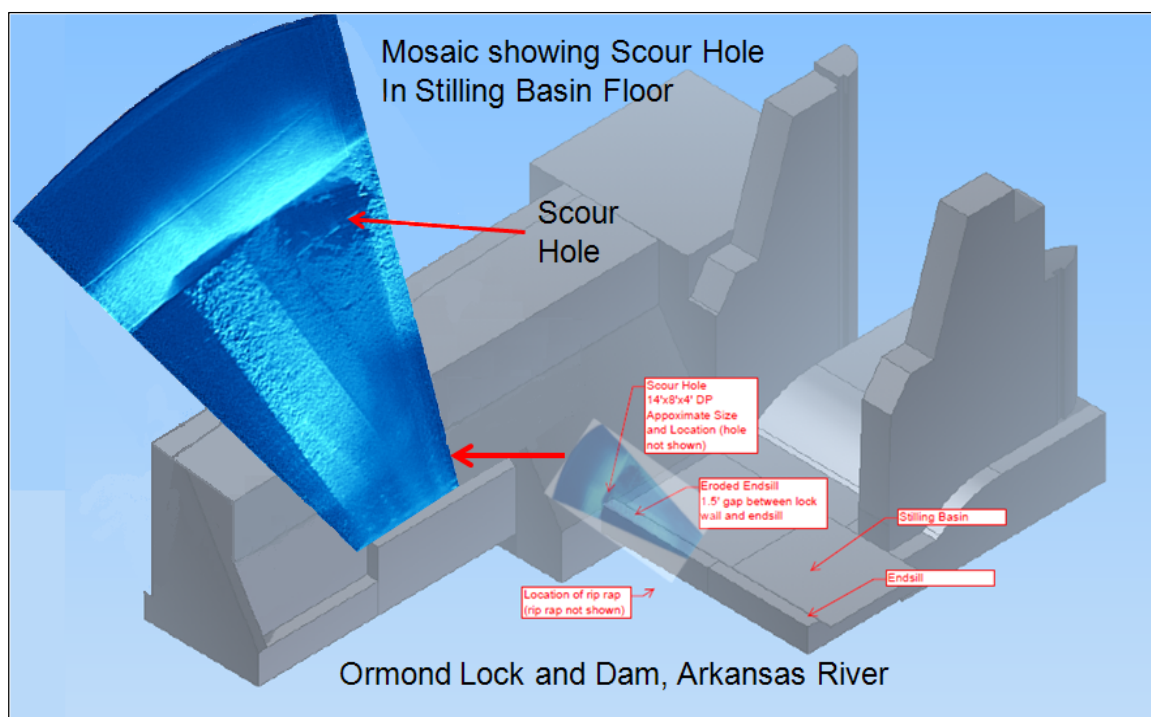
ERDC
INNOVATIVE SOLUTIONS
for a safer, better world

Navigation Systems Research Program

Underwater Inspection of Navigation Structures with an Acoustic Camera

James A. Evans, Terry W. Warren, and Richard W. Haskins

August 2013



The US Army Engineer Research and Development Center (ERDC) solves the nation's toughest engineering and environmental challenges. ERDC develops innovative solutions in civil and military engineering, geospatial sciences, water resources, and environmental sciences for the Army, the Department of Defense, civilian agencies, and our nation's public good. Find out more at www.erdclibrary.army.mil.

To search for other technical reports published by ERDC, visit the ERDC online library at <http://acwc.sdp.sirsi.net/client/default>.

Underwater Inspection of Navigation Structures with an Acoustic Camera

James A. Evans, Terry W. Warren, and Richard W. Haskins

*Information Technology Laboratory
US Army Engineer Research and Development Center
3909 Halls Ferry Road
Vicksburg, MS 39180-6199*

Final report

Approved for public release; distribution is unlimited.

Prepared for Headquarters, US Army Corps of Engineers
Washington, DC 20314-1000

Abstract

The US Army Corps of Engineers' (USACE) operations within turbid waters creates a need for better ways to inspect, quantify, monitor, and locate infrastructure in a difficult environment. Inspection methods have included dewatering, tactile diver inspection, and side-scan or multi-beam sonars. These older approaches can have high cost, inherent danger, and/or limited output quality. Newer technologies that use highly focused acoustic beams could greatly improve underwater observation.

The research described in this report addresses the limitations and expands the capabilities of an underwater, high-resolution acoustical imaging system for USACE. These efforts have produced new hardware and software and associated methods that address specific needs in system deployment, data collection, and analysis. During this research, continuous leveraging of reimbursable needs within USACE districts has produced an invaluable view of performance, capabilities, and limitations. It is believed that acoustical imaging technology will be a catalyst for the development of other advanced inspection capabilities within the Corps' navigation system.

DISCLAIMER: The contents of this report are not to be used for advertising, publication, or promotional purposes. Citation of trade names does not constitute an official endorsement or approval of the use of such commercial products. All product names and trademarks cited are the property of their respective owners. The findings of this report are not to be construed as an official Department of the Army position unless so designated by other authorized documents.

DESTROY THIS REPORT WHEN NO LONGER NEEDED. DO NOT RETURN IT TO THE ORIGINATOR.

Contents

Abstract.....	ii
Figures	v
Preface	viii
Unit Conversion Factors.....	ix
1 Introduction.....	1
1.1 Limited vision in turbid waters.....	1
1.2 Underwater inspection and imaging technologies	1
1.3 Enhancements for post-processing and deployment.....	2
1.4 Leveraging reimbursable jobs and research and development funding.....	4
2 DIDSON Underwater Acoustic Camera.....	5
2.1 Theory of operation	5
2.2 Understanding the images.....	8
3 Developed Capabilities	14
3.1 Deployment methods	14
3.1.1 Deployment history	14
3.1.2 Boat-mounted pole.....	18
3.1.3 Acoustic camera carried by diver.....	19
3.1.4 Tethered camera.....	20
3.2 Additional sensors to support geospatial position awareness	20
3.3 Software capabilities.....	20
3.3.1 Data enhancement through image integration and mosaicing	21
3.4 ClearSight.....	24
3.5 EdgeDetect software	26
3.6 DDF Parser software	26
4 Inspections Performed.....	28
4.1 Overview of inspection types	28
4.2 Arkansas River, May 2012	28
4.2.1 Lock and Dam 6, David D. Terry Lock and Dam.....	28
4.2.2 Lock and Dam 9, Ormond Lock and Dam	31
4.3 Mississippi River, November 2011.....	32
4.3.1 Lock and Dam 25, Mississippi River, scour hole inspection	32
4.4 Illinois River, July 2006	34
4.4.1 Starved Rock Lock and Dam, scour hole inspection	34
4.5 Additional case studies	34
5 Guidelines for Acoustic Camera Inspections.....	57

6	Conclusions.....	58
	References.....	59
	Appendix A: AcousticView User Guide, ClearSight Software	60
	Appendix B: DDF Parser User Manual.....	71
	Appendix C: DIDS0N Acoustic Camera Specifications	81
	Appendix D: EdgeDetect User Manual	83
	Report Documentation Page	

Figures

Figures

Figure 1-1. Downrange representation of the acoustic camera.....	2
Figure 1-2. Acoustic camera mounted on a survey boat.....	3
Figure 1-3. Block diagram of boat-mounted acoustic camera system.	4
Figure 2-1. Sample acoustic camera image of the stilling basin end sill and riverside lock wall at Lock and Dam 9 on the Arkansas River.....	7
Figure 2-2. Relationship between area viewed and camera display.....	7
Figure 2-3. Grazing angle of 90° and corresponding display.....	8
Figure 2-4. Acoustic camera image obtained with a 90° grazing angle.	8
Figure 2-5. Acoustic camera image of a lock wall scour hole outline obtained with a 90° grazing angle.....	9
Figure 2-6. Acoustic camera output perspectives.	10
Figure 2-7. Camera orientation effects.....	11
Figure 2-8. Horizontal and vertical surfaces imaged by the DIDSON.	12
Figure 2-9. Laboratory experiment to demonstrate DIDSON image artifacts.	13
Figure 3-1. DIDSON attached to an underwater ROV.	14
Figure 3-2. Boat with pole-mount deployment system.....	15
Figure 3-3. Typical measurements provided by the acoustic camera system sensors.	16
Figure 3-4. Mosaic image and corresponding GIS data.	16
Figure 3-5. Images of a barge lift gate at Lock and Dam 24 on the Mississippi River.	17
Figure 3-6. Acoustic camera deployment mechanism for culvert inspection.	17
Figure 3-7. Resultant mosaic images from culvert inspections.....	18
Figure 3-8. Manually created mosaic image.	19
Figure 3-9. Mosaic generated using a least mean square search.....	22
Figure 3-10. Image enhanced using the SIFT algorithm.	23
Figure 3-11. Images of the bottom of a concrete barge gate.	24
Figure 3-12. ClearSight user interface window.	25
Figure 3-13. EdgeDetect window.....	27
Figure 4-1. Lock and Dam 6 on the Arkansas River. (continued).....	29
Figure 4-2. A 3D surface plot of scour hole in the lock wall at Lock and Dam 6 on the Arkansas River.	31
Figure 4-3. Mosaic image of the scour hole at Lock and Dam 9 on the Arkansas River.	32
Figure 4-4. Lock and Dam 25 on the Mississippi River and areas damaged by scour.	33
Figure 4-5. Scour hole outline under the downstream riverside lock wall.....	34
Figure 4-6. Scour area under the end of Lock 25 on the Mississippi River.	35
Figure 4-7. Starved Rock Lock and Dam, Illinois River, dam and river bottom intersection.	36
Figure 4-8. Damaged concrete section.....	37

Figure 4-9. Example of concrete structure imaging.....	37
Figure 4-10. Damaged section of the underside of a concrete barge gate in New Orleans.....	38
Figure 4-11. Masonry wall comparison of visible image and acoustical image, downtown landing, Mississippi River, Vicksburg.....	39
Figure 4-12. Mosaics of river matting.	40
Figure 4-13. Underwater riprap section mosaic created from acoustical camera frames.	40
Figure 4-14. Vegetation mosaic created from acoustical camera images.	41
Figure 4-15. Sunken barge visible in river bottom silt.	41
Figure 4-16. Graph of the camera track in acquiring acoustic camera images of sunken barge.	42
Figure 4-17. Acoustic camera mosaics of scour areas.	43
Figure 4-18. Additional upstream structural elements exposed by scour.	43
Figure 4-19. Profile and surface views of differing types of sheet piles.	44
Figure 4-20. Acoustical camera images of the interfaces of structural components.	44
Figure 4-21. Mosaic of a scour hole at the intersection of a lock or dam wall and the river bottom.	45
Figure 4-22. Image of organic material in a scour area.	46
Figure 4-23. Exposed pilings in a scour area under a structural component.	46
Figure 4-24. Scour hole mosaic.	47
Figure 4-25. Mosaic image of scour patterns.	47
Figure 4-26. Mosaic image of timber piles.	48
Figure 4-27. Upstream face of a miter gate.	48
Figure 4-28. Downstream side of the miter gate.	49
Figure 4-29. Acoustic camera mosaics of underwater lock components and a corresponding visible image.	50
Figure 4-30. Lock chamber retrofit of a vent.....	50
Figure 4-31. Acoustical images of a tainter gate.....	51
Figure 4-32. Acoustic camera image acquisition information.	51
Figure 4-33. Images that indicate the location of debris.	52
Figure 4-34. Images showing intertwined debris and lock wall pilings.....	52
Figure 4-35. Steel service gate with binding issues.	54
Figure 4-36. Acoustical images of service gate and guideway at Delaware Lake.	54
Figure 4-37. Image of track groove and surrounding concrete taken with acoustic camera pointed normal to the surfaces.....	55
Figure 4-38. Deployment mechanism for conduit inspections.....	55
Figure 4-39. Mosaics from acoustic camera culvert scans.	56
Figure 4-40. Miscellaneous objects encountered during scans.	56
Figure A-1. ClearSight console.	62
Figure A-2. Project pane objects.	63
Figure A-3. Mosaic tools available in the Viewer pane.....	65
Figure A-4. Binary file structure.	66
Figure A-5. The transition from GPS coordinates to pixels.	67

Figure A-6. Scanning data with the DIDSON forward-looking sonar.....	67
Figure A-7. The DIDSON scans over a range of depth using a moving acoustic lens that changes the focus of the ultrasonic sound to cover the full downrange.	68
Figure A-8. The imaging geometry of an acoustic camera.....	68
Figure A-9. Mosaic created by applying a coordinate system transformation to align images.	70
Figure B-1. DDF Parser (no file selected).	72
Figure B-2. (a) Original image; (b) contrast scaled image; (c) contrast scaled image with low threshold: 20% and lower alpha static: 100%.....	74
Figure B-3. (a) Using lens correction; (b) original image stored in .ddf.	74
Figure B-4. (a) Image fill ratio: 0; (b) image fill ratio = 1.	76
Figure B-5. (a) Low threshold: 0%; (b) low threshold: 20%.....	77
Figure B-6. Each image has a low threshold value of 20%; (a) lower alpha static: 0%; (b) lower alpha static: 50%; (c) lower alpha static: 100%.	77
Figure B-7. Each image has a low threshold value of 20%; (a) low transparency dynamic: 0%; (b) low transparency dynamic: 50%; (c) low transparency dynamic: 100%.....	78
Figure B-8. (a) High threshold: 90%; (b) high threshold: 50%.....	78
Figure B-9. Each image has a high threshold value of 50%; (a) upper alpha static: 0%; (b) upper alpha static: 50%; (c) upper alpha static: 100%.	79
Figure B-10. Each image has a high threshold value of 50%; (a) upper transparency dynamic: 0%; (b) upper transparency dynamic: 50%; (c) upper transparency dynamic: 100%.....	80
Figure D-1. EdgeDetect user interface window.	84

Preface

The lack of visibility in rivers and impoundments due to suspended material (turbidity) presents challenges for Corps of Engineers personnel. Lack of clarity can hinder assessing the general condition of underwater structures such as gates and concrete piers (operation and maintenance); positioning float-in structures (construction); investigating archeological sites; and detecting endangered species. Currently, assessment involves the use of divers to inspect and record the condition of underwater structural components. However, diver deployments can be hazardous. The objective of this research is to evaluate and improve application of high-resolution acoustical imaging cameras such as the Dual Frequency Identification Sonar (DIDSON) for use by the Corps.

Funding to evaluate the camera and develop the acoustical imaging system was provided by the Navigation Systems Research Program (NavSys). The research was performed by James A. Evans, Principal Investigator, along with Terry W. Warren, Richard W. Haskins, and Ken Switzer, all of the Computational Science and Engineering Division (CSED), Information Technology Laboratory (ITL), US Army Engineer Research and Development Center (ERDC). Development efforts were aided by Steven Bunkley, CSED.

Charles E. Wiggins, Coastal and Hydraulics Laboratory (CHL), ERDC, was NavSys Manager. Dr. Michael Sharp was Technical Director for Navigation. Jeffrey A. McKee was the Navigation Business Line Leader, Headquarters, US Army Corps of Engineers (HQUSACE).

This report was prepared by Evans, Warren, and Haskins. Bruce C. Barker was Chief, Sensors, Measurement, and Instrumentation Branch (SMIB); Dr. Robert M. Wallace was Chief, CSED; Patti S. Duett was Deputy Director, ITL; and Dr. Reed L. Mosher was Director, ITL.

COL Jeffrey R. Eckstein was Commander, ERDC, and Dr. Jeffery P. Holland was Director.

Unit Conversion Factors

Multiply	By	To Obtain
feet	0.3048	meters

1 Introduction

1.1 Limited vision in turbid waters

The US Army Corps of Engineers (USACE) is responsible for operating and maintaining flood control and navigation structures on almost all waterways in the United States. Assessments to ensure structural integrity are of utmost importance to protect lives and property and prevent the disruption of river traffic.

In clear water and with proper lighting, visibility can extend 50 ft. In inland waterways, turbid (murky) conditions can restrict visibility to a few inches (Belcher et al. 2002). Ways to provide timely structural inspections in these conditions are necessary, particularly as the country's navigation structures age, often exceeding their design life spans.

1.2 Underwater inspection and imaging technologies

There are various means of assessing an underwater structure's condition. One is divers who move about, feeling with their hands. While yielding useful results, generally the divers only can report approximations of damage. Also, they can't capture objective information or a global picture.

Other technologies for viewing underwater environments include side-scan and multi-beam sonars. They produce still images that are typically lower in resolution.

Ultrasonic imaging technology used in the health care industry has been expanded to allow improved imaging in turbid underwater environments. Underwater inspections require a significant downrange capability, compared to ultrasonic imaging systems used by health care providers. The downrange is how far forward the camera can see (Figure 1-1). It is controlled partly by the power transmitted. These acoustic cameras, also called forward-looking sonars (FLS), use a variety of design approaches. The most common employ line, cylindrical, and conformal arrays, and multiple fixed-beam elements. Beams are formed by mechanical means (stepper motors), electronic means (analog delay lines), digital delay lines, and acoustic lenses.

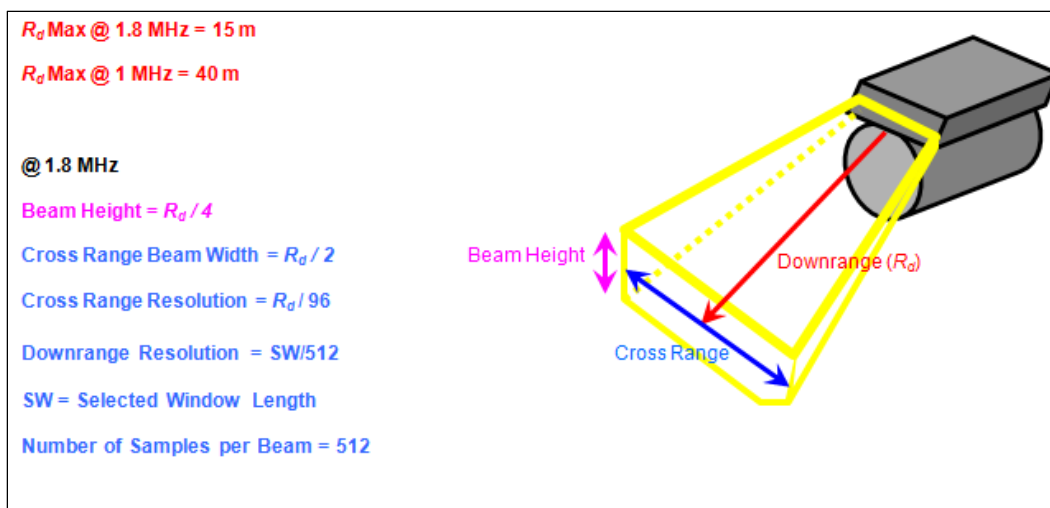


Figure 1-1. Downrange representation of the acoustic camera.

To inspect underwater structures, a system must be capable of focusing across a wide range of depths and distances. Highly resolved details are best obtained at distances of 1 or 2 m, while more global and wider fields of view are achieved at distances of 50 m or more. An FLS called the DIDSON, Dual Frequency Identifying Sonar, was developed by the Applied Physics Laboratory (APL) of the University of Washington. It proved to be a good candidate for making underwater structural inspections. The DIDSON can operate at two frequencies, 1 MHz and 1.8 MHz, thereby providing flexibility in its range and resolution.

1.3 Enhancements for post-processing and deployment

The DIDSON provides high-resolution imaging capabilities but has inherent limitations that require enhancements to increase its usefulness. Navigation structures are much larger than the camera's field of view. Therefore, a mosaicing capability is necessary to stitch together individual images to create a larger field of view. Also, unprocessed images tend to be grainy and require processing to sharpen resolution. Proper averaging during the mosaic process improves the quality and resolution by reducing non-stationary noise and enhancing weak reflectors.

Navigation structures are surrounded by moving water. A remotely operated vehicle (ROV) has been one means of deploying the camera tested, but commercially available ROVs within the range of funds allocated to this work lack the ability to operate in the high-current conditions of a river. A bottom-crawling vehicle could prove useful, but movement is limited by structural components or naturally occurring bottom contours.

Two means of deployment have been used by the development team. The primary means has been a system of extendable poles mounted to the side of a boat (Figure 1-2). A pan-and-tilt device is attached to the bottom pole and the acoustic camera attaches to the bottom of the pan-and-tilt. A 12-VDC electric winch is used to raise and lower the poles. A pressure sensor and a water column position sensor are attached at the camera level to provide camera depth in the water and altitude above the bottom. A block diagram is shown in Figure 1-3.

The other means of deployment has been to use divers who respond to verbal directions for camera positioning. More recently, helmet-mounted video glasses worn by the divers also have been provided. When the camera is used in this way, a minimal system consisting of the acoustic camera, topside breakout box, acoustic camera power supply, and topside PC can be employed. This makes for a portable system. However, positioning information is sacrificed when operating in this mode.



Figure 1-2. Acoustic camera mounted on a survey boat.

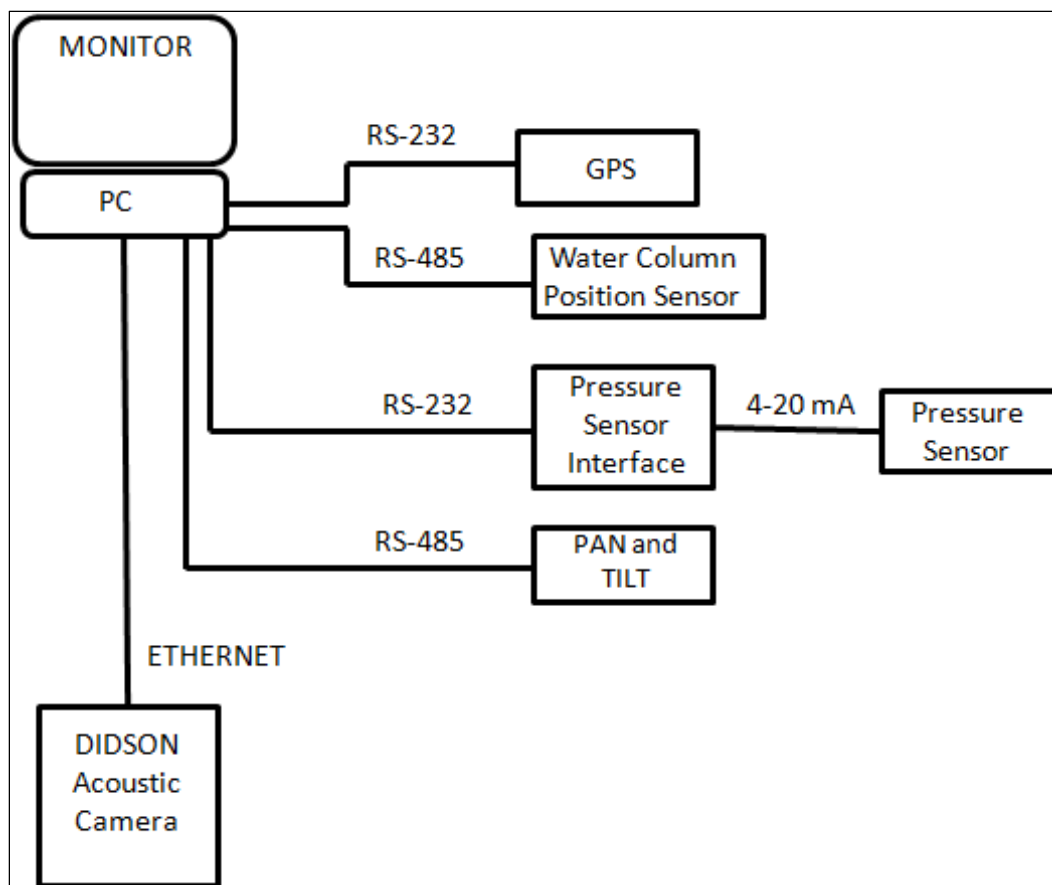


Figure 1-3. Block diagram of boat-mounted acoustic camera system.

1.4 Leveraging reimbursable jobs and research and development funding

During the ongoing research and development efforts to improve the Corps' capabilities of underwater inspection of structures in turbid water by using the acoustic camera, numerous district field requests have been met for a variety of needs and in a wide range of conditions. The result has been a means of field evaluation of new systems, software, methods, etc., providing valuable insight of system limitations, development needs, and ultimately tech transfer of the overall capability. The districts have benefited from the various enhancements and support tools, allowing for improvement of the inspection tools the Districts have available. The methods of deployment have included boat-mounted pan and tilt on the bottom of a pole system, diver held, and tethered cable. The needs have been varied and included scour inspection, crack detection, and object location. Objects or structures have included miter, tainter, and vertical gate, and walls.

2 DIDSON Underwater Acoustic Camera

2.1 Theory of operation

This chapter provides the theory of operation and the technical specifications of the DIDSON underwater acoustic camera. When a sound source projects a sound (stress wave), the acoustic energy will travel in the direction projected as long as it is unscattered or until the acoustic energy is attenuated. If the energy encounters another object, some of it will be reflected or scattered back to the detection transducer. The amount of reflected energy detected by the receiver is a function of the material impedance, incidence angle, surface texture, and size of the reflector.

The DIDSON is a forward-looking sonar (FLS) device that projects and focuses sonar signals in transmission and reception. This device measures the returned signals by utilizing a linear array of detection elements. The returned signals are sampled, and an image is formed based on the returned signal strengths. The pseudo-3D optical image is created with the elements in the array forming the cross-range dimension, time forming the range position, and the intensity of reflections from the narrow fan beam creating the intensity variations.

To form an image, the user first selects the operating frequency: either low or high (1 MHz or 1.8 MHz). The lower frequency allows the camera to see greater distances, whereas the higher one maximizes the resolution of the images nearer to the camera. The user selects the viewing area by specifying the range to start imaging and the length of the viewing window. The latter two parameters are used to set the sampling parameters for the measured signals. Sampling begins in time, according to the result of:

$$t_{start} = \frac{w_{start}}{c_{water}} \times 2, \quad (1)$$

where

t_{start} = sampling start time, in seconds;

w_{start} = start of the viewing window, in feet or meters;

c_{water} = speed of sound in fresh water (4900 ft/sec).

Sampling ends in time, according to the result of:

$$t_{end} = \frac{w_{start} + w_{length}}{c_{water}} \times 2, \quad (2)$$

where

t_{end} = sampling end time, in seconds;

w_{start} = start of the viewing window, in feet or meters;

w_{length} = length of the viewing window, in feet or meters;

c_{water} = speed of sound in fresh water, 4900 ft/sec.

Note that each of the equations contains a multiplier of 2. This is because the sound wave must travel the distance to the object of interest and return the same distance back to the transducer. At the object of interest, a window can be set up and the returned signal is sampled and digitized 512 times between the window t_{start} and t_{end} points. This allows the user to increase (or decrease) the resolution of the camera by manually setting the digitizing window of interest length. This reduces the data storage requirements by only storing the data within the window. The minimum window size is 1 m and, within the window, the signal is sampled 512 times, resulting in a maximum resolution at 1 m.

$$Resolution = w_{length} \div 512, \quad (3)$$

where

w_{length} = length of the specified viewing window, in feet or meters.

Each digitized sample returns a value between 0 and 255. Therefore, each beam in the image is made up of 512 pixel values with a value in the 0 to 255 range. In low-frequency mode, there are 48 beams spaced 0.6° apart. In high-frequency mode, there are 96 beams spaced 0.3° apart. Therefore, the cross range always provides 29° of coverage. When all beams are displayed together, an image is formed. Figure 2-1 shows a sample image obtained using DIDSON. This image was recorded while operating in the 1.8 MHz (high-resolution) mode.

To properly image an area, the camera should be oriented so the acoustic wave is projected along the surface to be viewed at an appropriate angle of incidence, also called the grazing angle. Figure 2-2 shows a graph of how an image relates to the area viewed.

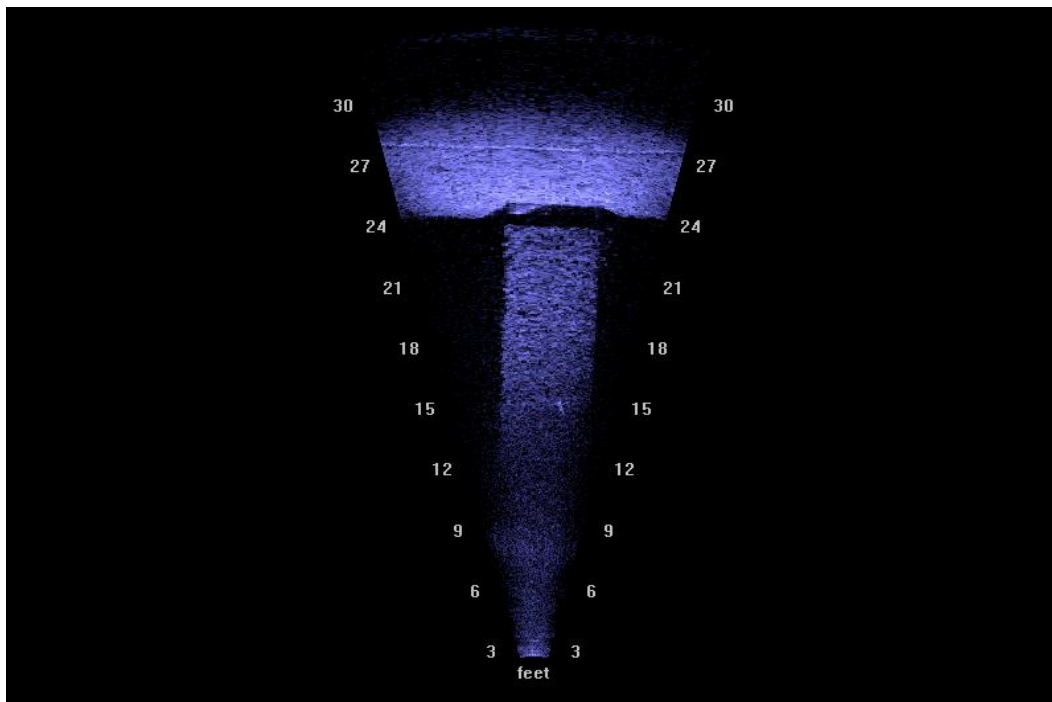


Figure 2-1. Sample acoustic camera image of the stilling basin end sill and riverside lock wall at Lock and Dam 9 on the Arkansas River.

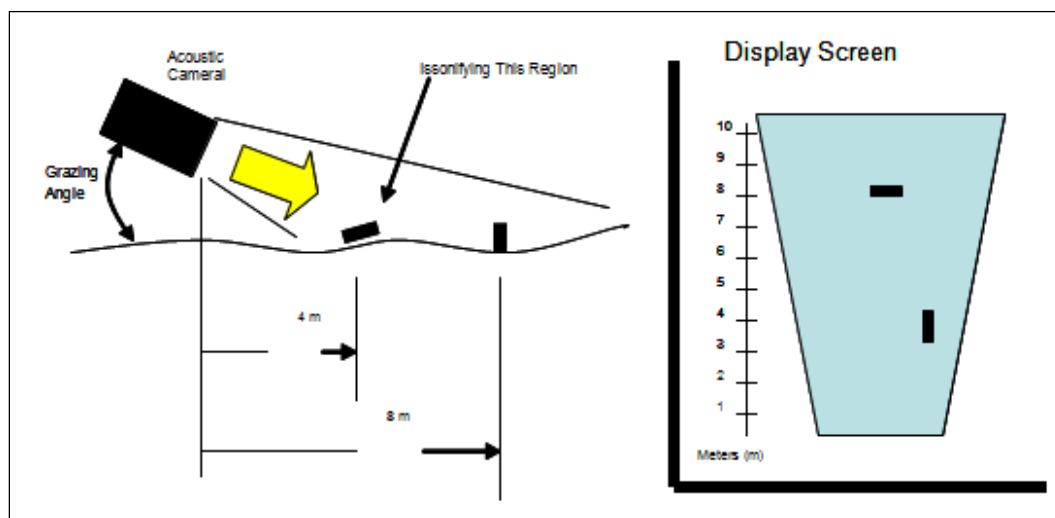


Figure 2-2. Relationship between area viewed and camera display.

If the grazing angle approaches 90° between the camera and a surface, as shown in Figure 2-3, almost all the acoustic energy will be reflected from the surface back to the camera and an image consisting of a straight line, similar to Figure 2-4, will be obtained. This occurs because the narrow angle of the fan beam hits the target at the same time. At times, an image obtained in this manner can be useful. Figure 2-5 is an image obtained with a 90° grazing angle that shows the outline of a lock wall scour hole at a particular elevation.

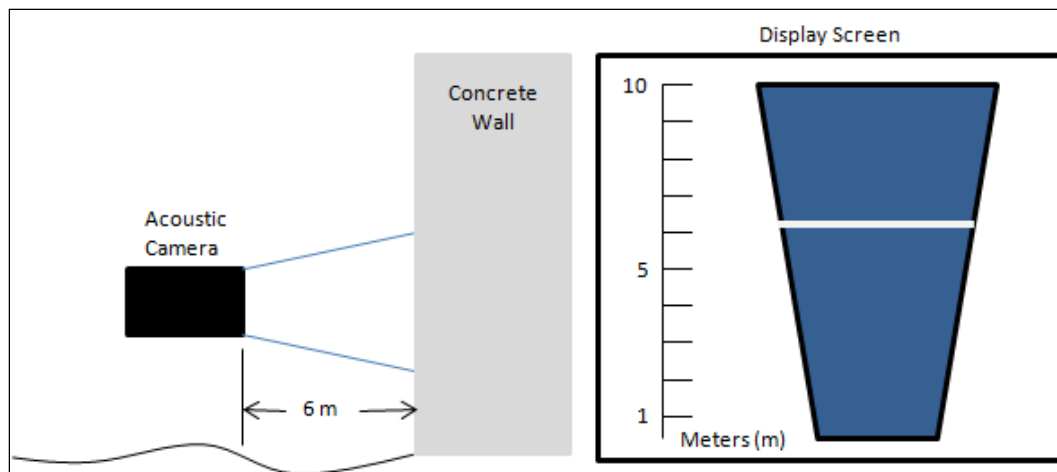


Figure 2-3. Grazing angle of 90° and corresponding display.

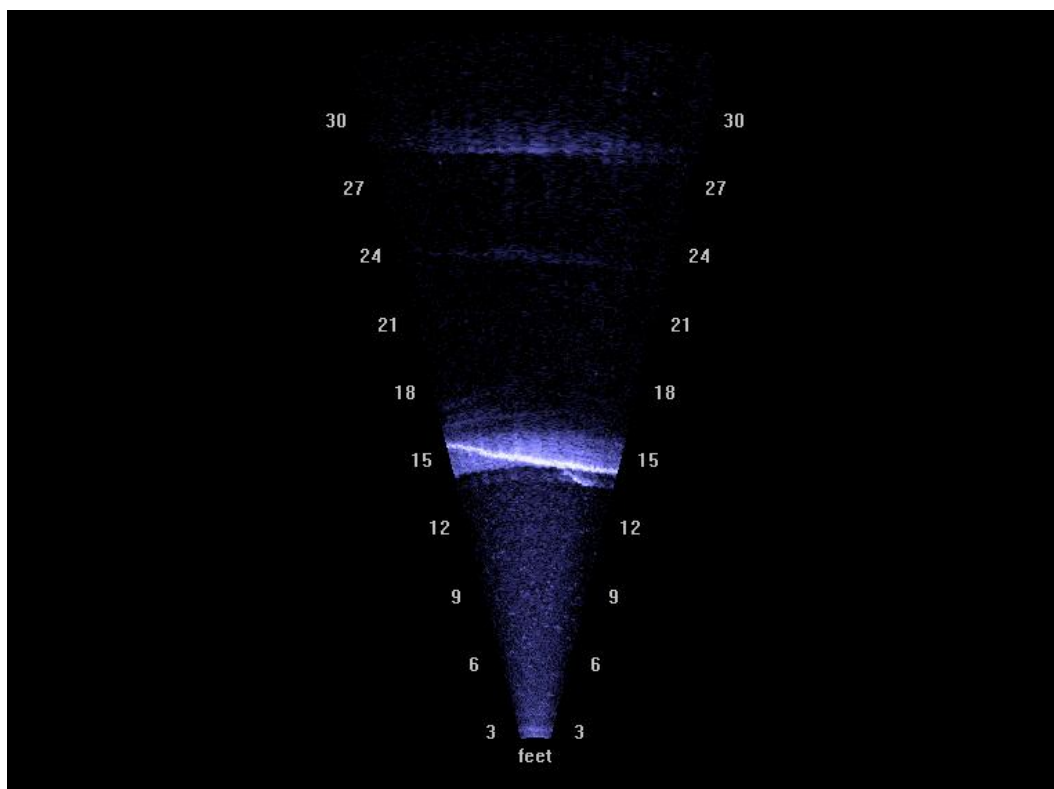


Figure 2-4. Acoustic camera image obtained with a 90° grazing angle.

2.2 Understanding the images

The DIDSON uses a mechanical lens system to focus an ultrasonic beam in both transmission and reception. The use of this system produces less side lobe or extraneous noise than typically seen in electronically beam-steered systems (Belcher et al. 1999). The transmitting and receiving element has a lead zirconate titanate (PZT) array of 96 elements. The multi-element PZT array generates the typically narrow dimension of the DIDSON image often

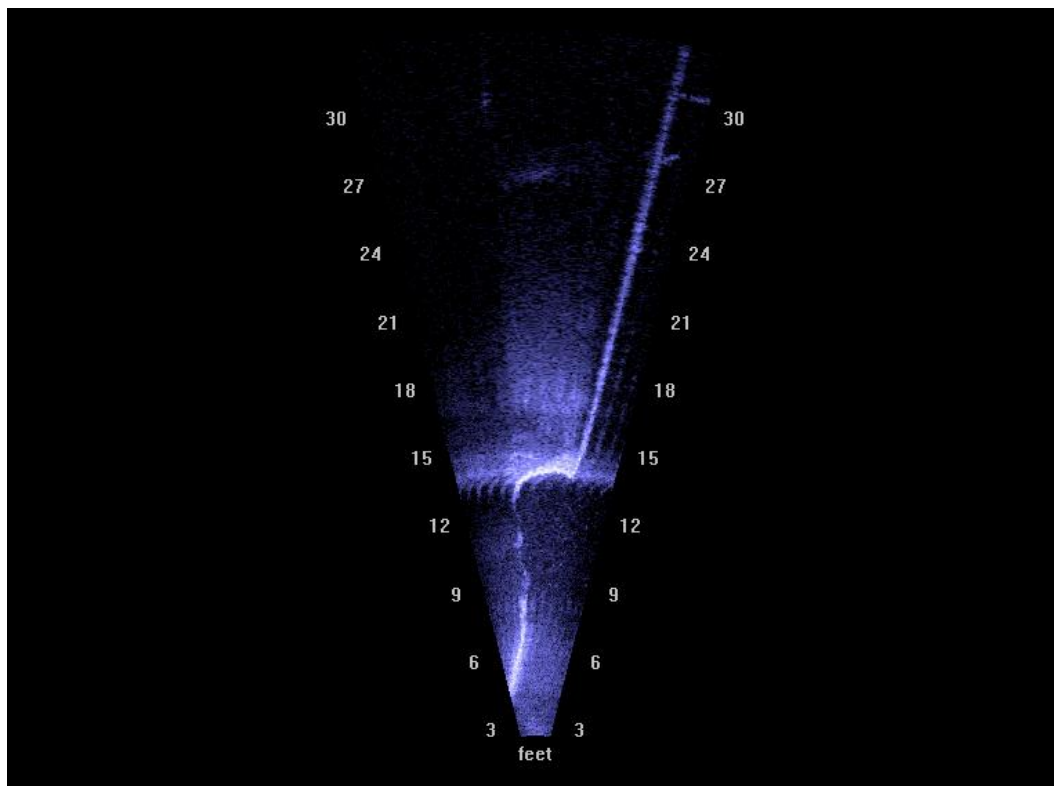


Figure 2-5. Acoustic camera image of a lock wall scour hole outline obtained with a 90° grazing angle.

displayed in a curvilinear fashion. The acoustic fan beam spreads wide in the dimension of the PZT array and narrow in the orthogonal dimension. The reflected signals are digitized and displayed as a function of time. Because the signal has a generally uniform propagation velocity, the time display is represented accurately by a depth or downrange mapping. While the DIDSON display appears to be an optical image, it is actually a sound-based representation. Therefore, unique differences and occurrences are encountered during deployment. Some examples are perspective shifts, apparent transparencies, reverberations, acoustic mirrors, and multipath returns. This section aims to clarify DIDSON output and how it is affected by deployment and environmental conditions. The DIDSON generally does not have problems seeing through low-level turbulence, unless the concentration is very high. Air bubbles and high levels of silt generally can be seen when the camera is in close range.

Figure 2-6 shows how the DIDSON's output has a perspective shift. This shift is due to the depth, or z-axis, actually being time. The image above shows that, when the DIDSON is near the floor, looking at the cinder block, the output appears as if someone is looking down on the cinder block.

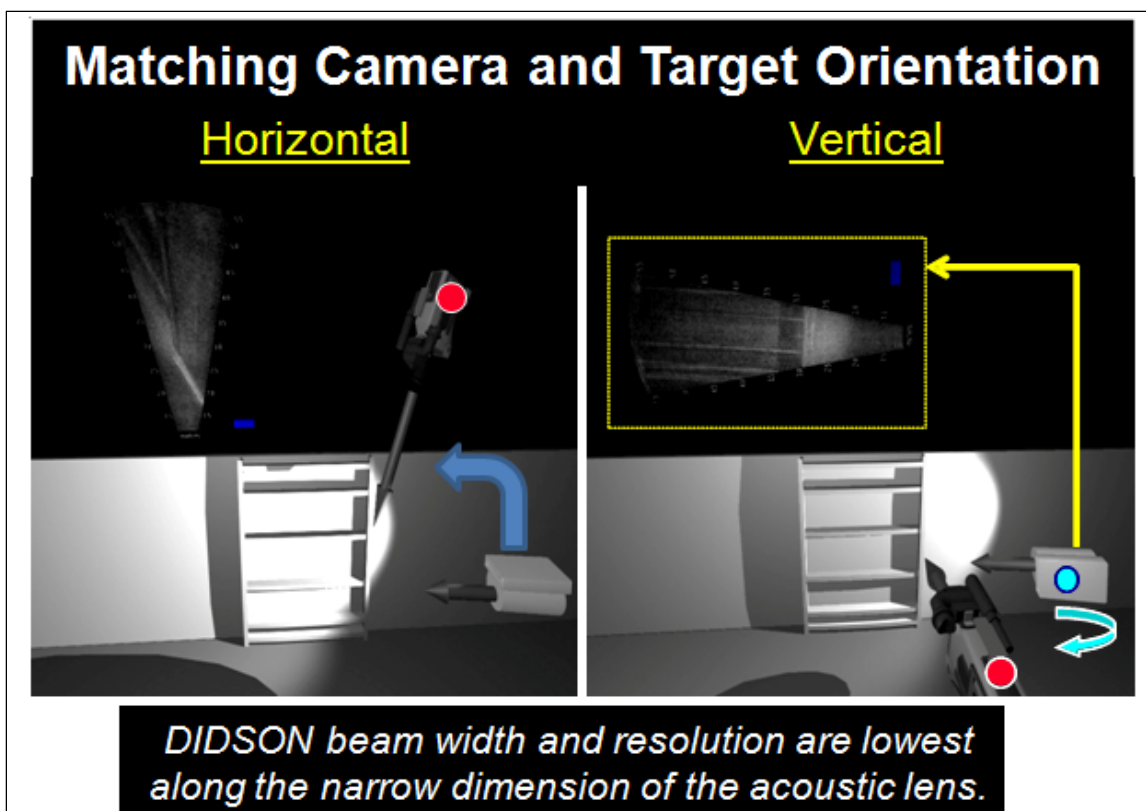
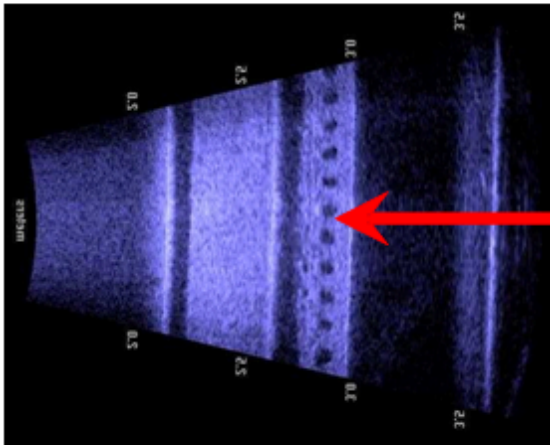


Figure 2-7. Camera orientation effects.

In the laboratory, several objects were placed on a turntable. The DIDSON was fixed and imaged these objects as they were rotated. Figure 2-9 shows the same target from multiple perspectives and some of the artifacts discussed in the earlier section. One thing that can be seen in the two DIDSON images on the left is an apparent transparency of the cinder blocks. This occurs because the sound is traveling up, into the block, and the image is being perceived from a rotated perspective. Therefore, it seems the camera operator is looking through the cinder block. The 3D models were made transparent to help illustrate these details. Also seen in the image on the lower right is the concrete floor acting as an acoustic mirror and reflecting the cinder block back at the camera. It is common in field deployments to have this effect from the surface of the water. When there are some wind or water ripples, it is generally clear that the camera is pointing at a reflection, not directly at the target.

Vertical Orientation



Acoustical Image
of Lower-Casing
End Plate

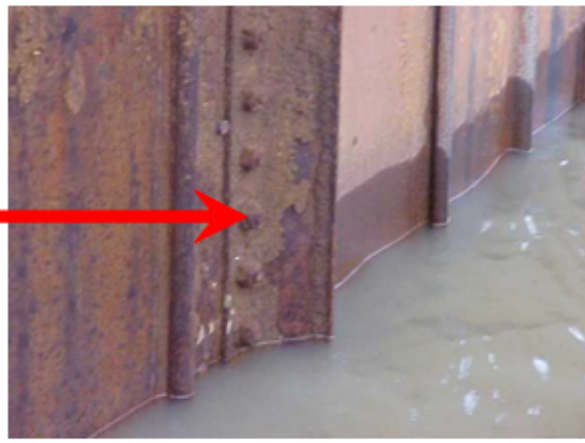
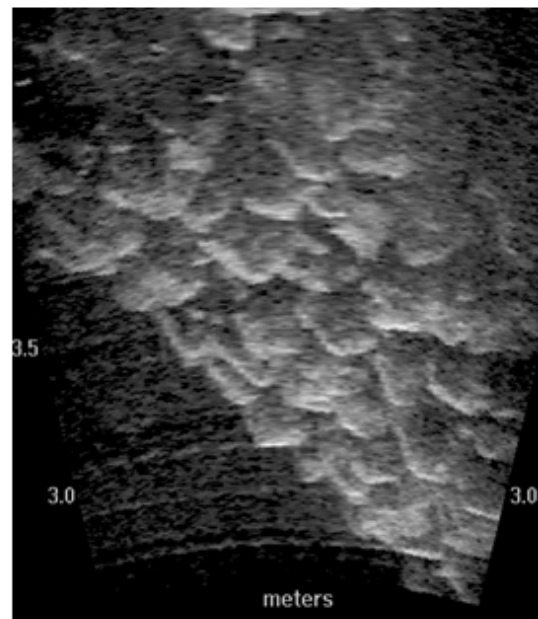


Photo
of Upper-Casing
End Plate

Horizontal Orientation



Objects on Concrete Floor



Limestone Rocks

Figure 2-8. Horizontal and vertical surfaces imaged by the DIDSON.

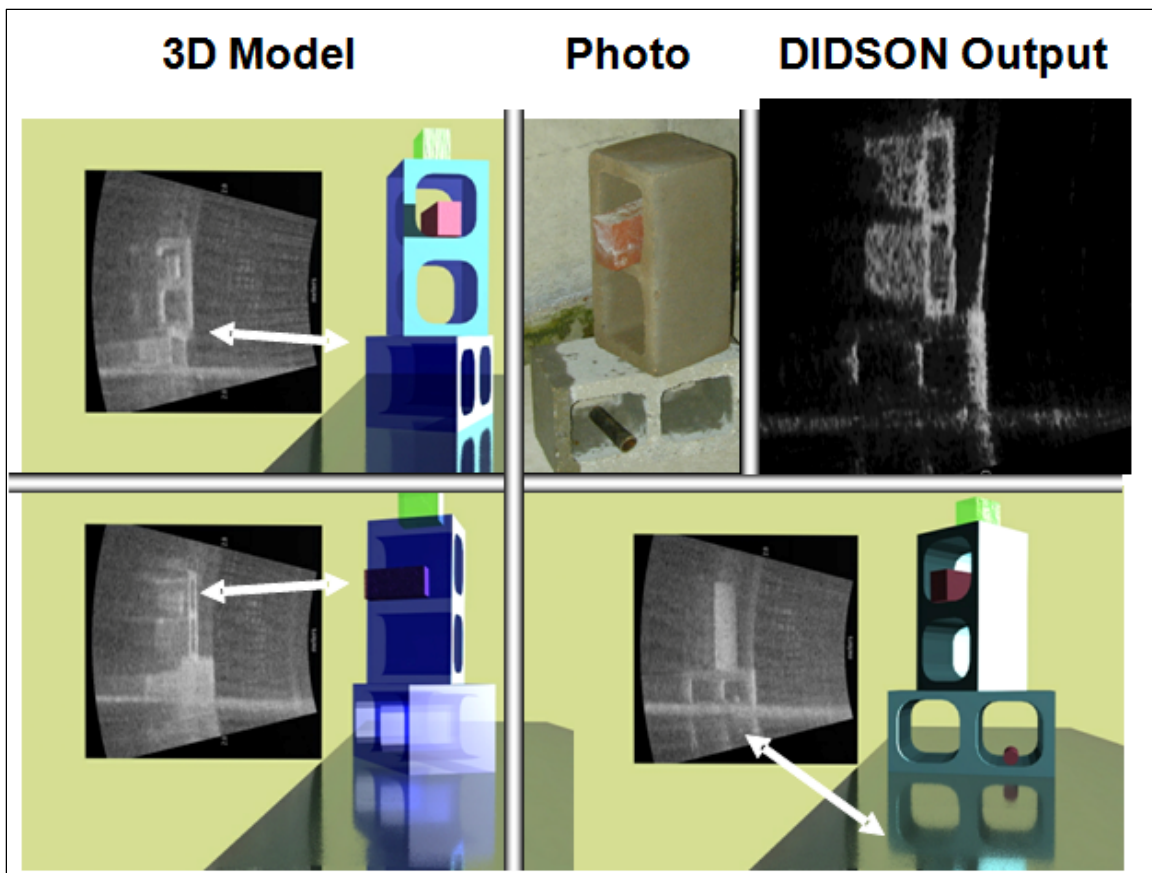


Figure 2-9. Laboratory experiment to demonstrate DIDSON image artifacts.

3 Developed Capabilities

3.1 Deployment methods

Versatility is of high importance when using the acoustic camera in moving water. To ensure proper imaging is obtained, the user must be able to:

- Manipulate the position of the camera in relation to the object being scanned (distance from the object and height in the water column);
- Manipulate the direction of the camera to ensure proper viewing angles;
- Regulate the speed of the movement of the camera.

No single method was successful for all situations, but three methods proved useful for structure assessments.

3.1.1 Deployment history

Every deployment opportunity has been a learning experience. Some iterative measures have been taken to improve the limitations of the various approaches. An early deployment attempt was made using an ROV (Figure 3-1). It was learned quickly that position, orientation, and control were challenging with the heavy DIDSON cable and nearly impossible once combined with any significant current. The preferred deployment method is from a telescopic boom, or pole, attached to the deployment boat with a pan-and-tilt head attached to the end of the boom (Figure 3-2).



Figure 3-1. DIDSON attached to an underwater ROV.

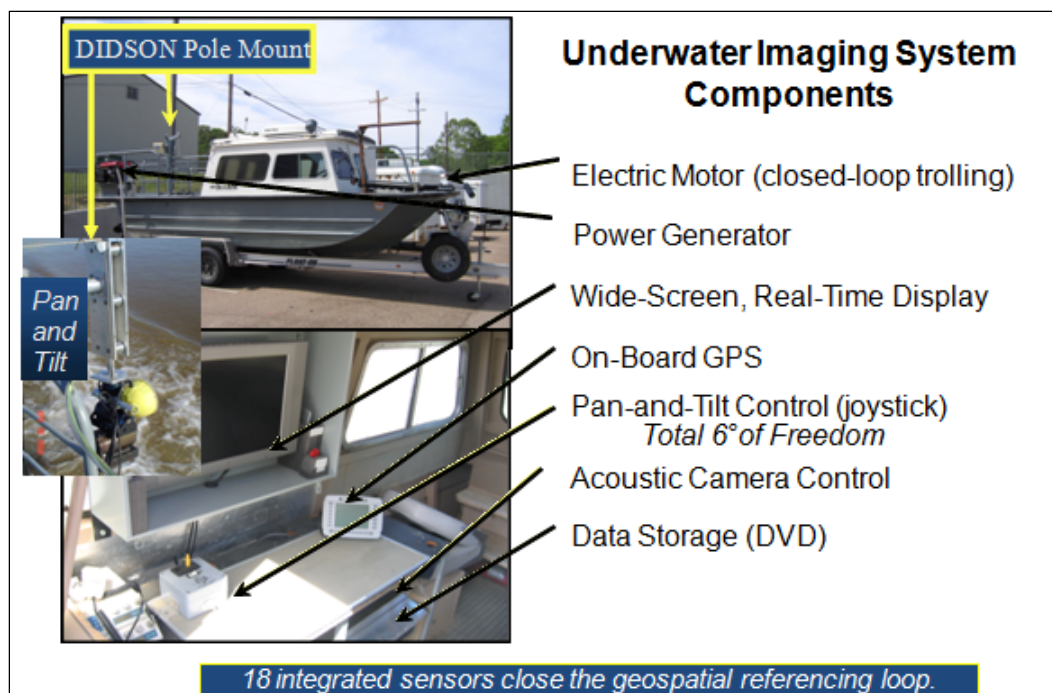


Figure 3-2. Boat with pole-mount deployment system.

Figure 3-3 shows plots of some of the collected sensor data. This data is indexed into the native DIDSON ddf files and used for various purposes. One piece of software extracted the acoustic camera's direction and angle to display a 3D arrow on the screen during deployment (left side of the image). This arrow was not affected by boat rotation and, therefore, allows quick, real-time feedback regarding the angle and direction of the camera. Figure 3-4 shows additional overlays, with depth, GPS position, and angle plotted with respect to a collected mosaic of a sunken barge.

In some cases, it is not practical or possible to deploy the camera from the boat using the pan-and-tilt mechanism. One example is deep scour holes imaged at Locks and Dams 24-27 on the Mississippi River. The acoustic camera needed to be deep enough to see under the concrete ledge, meaning any translation of the boat would be dangerous to the hardware and possibly personnel. Voice instructions were used to guide the diver's rotation, tilting, and orientation of the camera based on the images viewed from the topside.

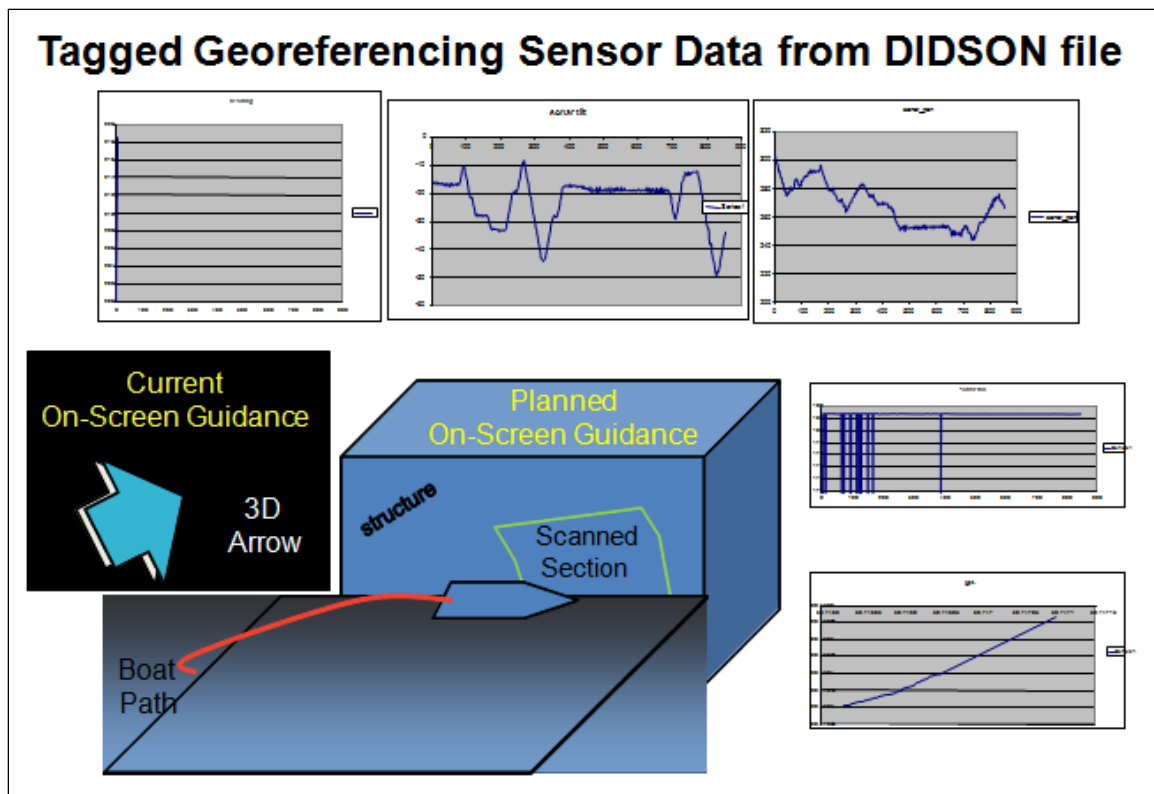


Figure 3-3. Typical measurements provided by the acoustic camera system sensors.

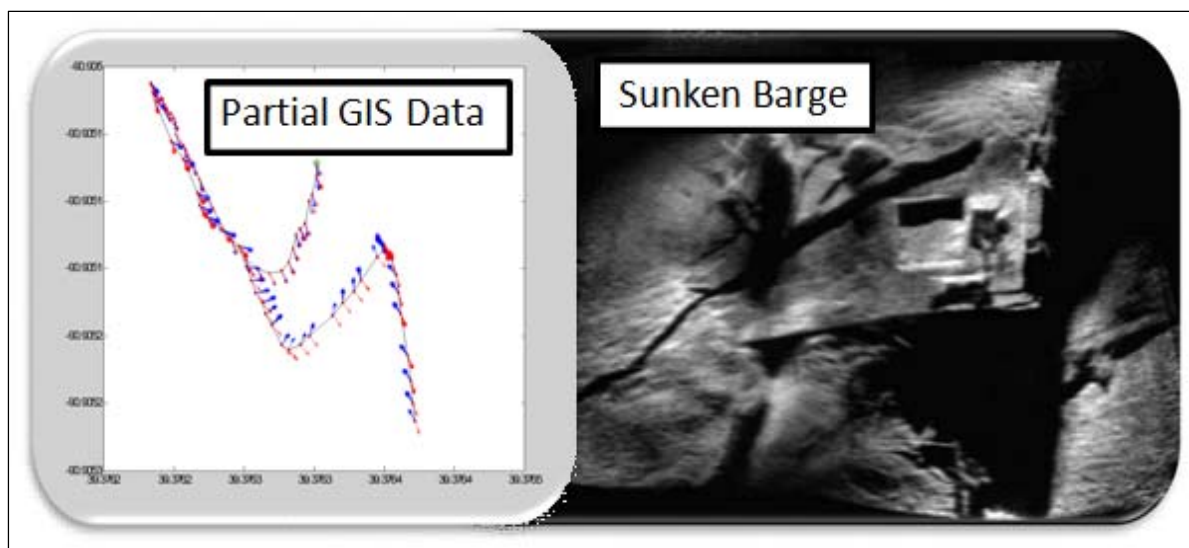


Figure 3-4. Mosaic image and corresponding GIS data.

Since then, heads-up display capabilities have been pursued and accomplished with some success. The barge lift gate shown in Figure 3-5 was the result of a deployment in which the only means of access was a qualified diver.

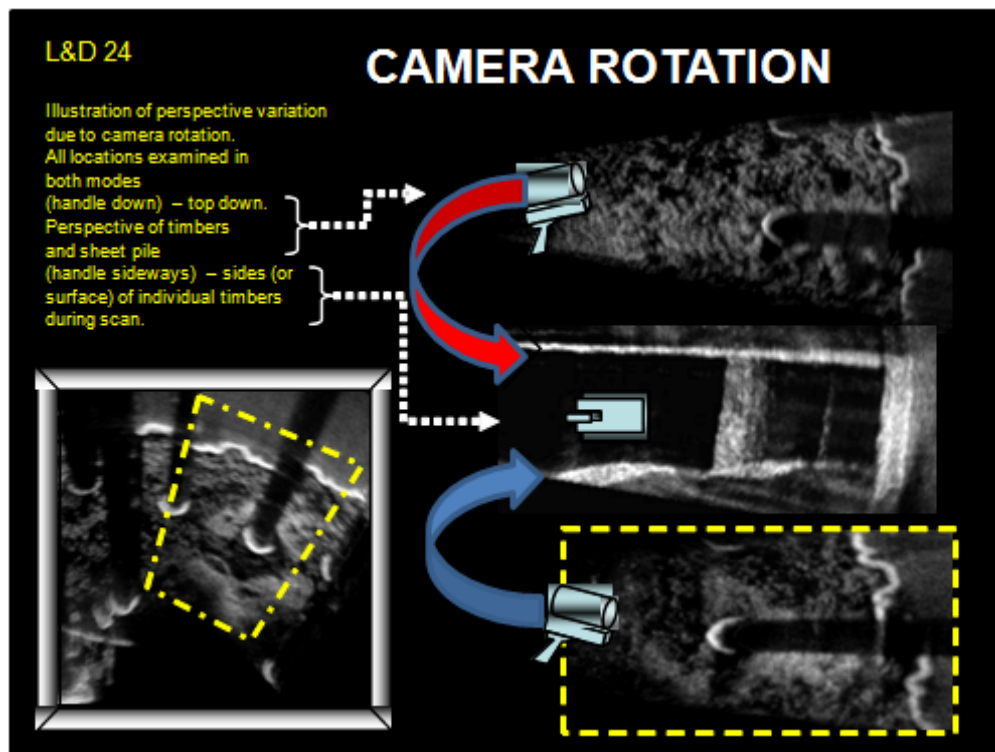


Figure 3-5. Images of a barge lift gate at Lock and Dam 24 on the Mississippi River.

In another deployment condition, the DIDSON was pulled on guide ropes through 3-ft-diameter culverts as long as 80 ft. The setup and resultant images are shown in Figures 3-6 and 3-7.

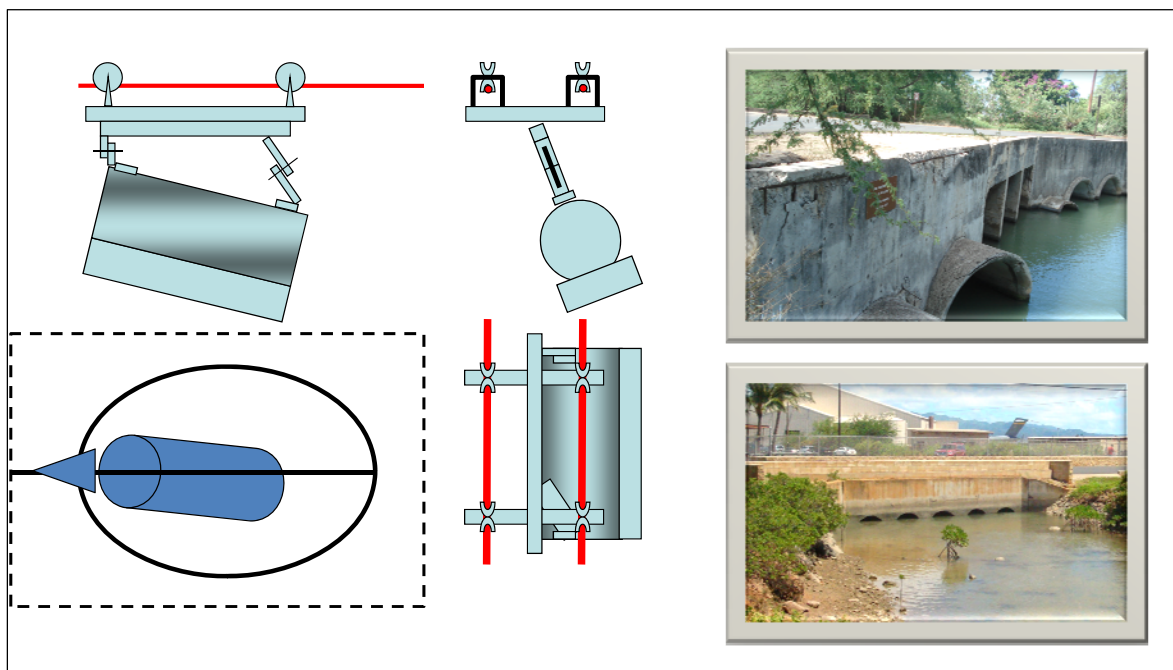


Figure 3-6. Acoustic camera deployment mechanism for culvert inspection.

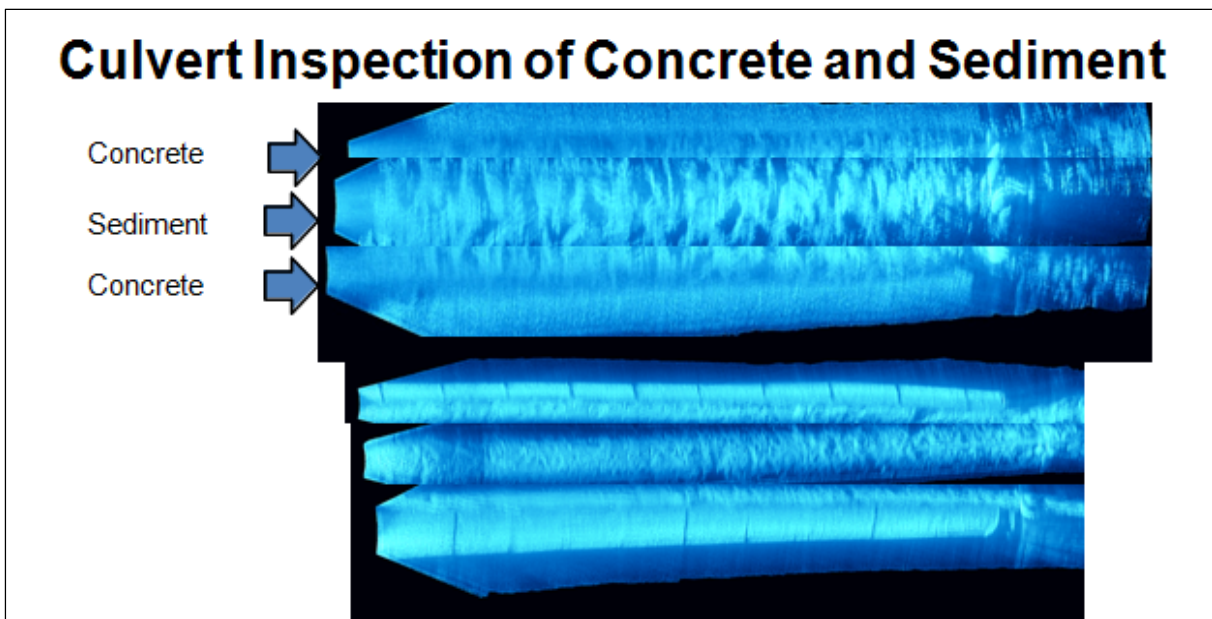


Figure 3-7. Resultant mosaic images from culvert inspections.

3.1.2 Boat-mounted pole

The most used method of deployment has been a mount that allows the camera and a pan-and-tilt device to be dropped over the side of a boat. The mount is fastened to the deck of the boat and has an arm that extends over the side of the boat. The arm is attached to a vertical mechanism with rollers that holds a segmented pole. The pan-and-tilt is attached to the bottom of the pole. The acoustic camera attaches to the pan-and-tilt. Figure 1-2 shows the mount.

On the bottom of the lowest pole, a metal plate is attached that has an eye to which a cable from a 12-V DC electric winch is attached. By letting cable out on the winch, gravity pulls the camera and poles down to lower the camera to the desired depth in the water. By retracting cable, the camera is raised toward the surface to the desired depth.

Other equipment and sensors used on a boat-mounted setup are a precision differential GPS, a water column position sensor, and a 4 to 20 mA pressure sensor to provide water column depth. Also, 12-V DC and 24-V DC power supplies are on board to power the equipment. A Honda generator supplies 120-V, 60-Hz AC power.

The boat used for this work was a 23-ft-long Sea Ark outfitted with a 170-hp diesel engine and a 105-lb thrust trolling motor.

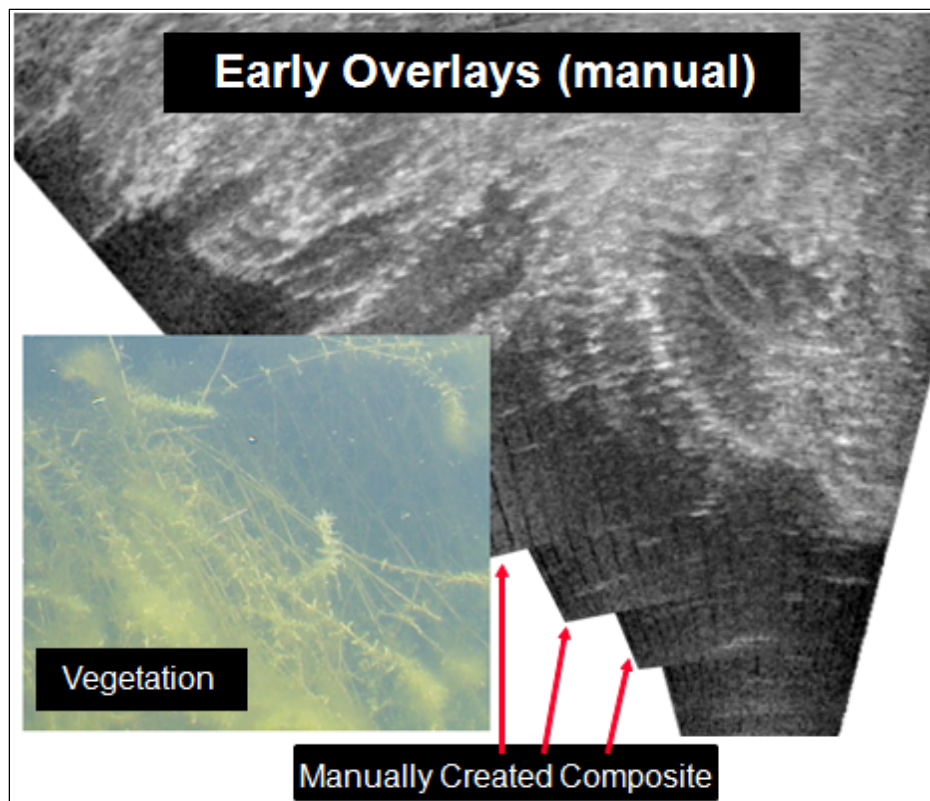


Figure 3-8. Manually created mosaic image.

3.1.3 Acoustic camera carried by diver

Hazards to using the boat-mounted system included unknown underwater obstacles, particularly rough surface water conditions, and deep targets with a current involved. Also, the time and distance to transport the boat were prohibitive. If only imaging was desired and absolute position information was deemed unnecessary, divers held the camera, responding to verbal commands to position themselves in relation to the desired targets. Also given verbally were commands as to the desired tilt and pan angles of the camera.

Advantages of a diver-carried camera:

- Minimal equipment (laptop PC, acoustic camera power supply, acoustic camera and cables);
- Almost unlimited positioning ability.

Disadvantages:

- Lack of camera position information;

- Slower camera movement;
- More restricted coverage area;
- Risk of harm to personnel.

3.1.4 Tethered camera

In a special case, where the condition of culverts was to be assessed, the camera was attached to ropes via a mechanism that allowed an angle to be set and maintained while the ropes were used to move the camera the length of the culverts.

3.2 Additional sensors to support geospatial position awareness

The acoustic camera contains an internal compass, tilt, and roll sensors to provide orientation information to the user. For structural inspections, knowledge of the camera's location must be known as well. To accomplish this, a precision differential GPS was installed to measure longitude and latitude. To know the depth of the camera below the surface of the water, an underwater inertial guidance sensor was purchased. It contained a pressure sensor that provided depth measurements via an RS-232 interface. The inertial guidance sensor also contained sensors to provide pitch, roll, and yaw measurements that provided redundancy for the corresponding sensors in the acoustic camera. Another sensor that was incorporated was an altimeter, which reports the distance from the sensor to a target. In this case, the altimeter was mounted at the level of the camera lens and pointed straight down to provide the height of the camera above the bottom. This sensor communicated with the PC through an RS-485 interface.

3.3 Software capabilities

The acoustic camera transfers data from the sonar unit to a topside PC via an Ethernet connection. Data consists of either 512x96 (high-frequency mode) or 512x48 (low-frequency mode) element frames and associated header information. The topside PC uses software provided by Sound Metrics Corp., the acoustic camera manufacturer. The software accepts the data from the sonar unit, displays it on the PC monitor, and stores it to the PC disc drive when recording has been selected. The acoustic camera software has many processing features built in, as well. They are detailed in the program's Help system.

During the development of this inspection system, the need for information not provided by the acoustic camera had to be addressed. A differential GPS system was added. An altitude sensor was added. A pressure sensor to measure the water depth was added. The pan-and-tilt mechanism was added. In each case, Sound Metrics modified the DIDSON software so the measurements from the added sensors could be stored with the image data.

3.3.1 Data enhancement through image integration and mosaicing

Early in the program, it was determined that, while the output was an improvement over existing technologies, some issues could be improved (Kim et al. 2004). The camera output was grainy, sometimes noisy, and displayed a limited field of view (Kim et al. 2004). It was time consuming to review the collected video data, and the data video file sizes were large and not easy to transfer or present. The solution was determined to be mosaicing and averaging the collected data into a composite image with a wider field of view. The first mosaicing was of hydrilla plants (Figure 3-8). The figure contains a video image obtained at the same general area as the mosaic. Note the level of detail captured by the acoustic camera.

Figure 3-9 shows the results of using a MATLAB least mean square search for mosaicing. As indicated in the figure, blurring occurred during slight rotations of the camera. Though the MATLAB routine was not robust in terms of its ability to handle intrinsic rotations in deployment, it clearly demonstrated not only improvement in aperture but also data quality, as the 8-bit image data with non-stationary noise was significantly enhanced from averaging. Attempts were made to include rotation in the MATLAB code using approaches such as cross correlation of radon transforms. Ultimately, the search criteria of displacement, rotation angle, and rotation point were computationally prohibitive using those approaches.

Further investigation revealed some emerging codes based on the scaled invariant feature transform (SIFT) algorithm. SIFT is an algorithm that registers unique features in images, thereby providing a mechanism by which features common among images can be matched for purposes such as creating a mosaic from multiple images. Commercially available software was found for automatic integration of digital camera photographs in panoramics. A MATLAB code was written to preprocess the DIDSON data output files and allow the images to be fed into the SIFT mosaicing software. Functions of this preprocessing code included stripping overlays from the image, setting transparency as the low-level reflection threshold, and

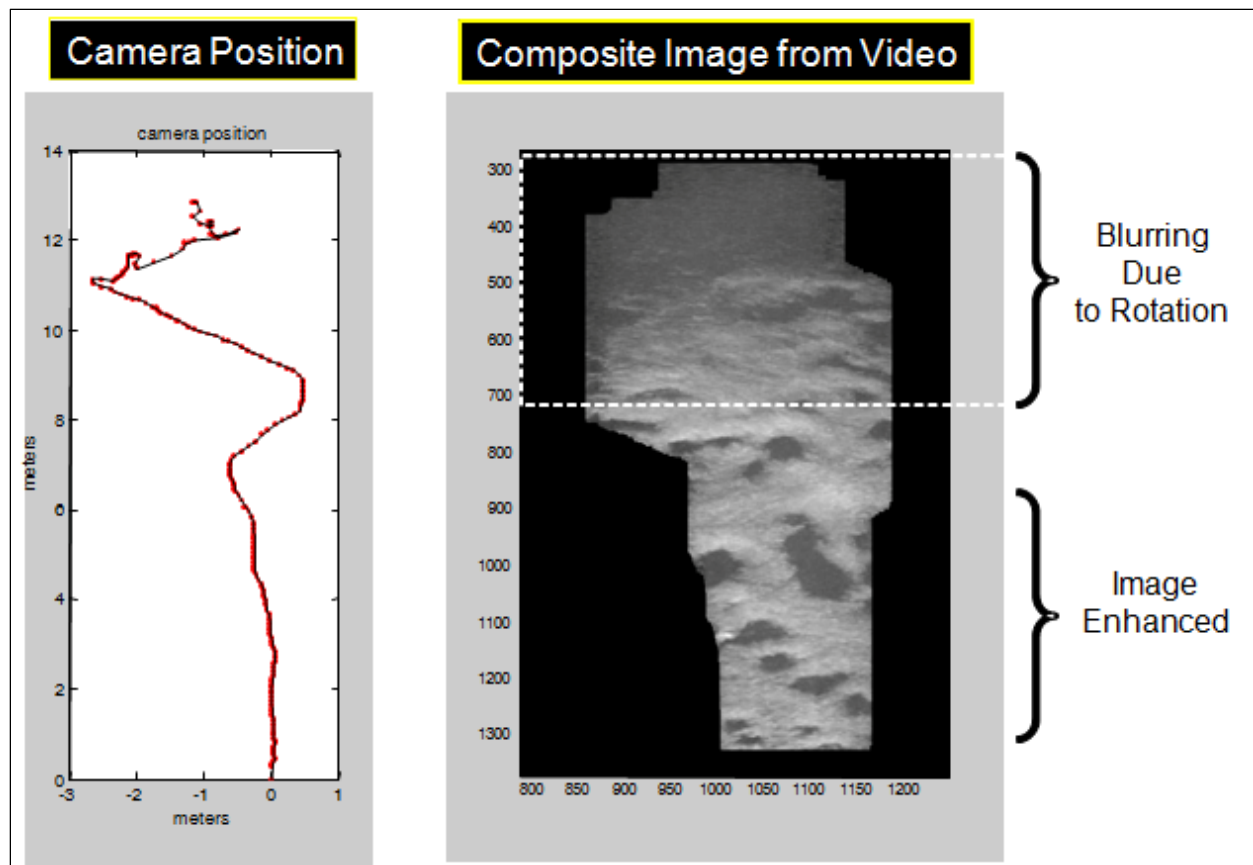


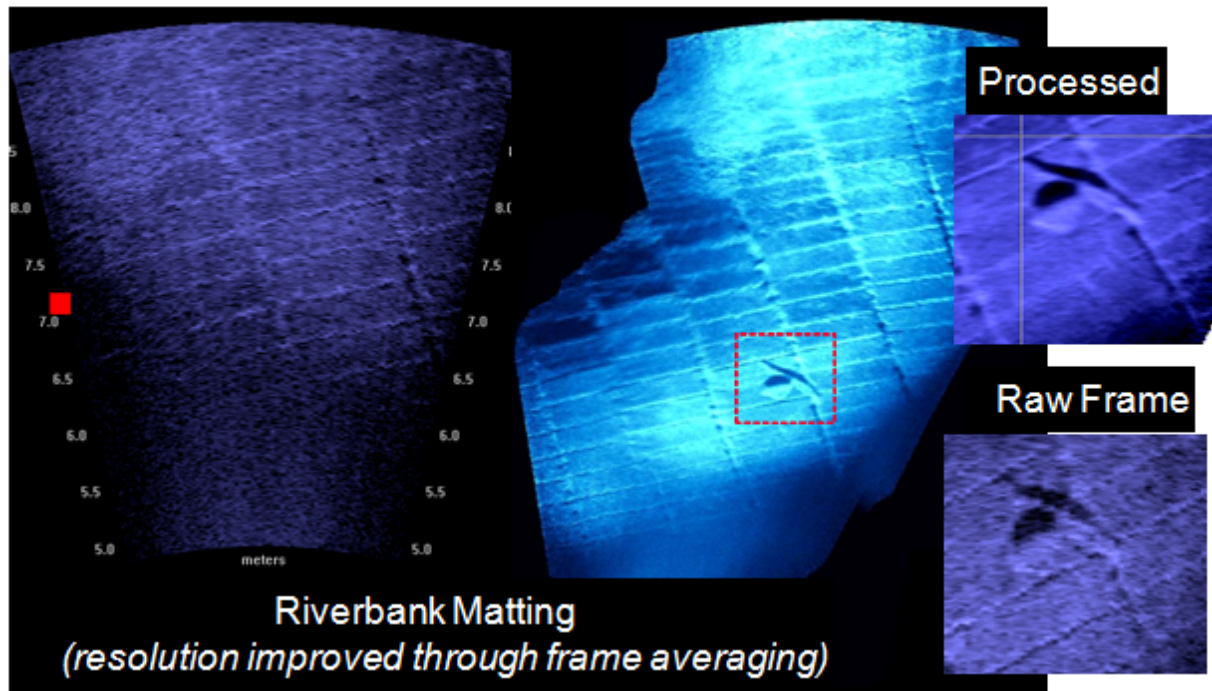
Figure 3-9. Mosaic generated using a least mean square search.

converting from .avi format to sequentially numbered .png files. Figure 3-11 shows early versions of the automated mosaicing and a comparison to the raw DIDSON data.

The commercial digital imaging code has advanced significantly. There are more options, particularly for handling moving objects, lens distortions, and image recombinations. The multithreading and higher memory, along with the improvement in hardware performance, mean larger datasets can be processed faster. Figure 3-11 shows a damaged section of concrete that was processed for detail, to determine the ability to detect concrete cracking. In addition to cracking of the concrete, entrapped air voids, marine growth, steel plating, and other details can be seen.

These improvements, along with enhanced preprocessing codes such as DDF Parser (Appendix B), mean many of the older panoramics/mosaics presented in this report could be improved by reprocessing the original data with the newer codes.

Automated Overlay and Mosaic



Improved Archive Format and Resolution

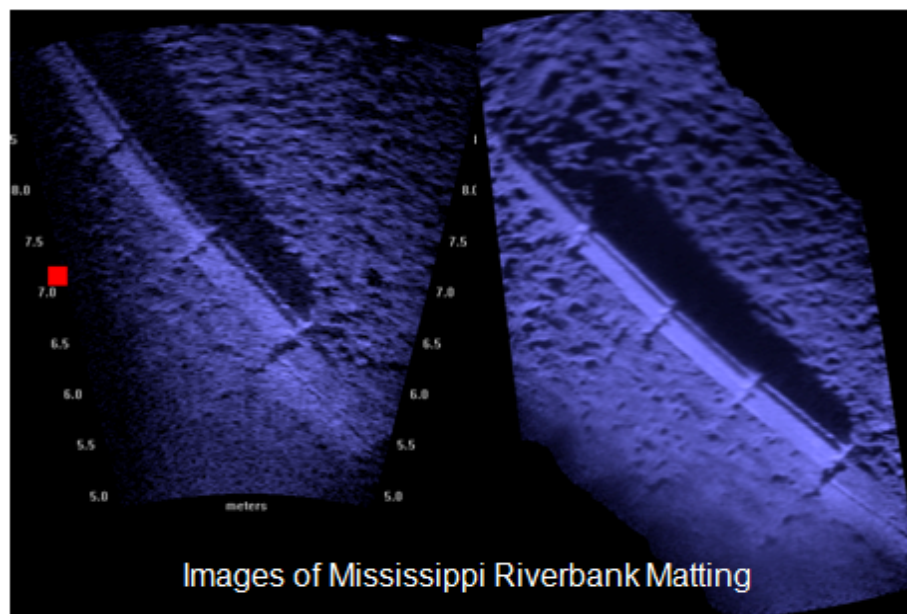


Figure 3-10. Image enhanced using the SIFT algorithm.

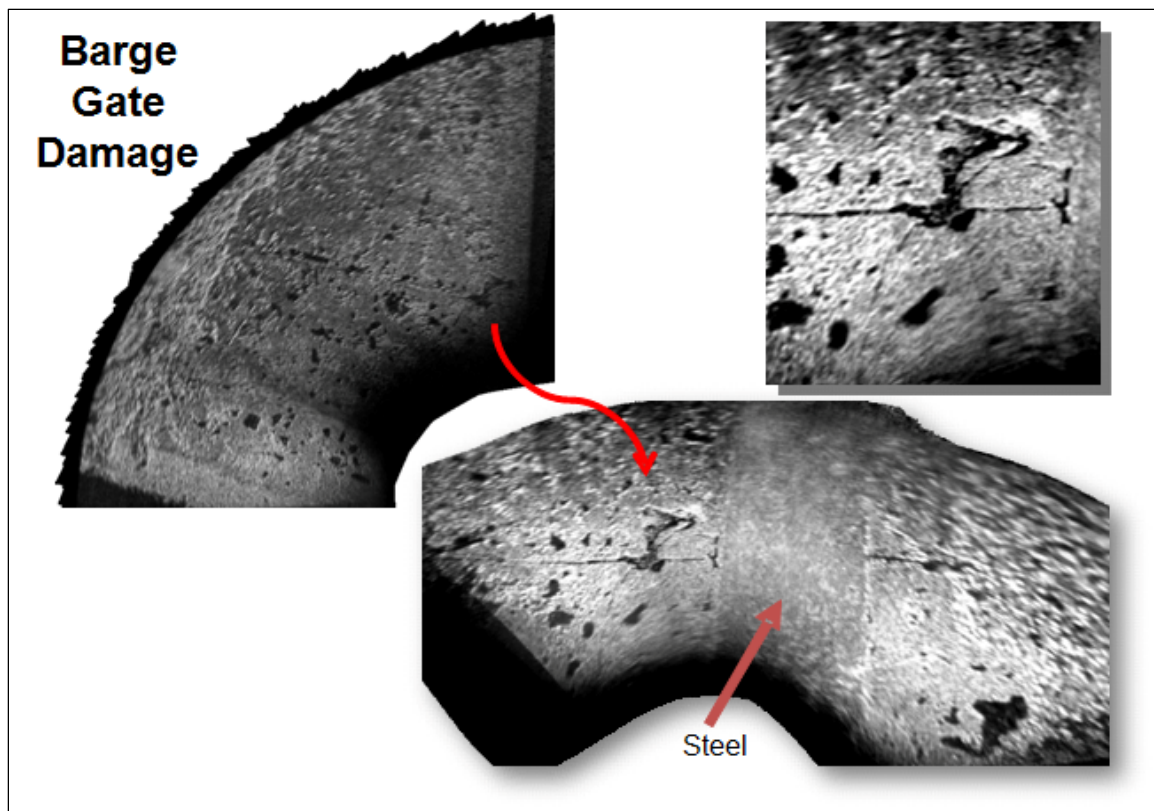


Figure 3-11. Images of the bottom of a concrete barge gate.

Ultimately, the ClearSight mosaicing software was developed in part by ERDC to increase speed and automation of acoustic camera data post-processing. The DDF Parser and SIFT codes are seen as complementary to ClearSight, which generally performs faster, while the SIFT code produces a superior output in some applications, though at the expense of time and parameter tweaking.

3.4 ClearSight (see Appendix A)

When assessing the condition of a structure or its components, different end results can be required depending on what is being examined and the information desired. Some projects require viewing only a small component, and live video from the acoustic camera will provide the needed information. The majority, however, require viewing large pieces of a structure, much larger than can be seen in a single camera frame. For these projects, the capability to stitch together frames to create a single image is crucial. Also, even small areas of a structure can have the imaging enhanced over single recorded images by using mosaic software for its noise-reduction capabilities. A number of commercial mosaic software packages were tested. A commercial package that uses the SIFT algorithm proved useful for data

recorded from a single point of reference while panning the camera. It proved less useful for data recorded in a push-broom fashion (i.e., the camera moves along a line while recording). Another drawback to the SIFT-based software was the time required to prepare the acoustic camera data to key in, along with the time required to put together a large number of frames.

To inspect a large area in the smallest time, the best way to record images is to move the camera platform in a continuous straight line. To create a mosaic of images collected in a push-broom manner, stitching software must be optimized to work with the data collected. To complete this task, a third-party software developer, AcousticView, was contracted. AcousticView developed a package called ClearSight. The camera should be moving at a constant velocity, but the velocity must be slow enough that approximately 60% overlap in consecutive images is achieved. If these conditions are met, ClearSight is a good tool for creating mosaic images that maintain position information of the pixels in the mosaic image. Figure 3-12 shows the ClearSight user interface and a generated mosaic of the downstream side of a lock miter gate.

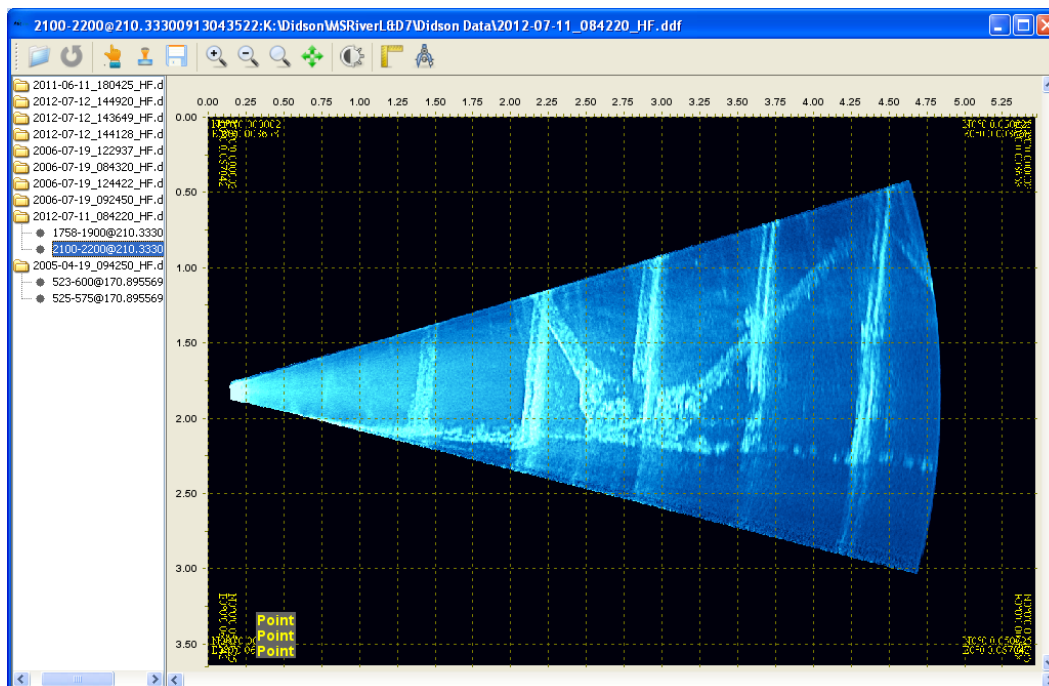


Figure 3-12. ClearSight user interface window.

An important feature of ClearSight is the ability to incorporate the GPS information recorded by the acoustic camera software into the mosaics it creates. ClearSight, by default, puts GPS coordinates in the corners of the

image window. The user can direct the program to put a GPS coordinate stamp at any location on the mosaic image by selecting the appropriate tool on the menu bar. The menu bar also contains a button to activate GPS tracking (i.e., a display updates the GPS coordinate display as the cursor is moved about the mosaic).

3.5 EdgeDetect software

The acoustic camera also has been used to record images of the outline of surfaces, such as scour holes in lock walls or the slope of a wall. Figure 3-13 shows this type of image. By recording these types of images at multiple heights in the water column, a surface map can be generated. To accomplish this goal, software called EdgeDetect was written by ERDC. Figure 3-13 shows the EdgeDetect window that is the user interface for this program. The EdgeDetect user manual is in Appendix D. Chapter 4 will show examples of the usefulness of EdgeDetect.

3.6 DDF Parser software

The DDF Parser software was developed by ERDC to provide a means of conveniently manipulating the acoustic camera's native data files. DDF Parser allows the user to pre-process data files that will be keyed in to two mosaic software packages, Kolor autopano giga and AcousticView synesthesia ClearSight. The user manual is in Appendix C.

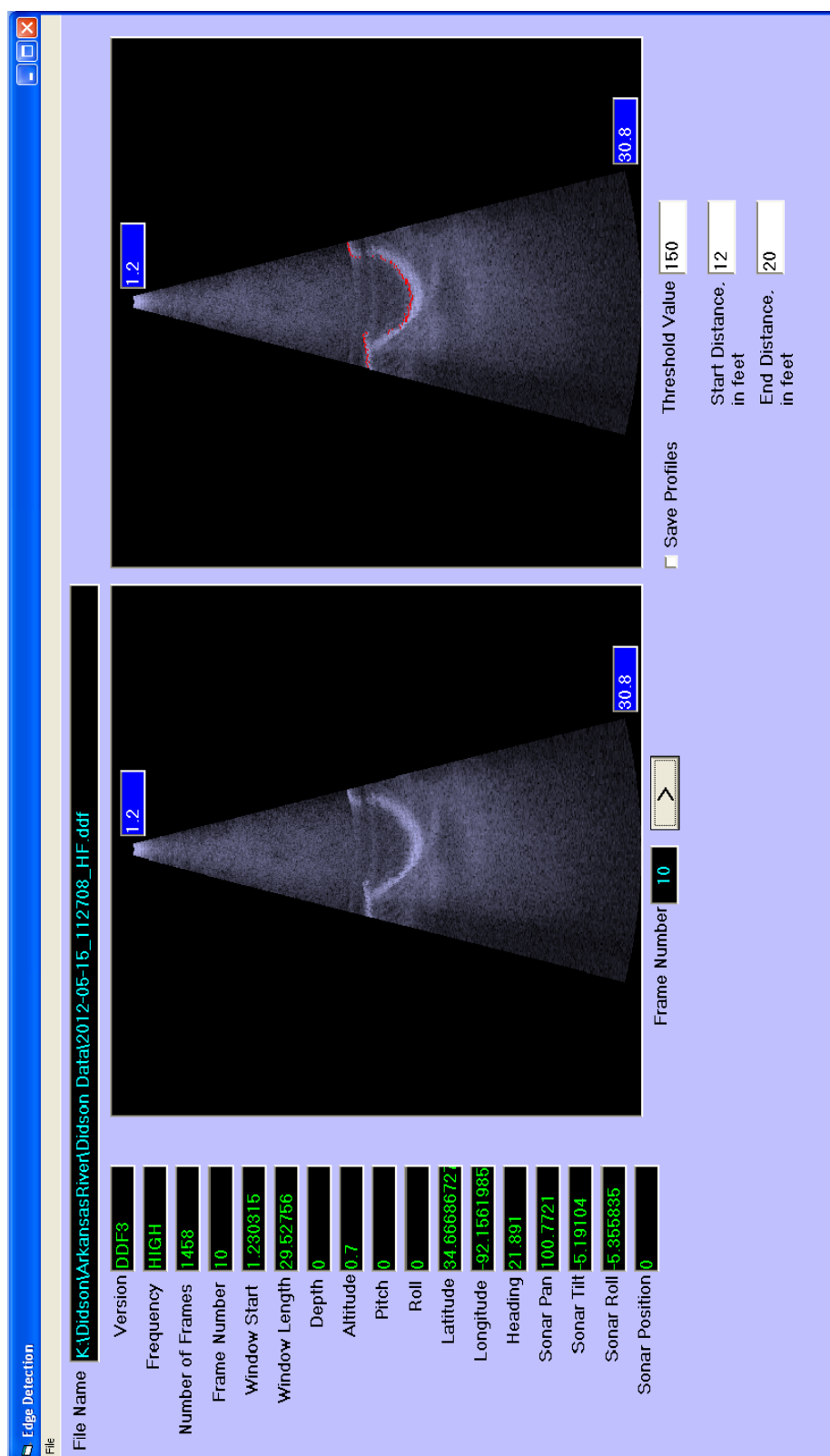


Figure 3-13. EdgeDetect window.

4 Inspections Performed

4.1 Overview of inspection types

The acoustic camera has been used to inspect various structural components to assess a variety of issues. One of the main and most persistent issues is scour holes that develop in and under lock walls, in approach channels, in stilling basins, etc. Three concrete scour projects are described in the next three sections.

Discussed at the end of this chapter will be some of the inspections performed during the last decade and the information obtained. This information will demonstrate the capabilities and expected output of the acoustic camera for underwater structural inspections across a broad range of deployments. Because some of these deployments date to earlier processing software, they all do not reflect the current data enhancement achievable. As covered in these studies, the camera has been used to determine the structural integrity of miter gates in lock chambers and tainter gates in dams. It also has been used to examine large and small culverts and to determine correct alignment of components such as a vertical gate fitting into a slot in a structure. These cases and others will be covered in the last section of this chapter.

4.2 Arkansas River, May 2012

4.2.1 Lock and Dam 6, David D. Terry Lock and Dam

The David D. Terry Lock and Dam is part of the McClellan-Kerr Arkansas River Navigation System (MKARNS). It is typical of the MKARNS lock dams, having a lock chamber that measures 110 ft wide and 600 ft long. The lock chamber has miter gates at each end. The dam consists of 17 tainter gates, each 60 ft wide and 27 ft high, that are used to regulate the amount of water that can pass, thereby controlling the upstream and downstream pool levels. The lock wall on the riverside and downstream of the dam in the area of the stilling basin end sill had developed a large scour hole. Also, the end sill had experienced significant erosion. An inspection was performed to document the amount of damage and to aid in contract specifications for repair work to the structure.

The work was performed from an ERDC survey boat. Because the water was rather rough, the boat was moored to a work barge provided by the USACE Little Rock District.

To map the size of the scour hole in the lock wall, the survey boat was positioned so the acoustic camera could be pointed directly at the scour area and so an outline could be obtained. To obtain contour lines, the outlines were recorded as the camera depth was varied. Figure 4-1 shows the images obtained. The images have been annotated to indicate the location of the lock wall and approximate dimensions of the scour area.

The EdgeDetect program generated a set of contours using the images in Figure 4-1. The contour points were loaded into MATLAB, and a surface was generated (Figure 4.2).

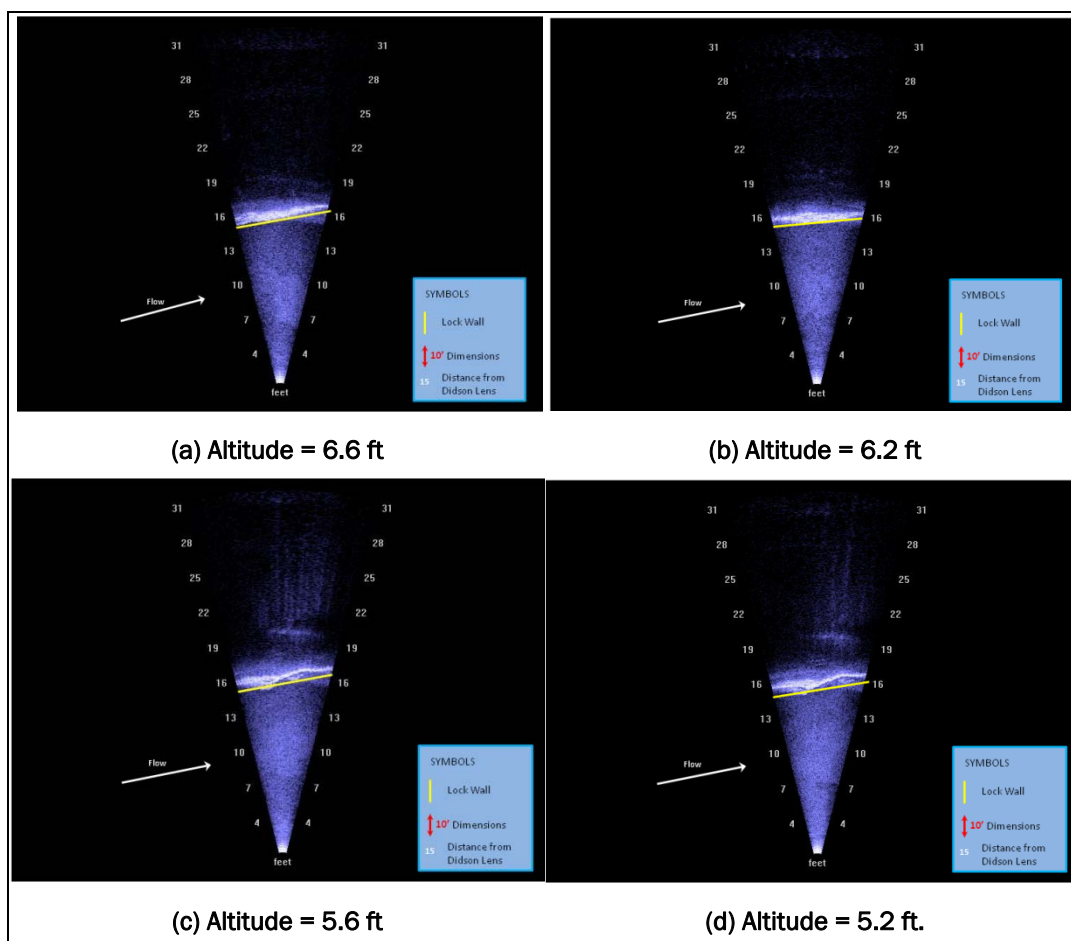


Figure 4-1. Lock and Dam 6 on the Arkansas River. (continued)

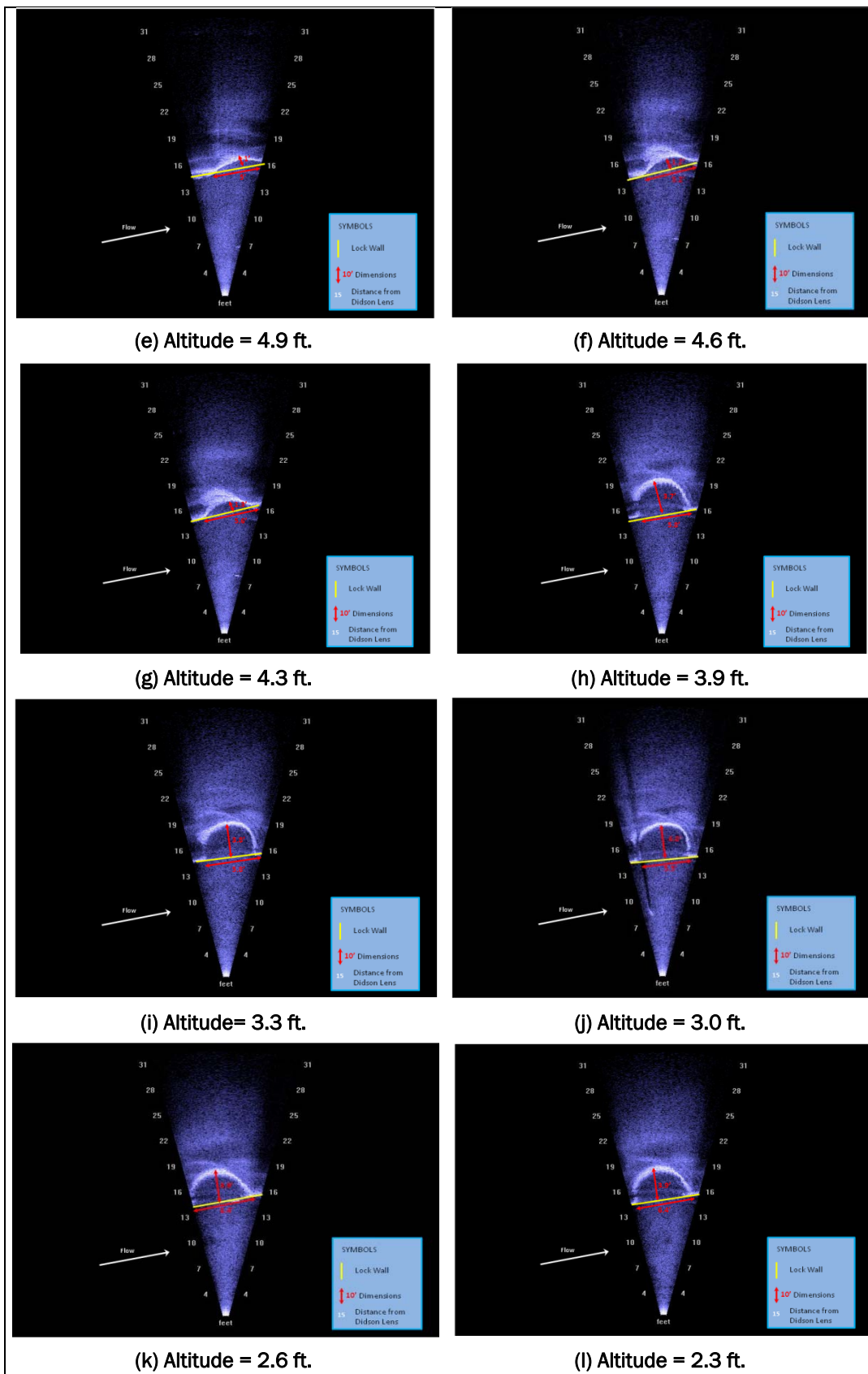


Figure 4-1. (concluded)

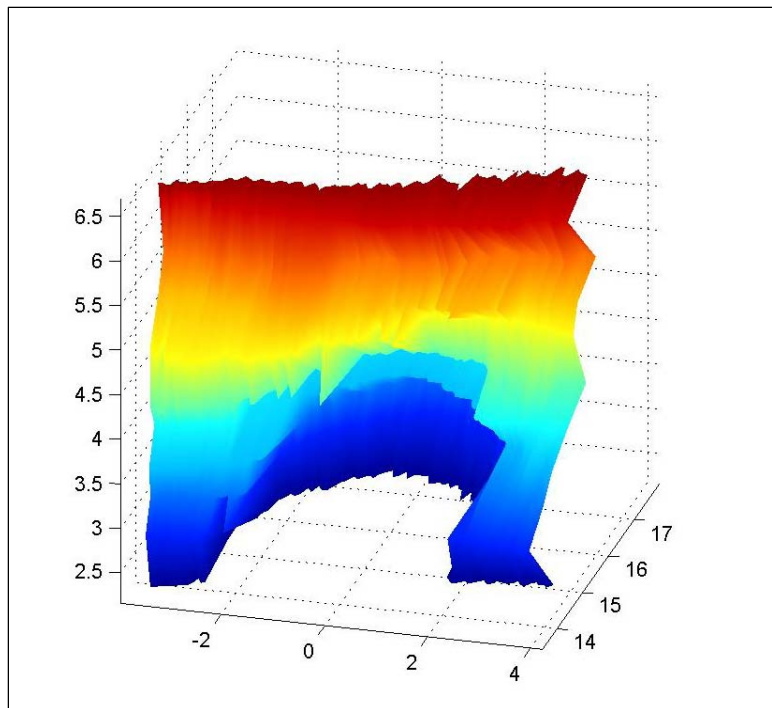


Figure 4-2. A 3D surface plot of scour hole in the lock wall at Lock and Dam 6 on the Arkansas River.

4.2.2 Lock and Dam 9, Ormond Lock and Dam

The Ormond Lock and Dam is part of the MKARNS, too. It also has a 110-ft-wide-by-600-ft-long lock chamber. The dam is formed by 14 tainter gates. An inspection was performed in May 2012 to locate and measure scour that had been reported during dive team inspections.

The imaging was performed with an ERDC survey boat. Because the water was calm, the survey boat was positioned using a combination of the inboard engine and ropes attached to the lock wall structure.

The scour hole is shown in Figure 4-3. This image was generated using the ClearSight mosaic software by combining frames 1470 through 1650 from the DIDSON data file named 2012-05-15_181940_HF.ddf.

The size of the scour hole (maximum depth, width, and length) was determined by reorienting the acoustic camera so the outlines of the hole could be observed.

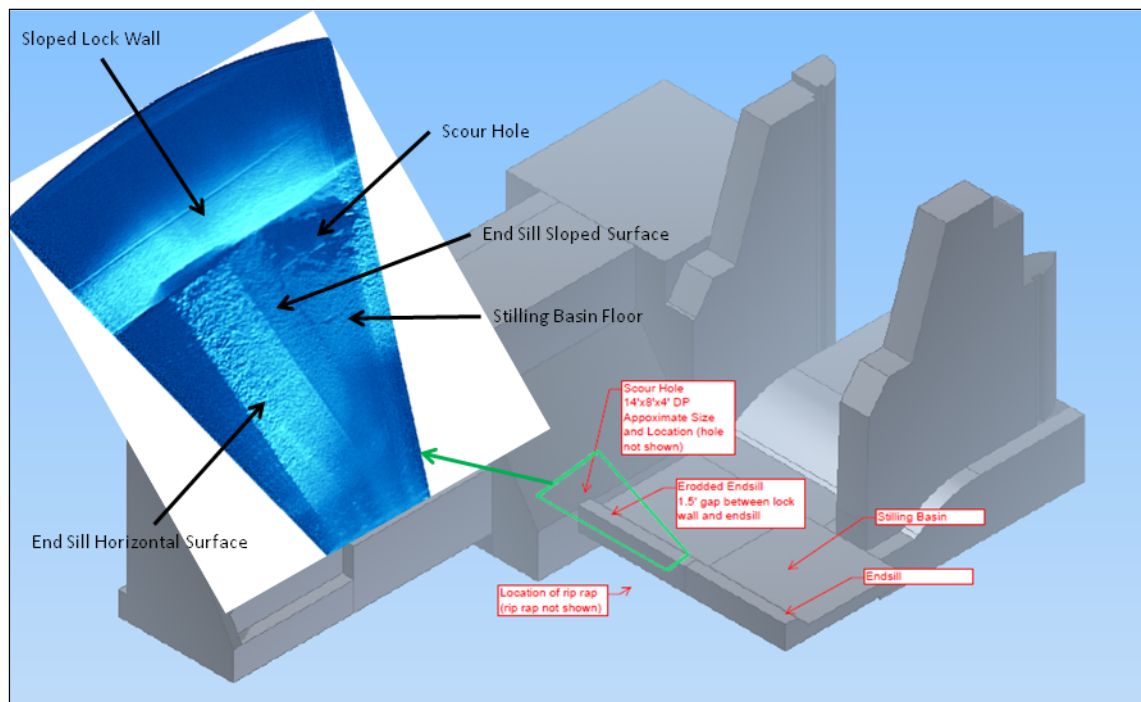


Figure 4-3. Mosaic image of the scour hole at Lock and Dam 9 on the Arkansas River.

4.3 Mississippi River, November 2011

4.3.1 Lock and Dam 25, Mississippi River, scour hole inspection

At this lock and dam near Winfield, Missouri, scour had developed under the downstream riverside lock wall. The scour was so vast that a large section of concrete that normally rests on the riverbed had broken, and the void continued well under the remaining lock wall. Figure 4-4 provides a not-to-scale plan view representation of the lock, and shows the location of the broken concrete section. Dive crews had probed beneath the lock wall with poles as long as 10 ft, according to verbal reports, and had not been able to locate the end of the scour hole. For safety purposes, divers were not permitted to go under the lock wall and into the scour area. It also was known that there was a smaller scour area under the lock floor concrete at the downstream end of the lock. Figure 4-4 shows an indication of the scour locations.

The USACE St. Louis District wanted to know the actual dimensions of the scoured areas, to plan and budget for repairs. A contract dive team was used to manipulate the acoustic camera for data collection.

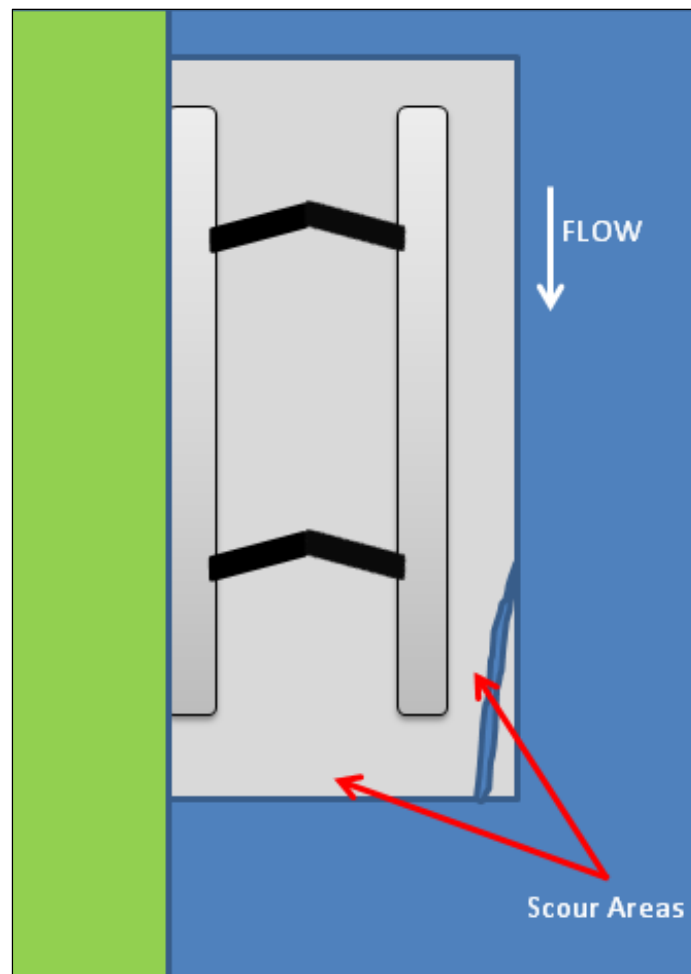


Figure 4-4. Lock and Dam 25 on the Mississippi River and areas damaged by scour.

To measure the depth of the scour hole beneath the riverside of the lock wall, the diver positioned himself in the area between the intact lock floor slab and the section of broken concrete. By pointing the acoustic camera in a vertical orientation, the outlines of the underside of the lock floor slab and the riverbed could be obtained. The depth of the scour hole was determined by the distance to the intersection of the riverbed and the underside of the concrete slab. The result obtained was a depth of approximately 22 ft and a height of approximately 6 ft at the location indicated in Figure 4-5. These are the best estimates from the images obtained. More accuracy could have been obtained if the diver could have backed far enough away to get the vertical edge of the concrete slab in the image, but he couldn't because a portion of the broken slab was in the way.

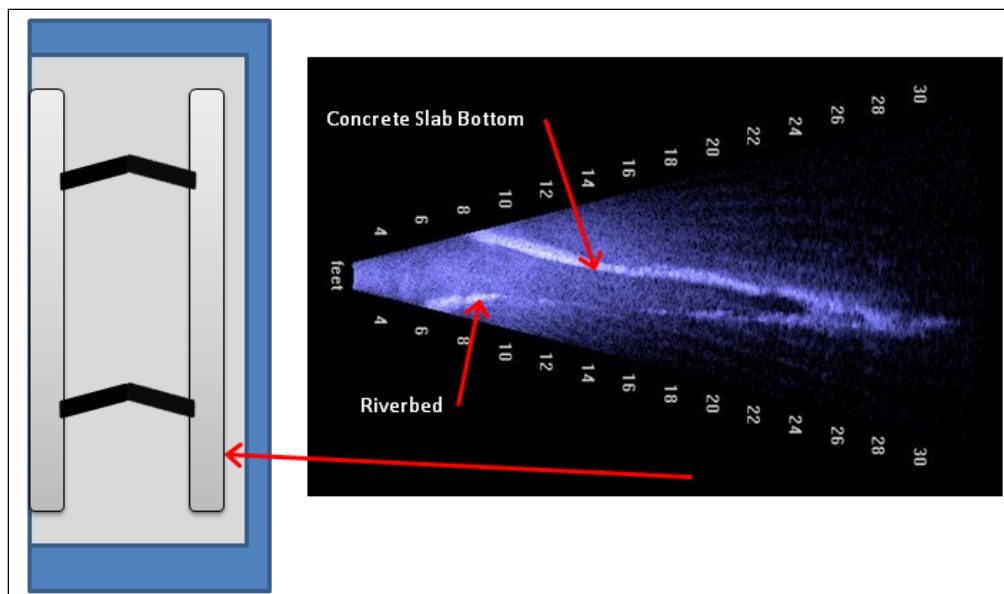


Figure 4-5. Scour hole outline under the downstream riverside lock wall.

The scour hole under the downstream edge of the lock floor was measured at three locations to provide an approximate contour of the void. Figure 4-6 provides the images at these locations.

4.4 Illinois River, July 2006

4.4.1 Starved Rock Lock and Dam, scour hole inspection

Depth soundings that had been taken at Starved Rock Lock and Dam near Ottawa, Illinois, indicated holes of sufficient depth to cause some concern. The holes were near the dam and raised the question of whether scour holes were developing under the structure. Acoustic camera scans along the downstream side of the dam monoliths revealed no scour beneath the dam. The vertical face of the monolith met the river bottom the length of the dam. The mosaic in Figure 4-7 is representative of the images viewed.

4.5 Additional case studies

The following section begins with damaged concrete and concrete features; next, steel; then, inspection of steel and concrete structures. Imaging of organic shapes or materials is presented separately from plants and rocks. It is important again to point out that post-processing methods and results have improved, and much of the older inspection scans have not been reprocessed with higher performance imaging software. Processing will be described or characterized where relevant. Some of the images in this section have been presented in other context in this report. For continuity and ease of referencing, they are reproduced here.

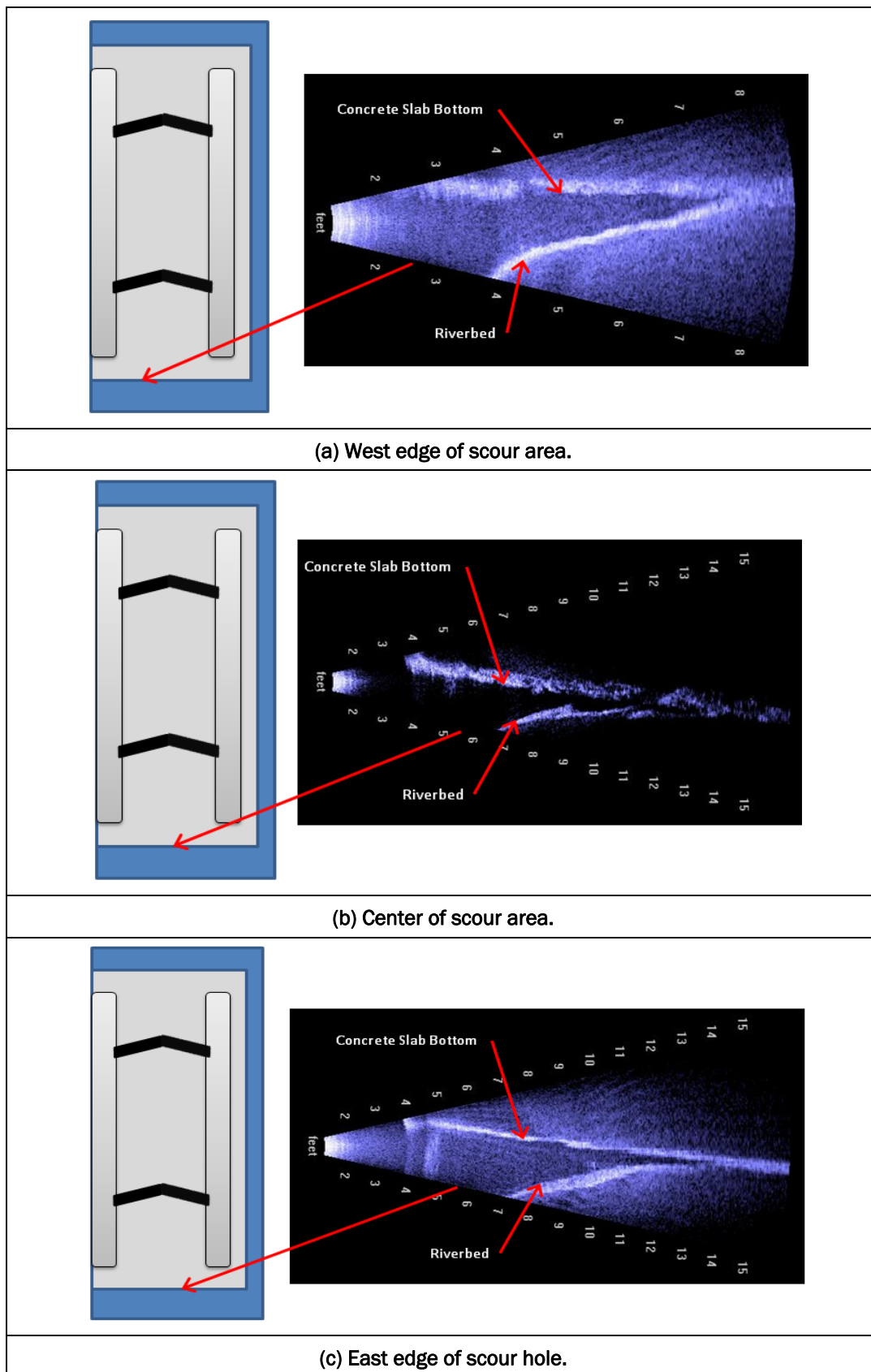


Figure 4-6. Scour area under the end of Lock 25 on the Mississippi River.

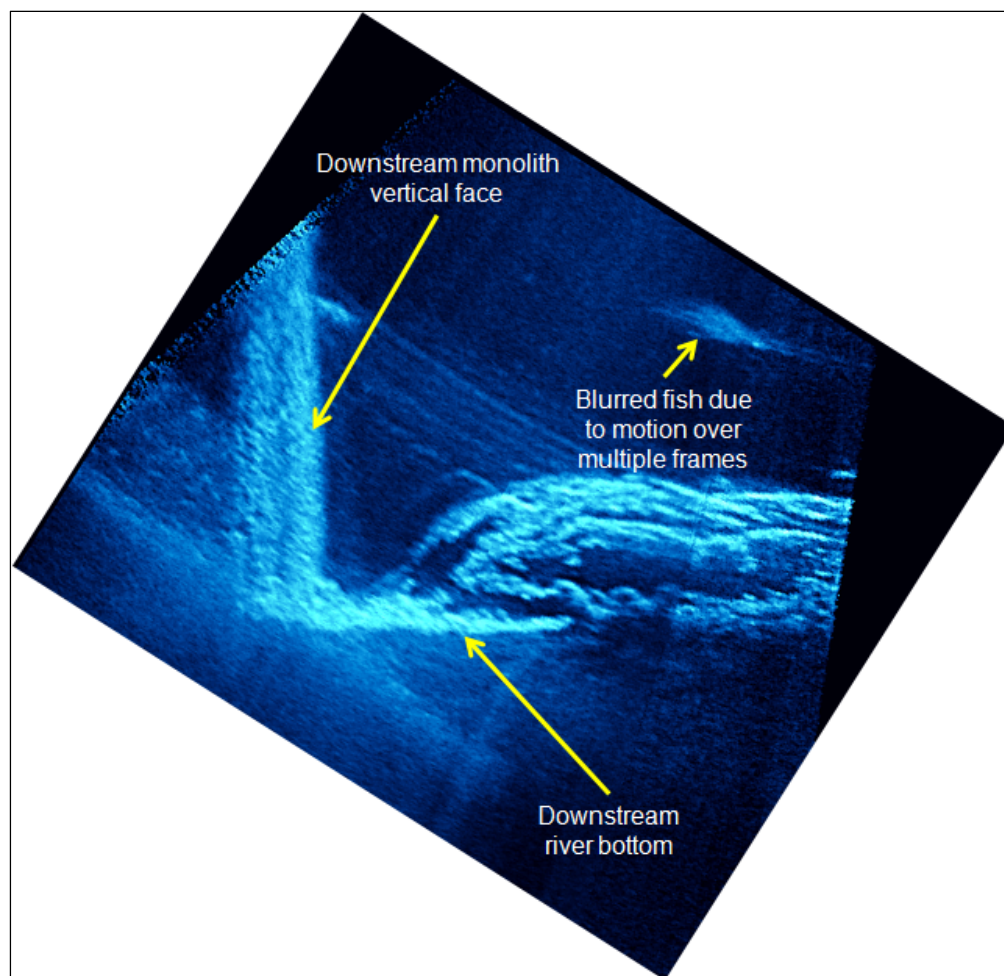


Figure 4-7. Starved Rock Lock and Dam, Illinois River, dam and river bottom intersection.

Figure 4-8 shows damaged concrete. The acoustic image (bottom) is a single-frame grab that has been high-process filtered and histogram equalized. The macroscopic cracks are of significant size to affect reflected acoustic energy from the plate's surface. When imaging cracked concrete, it is important to be aware of silt and biological materials that can coat the surface. Cleaning before scanning depends on age and environment.

Figure 4-9 shows a large concrete joint between two curved monoliths. Small spalling is detected and shown in the insets. Current methods use edge detection to get objective volume maps. This image was collected from diver-based deployment; however, boat deployment also is feasible here.

The New Orleans Barge Lift Gate's concrete floor was damaged when it was sunk on a piece of vertical scrap I-beam. Biological growth and silt were blown or wiped away, and the image was collected from diver-based

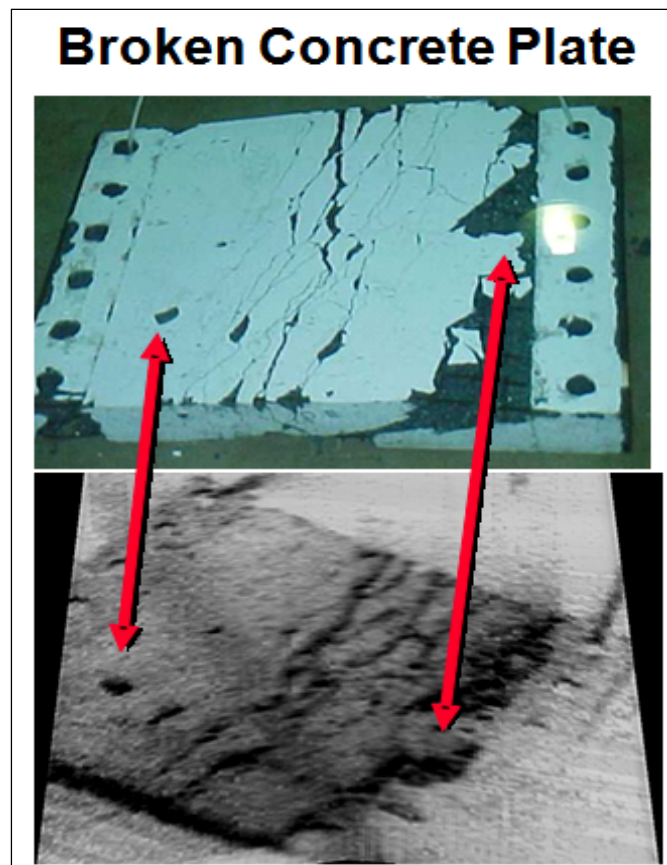


Figure 4-8. Damaged concrete section.

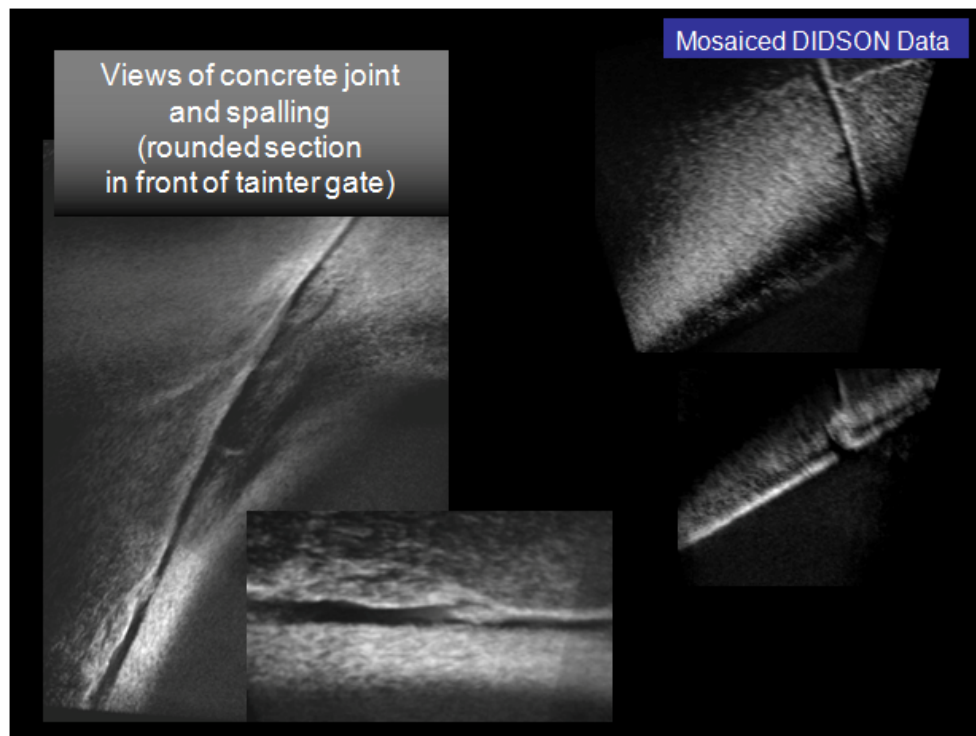


Figure 4-9. Example of concrete structure imaging.

deployment. This deployment method was used due to accessibility of this section of the structure. The steel skid pad shows up due to its different acoustic impedance. This is shown in the bottom image of Figure 4-10.

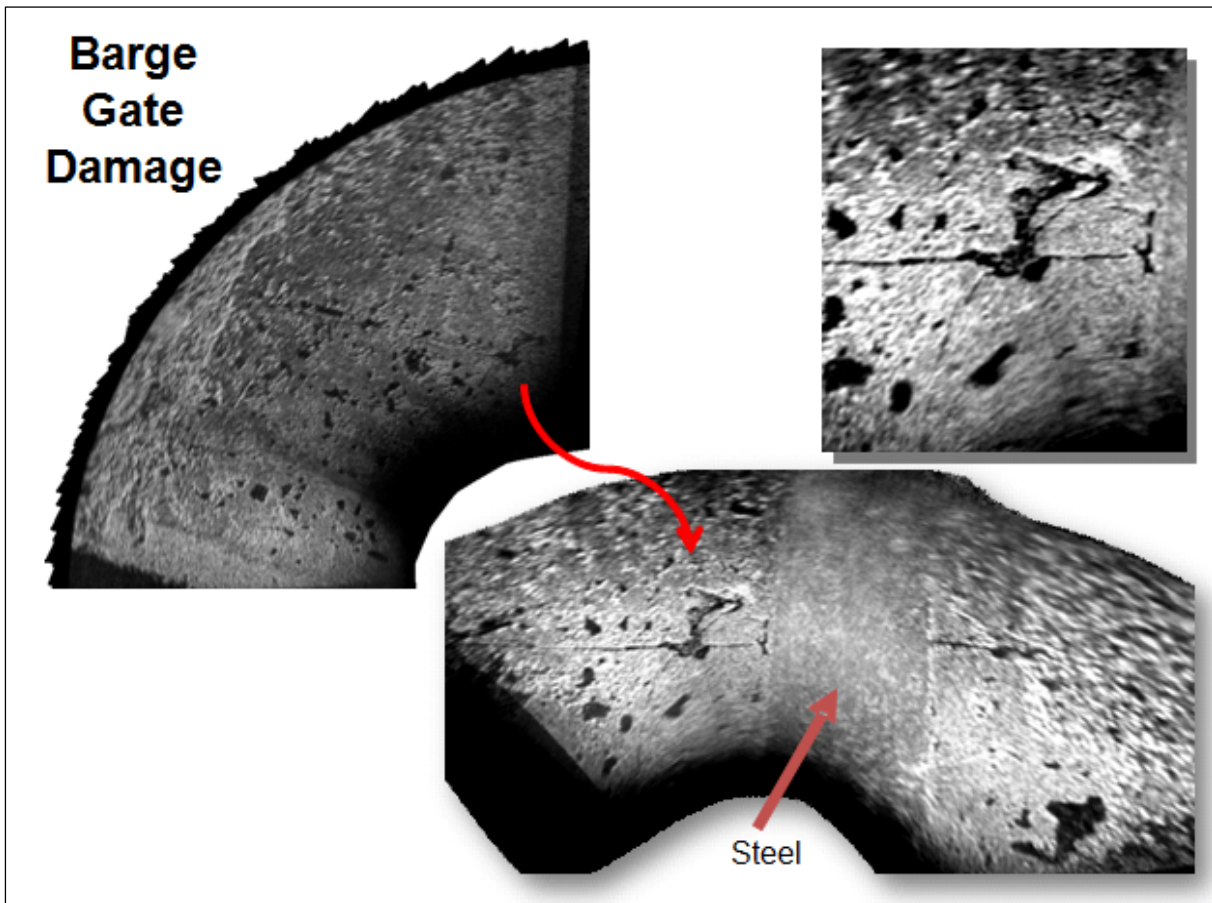


Figure 4-10. Damaged section of the underside of a concrete barge gate in New Orleans.

The photo in Figure 4-11 of the damaged stamped concrete at the river landing in downtown Vicksburg, Mississippi, was taken during low water. During high water the broken areas were rescanned with the underwater acoustic camera, and a mosaic was created. The large damage at this scale appears clearly captured in the mosaic output. Distance from the camera to the targets was 15 to 30 ft.

Matting for erosion protection has been placed along large sections of the Mississippi River. These are shown in several scales in Figure 4-12. The image on the left shows edge penetration for the sediment on the river bottom. The image on the right is a large mosaic. For scale, the mats are 4 ft long and 1.5 ft wide. Performance issues with repetitive patterns and low-contrast surface were addressed in early automated mosaic software efforts.

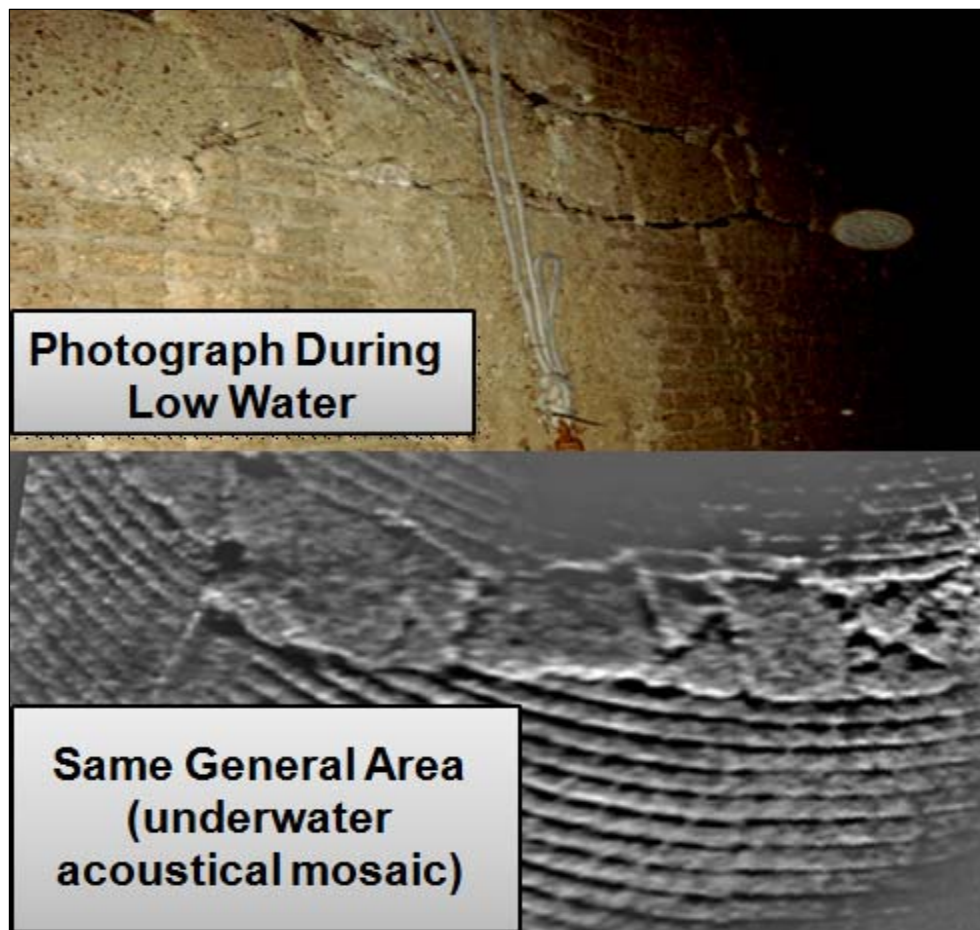


Figure 4-11. Masonry wall comparison of visible image and acoustical image, downtown landing, Mississippi River, Vicksburg.

Underwater rock or riprap is shown in the large mosaic in Figure 4-13. Debris (lower left) is encountered often. Common observations are milk crates, cinder block, chains, and fish and crab traps, which generally stand out due to their inorganic profiles.

Live and dead vegetation is seen clearly and characterized in acoustic camera scans (Figure 4-14). At higher frame rates (as many as 15 fps for DIDSON), species can be characterized by movements better captured as video.

The mosaics in Figure 4-15 show a contrast with a sunken barge from the 1960s that protrudes from the silt and debris. Recently, in a reimbursable effort, a sub-bottom profiler was used to supplement an acoustic camera-based search operation for a large steel-based structure lost in open waters.

The graph in Figure 4-16 shows collected GPS-based position, camera direction, and orientation.

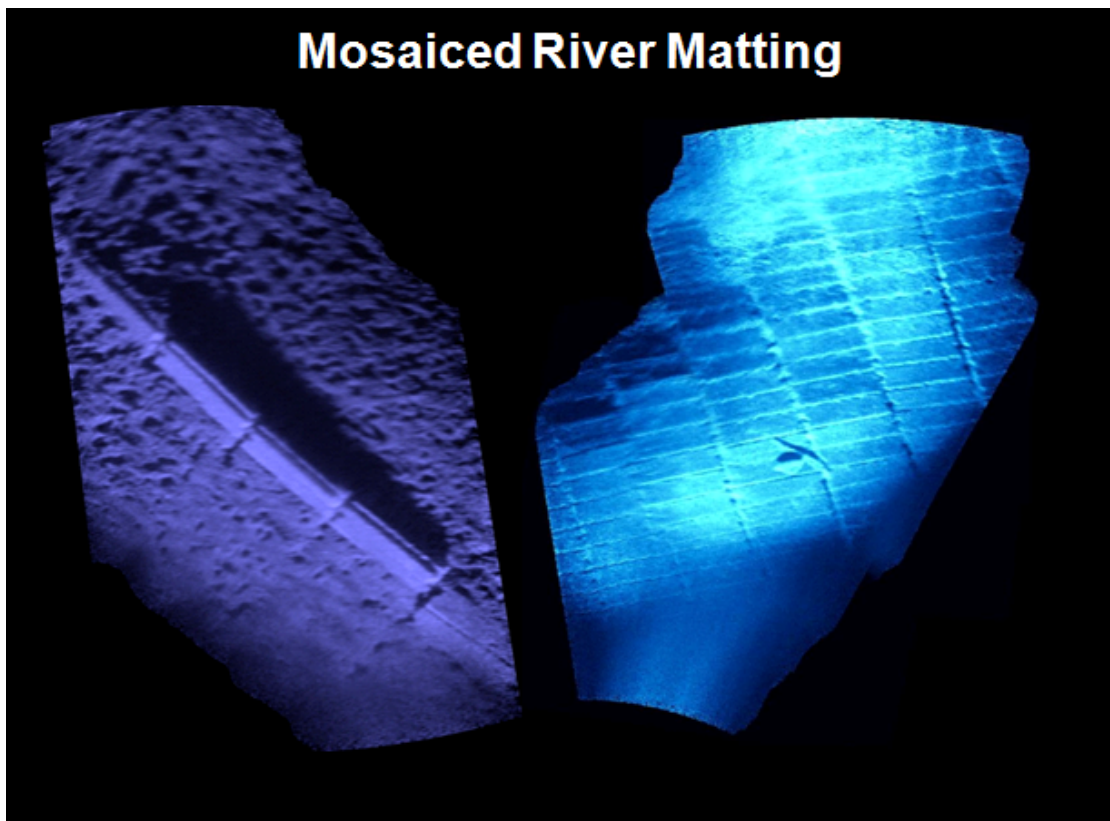


Figure 4-12. Mosaics of river matting.

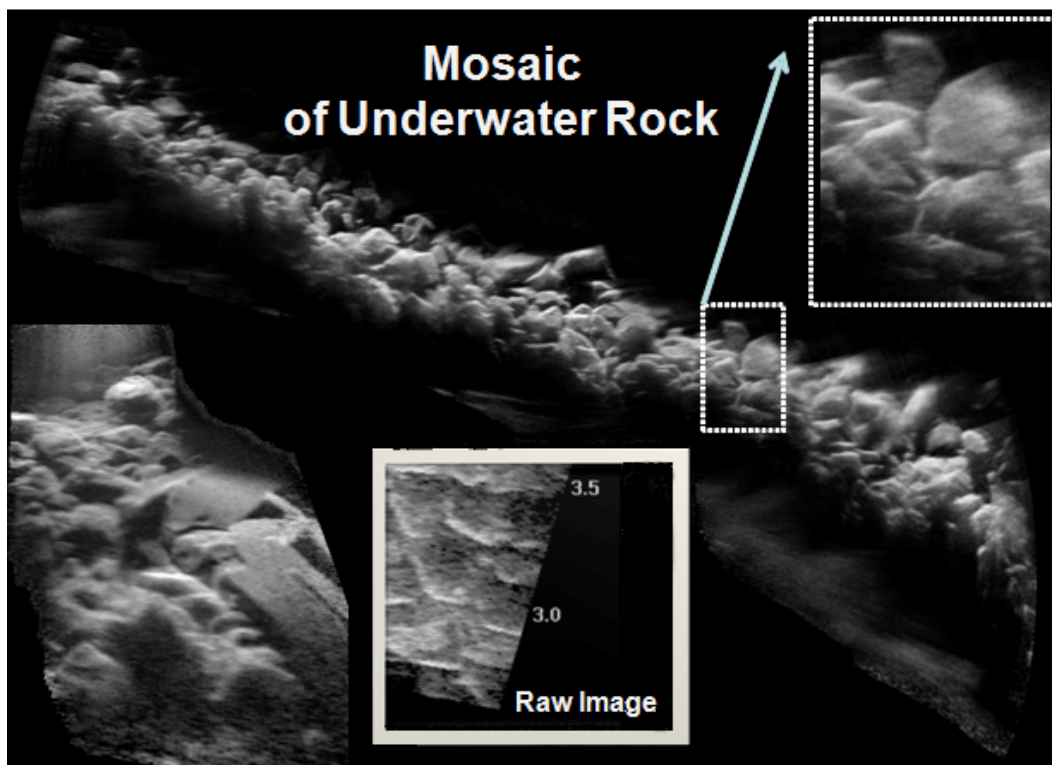


Figure 4-13. Underwater riprap section mosaic created from acoustical camera frames.

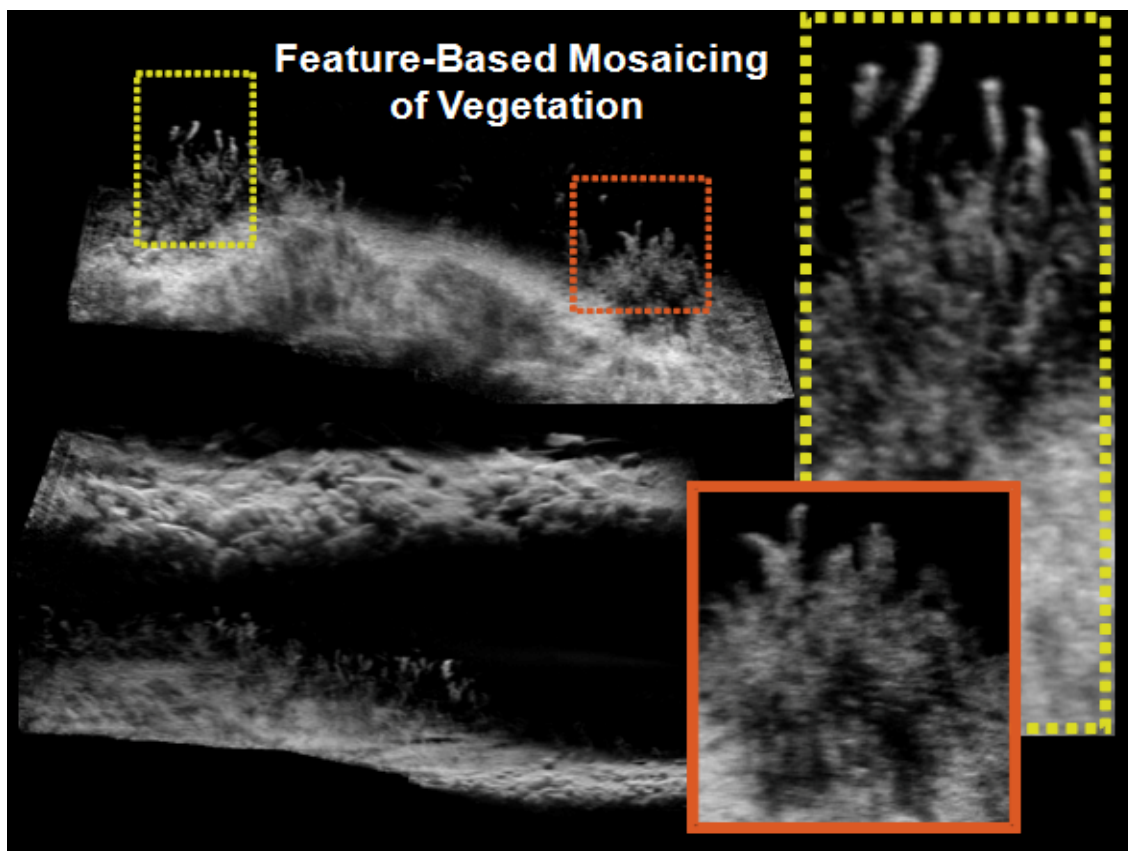


Figure 4-14. Vegetation mosaic created from acoustical camera images.

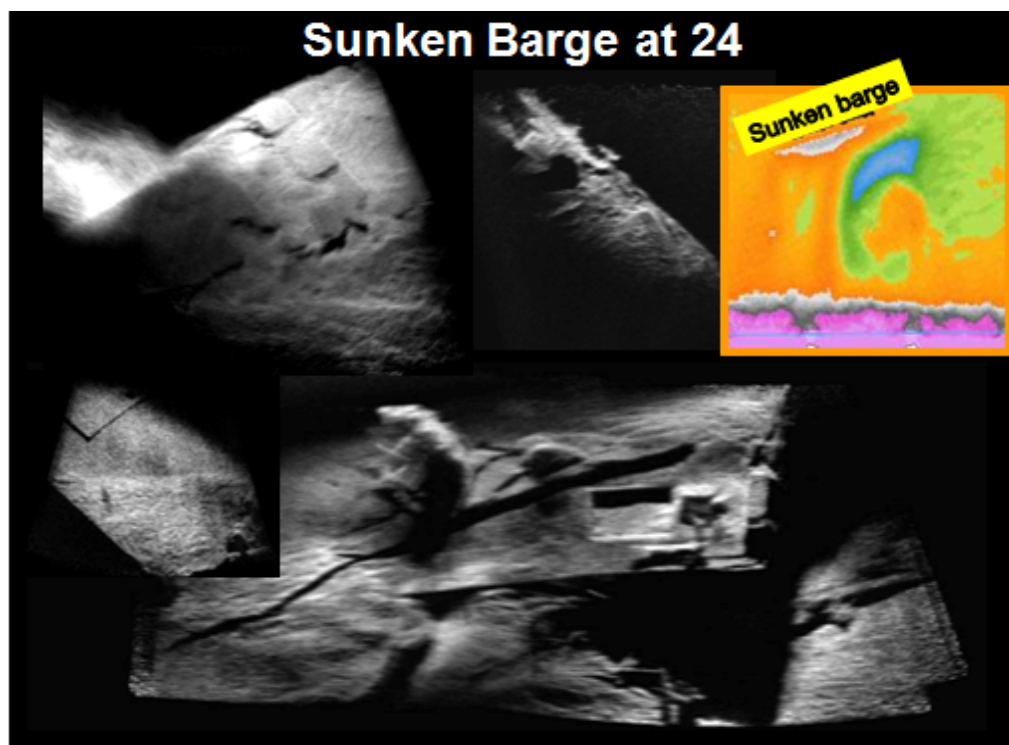


Figure 4-15. Sunken barge visible in river bottom silt.

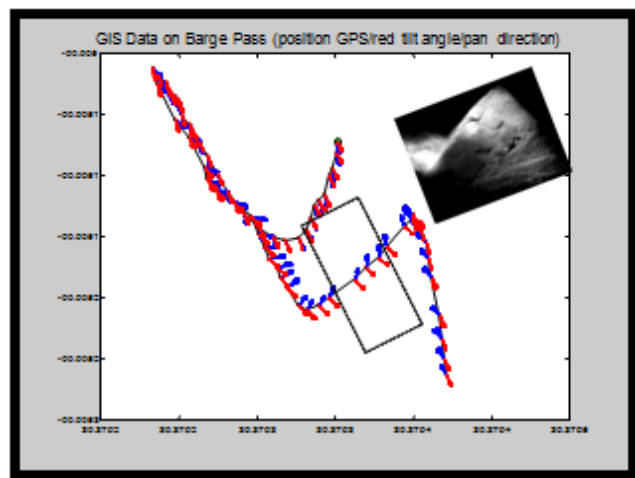


Figure 4-16. Graph of the camera track in acquiring acoustic camera images of sunken barge.

Figure 4-17 and the next several figures show upstream scour at several dams. The acoustic camera was diver deployed with topside engineers instructing the divers. Figure 4-17 shows scour-exposed timbers and sheet piles. Those images illustrate that changing the orientation of the camera highlights different features of the structure. The horizontal mode, in which the fan beams are parallel to the ground, is useful when inspecting the concrete bottom surface and timber cross section at various elevations. Irregular roundness of the piles indicates likely damage of the insonified surface. Notice that the vertical mode translates a perspective from which the objects are viewed by 90° . By scanning in these two modes, a comprehensive image of the object condition is possible.

Figure 4-18 presents more steel and timber exposed in upstream scour. These objects were imaged in areas not accessible by conventional side-scan or multi-beam deployments.

Figure 4-19 shows a profile and surface view of various sheet pilings. Figure 4-20 contains images of similar structures. Interfaces between the concrete, steel, and ground are interpreted clearly. Note, though, that deployment into holes, caverns, and conduits can be complicated by ghosting, meaning reflections come back simultaneously from the ground and ceiling, sides, etc.

The image in Figure 4-21 shows scour starting between the riverbed and the concrete structure.

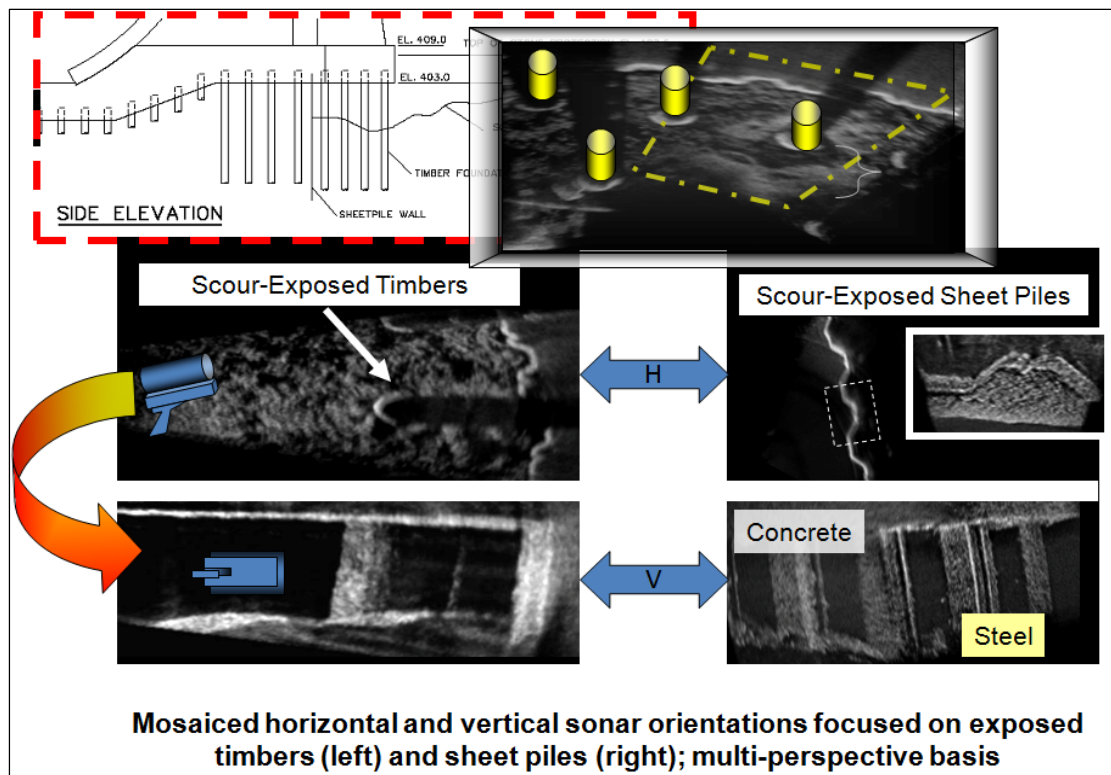


Figure 4-17. Acoustic camera mosaics of scour areas.

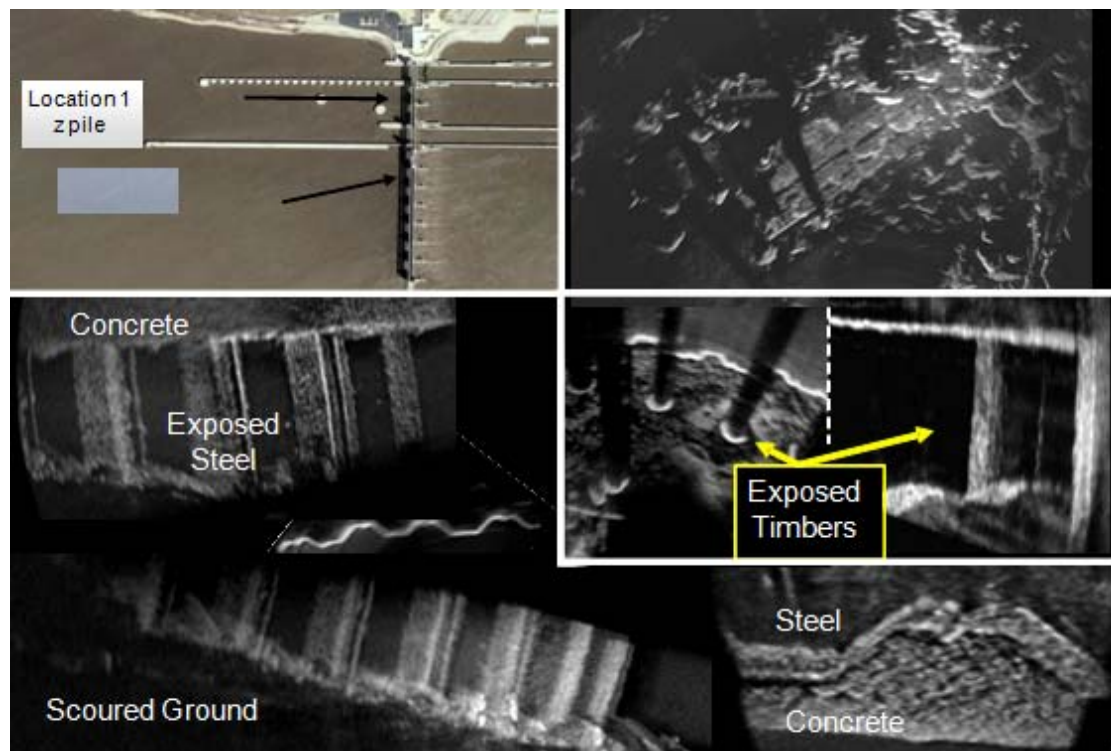


Figure 4-18. Additional upstream structural elements exposed by scour.

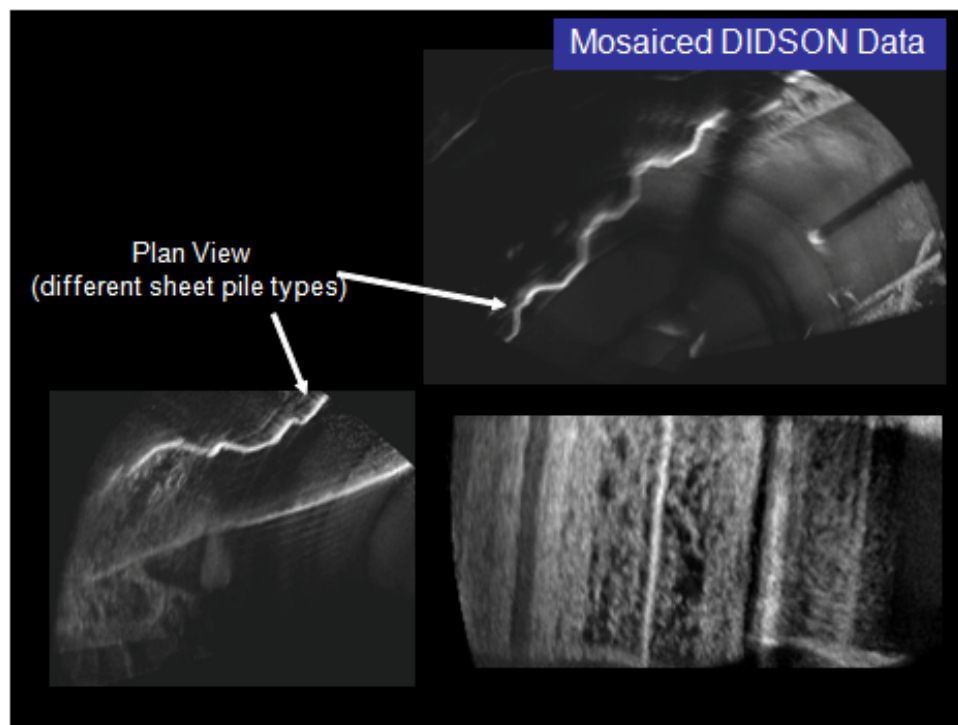


Figure 4-19. Profile and surface views of differing types of sheet piles.

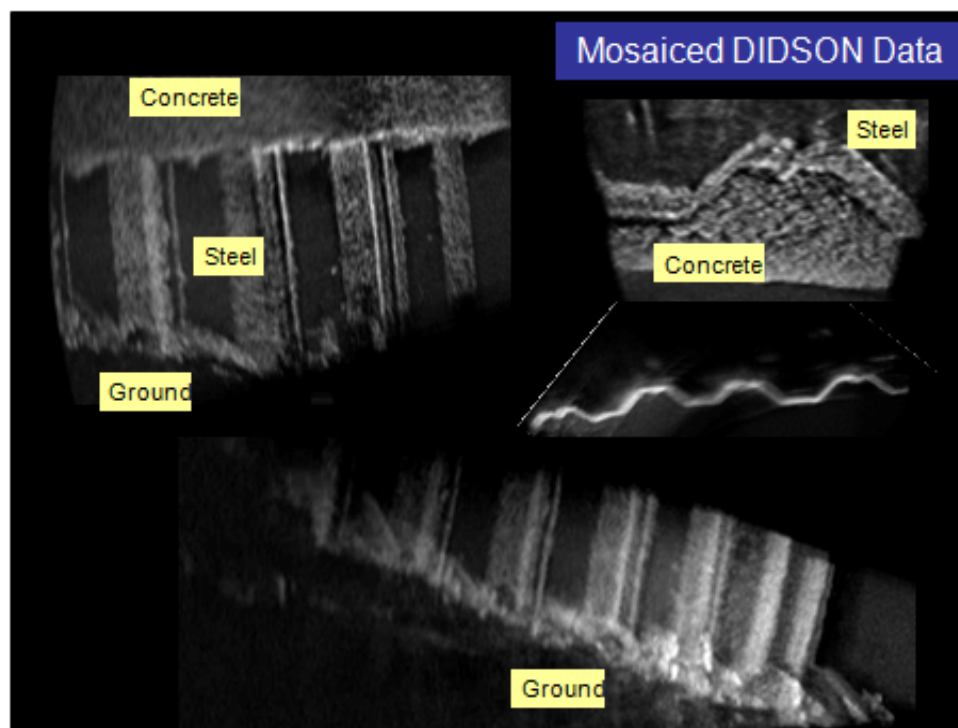


Figure 4-20. Acoustical camera images of the interfaces of structural components.

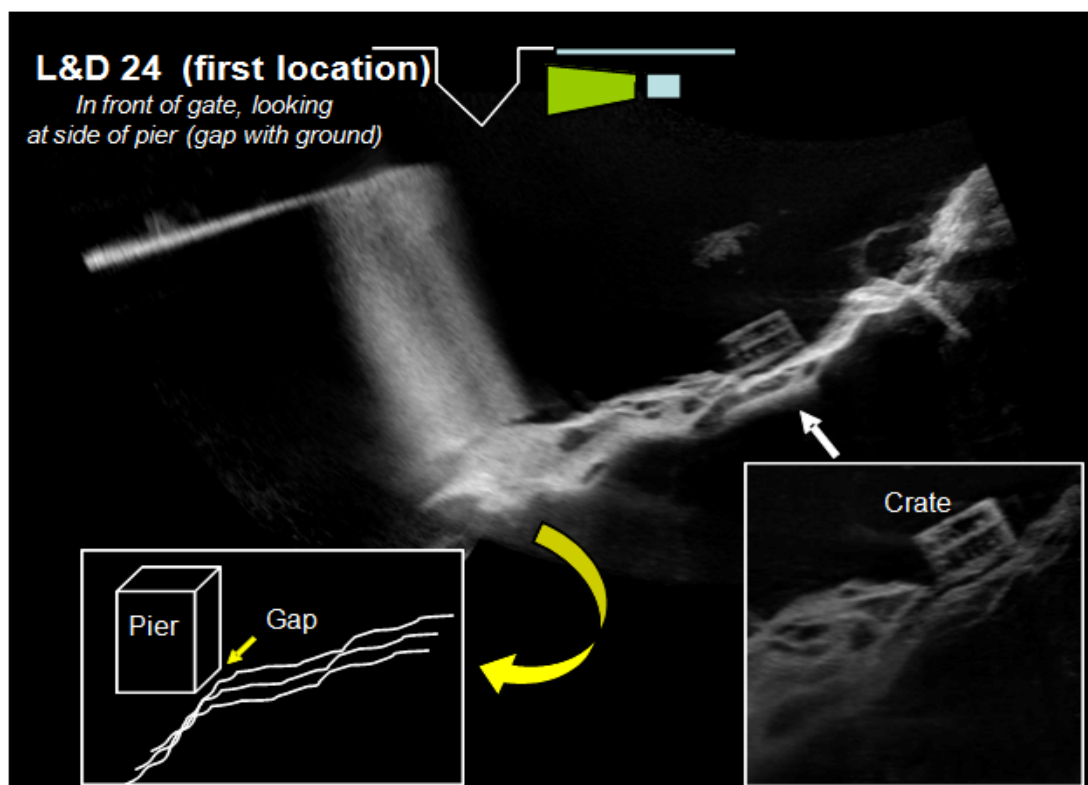


Figure 4-21. Mosaic of a scour hole at the intersection of a lock or dam wall and the river bottom.

Organic debris was detected in some of the upstream scour sections. An example is shown in Figure 4-22.

Scanning within the scour volume allowed pile sections to be independently scanned where acoustic shadowing allowed. This mode provides the best detail when characterizing damage, while the vertical mode provides better dimensions and quantifying of the shape.

Looking upstream in the large mosaic in Figure 4-24, the large rock was clearly still present in the bottom of the roughly 20-ft-deep scour hole.

Looking downstream in the image in Figure 4-25, the inset shows the scour patterns in the fines near the sheet pile.

The timber can be inspected, with position variation used to minimize shadows (Figure 4-26).

The images in Figure 4-27 were produced using older mosaic technology, and the results today could be improved significantly. They are shown because they are images of steel navigation structures. The outside of the lock gate is shown in the figure.

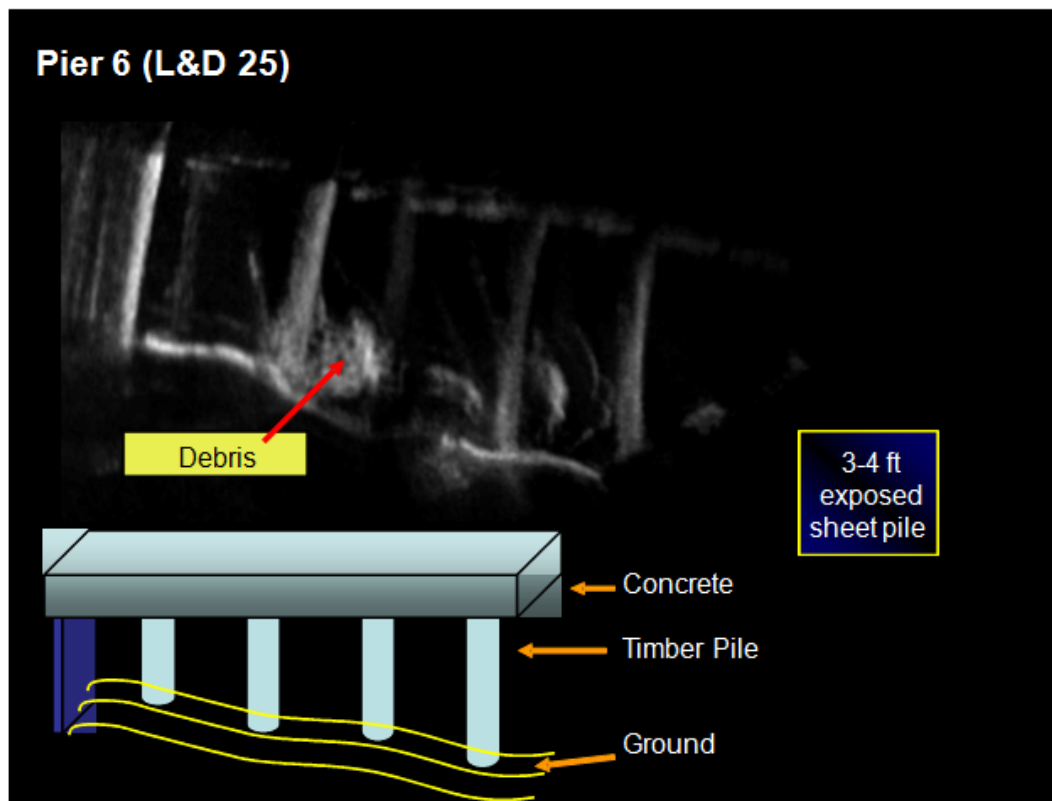


Figure 4-22. Image of organic material in a scour area.

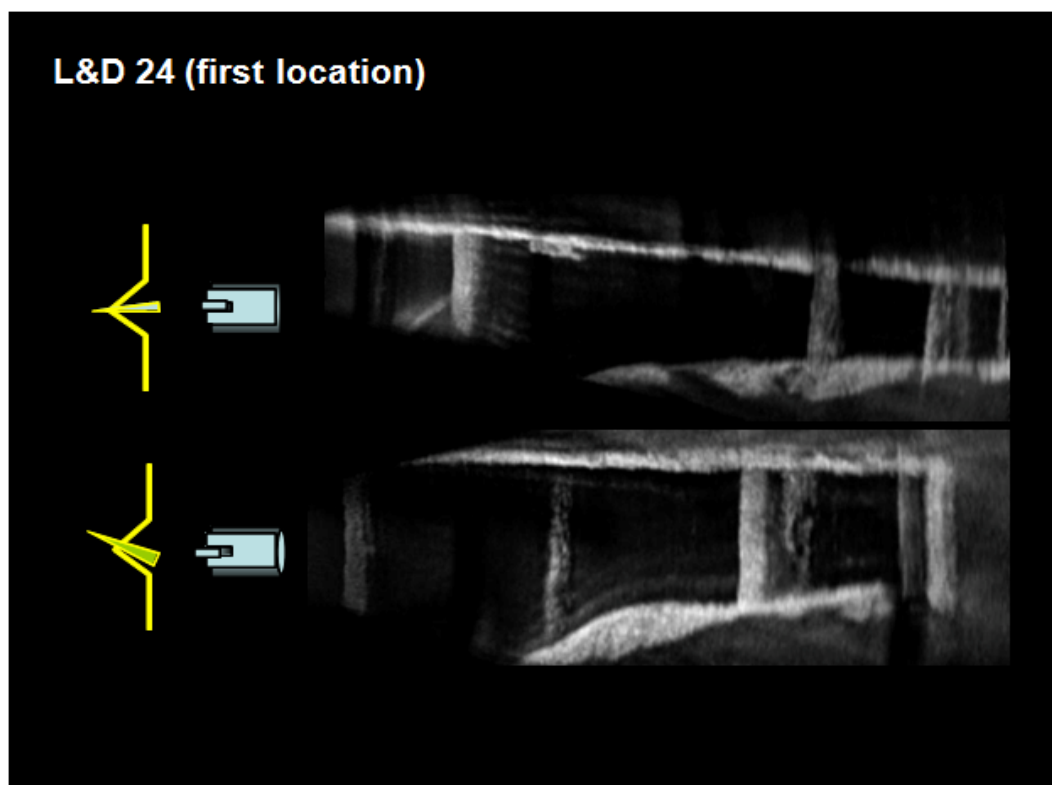


Figure 4-23. Exposed pilings in a scour area under a structural component.

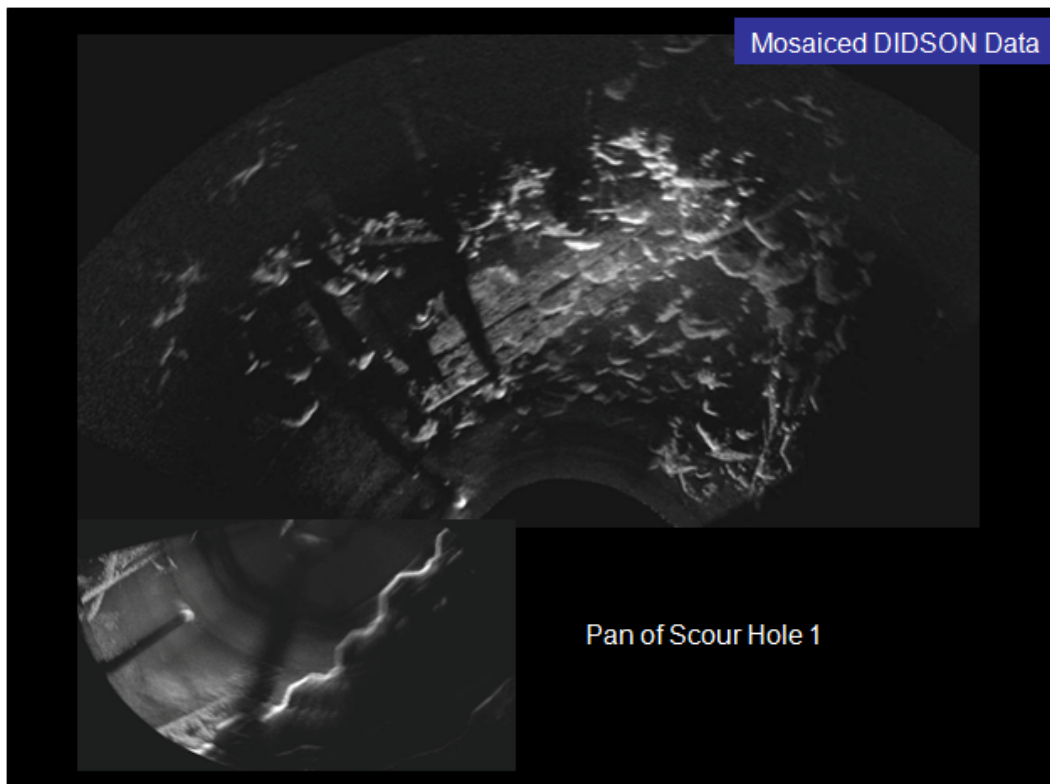


Figure 4-24. Scour hole mosaic.

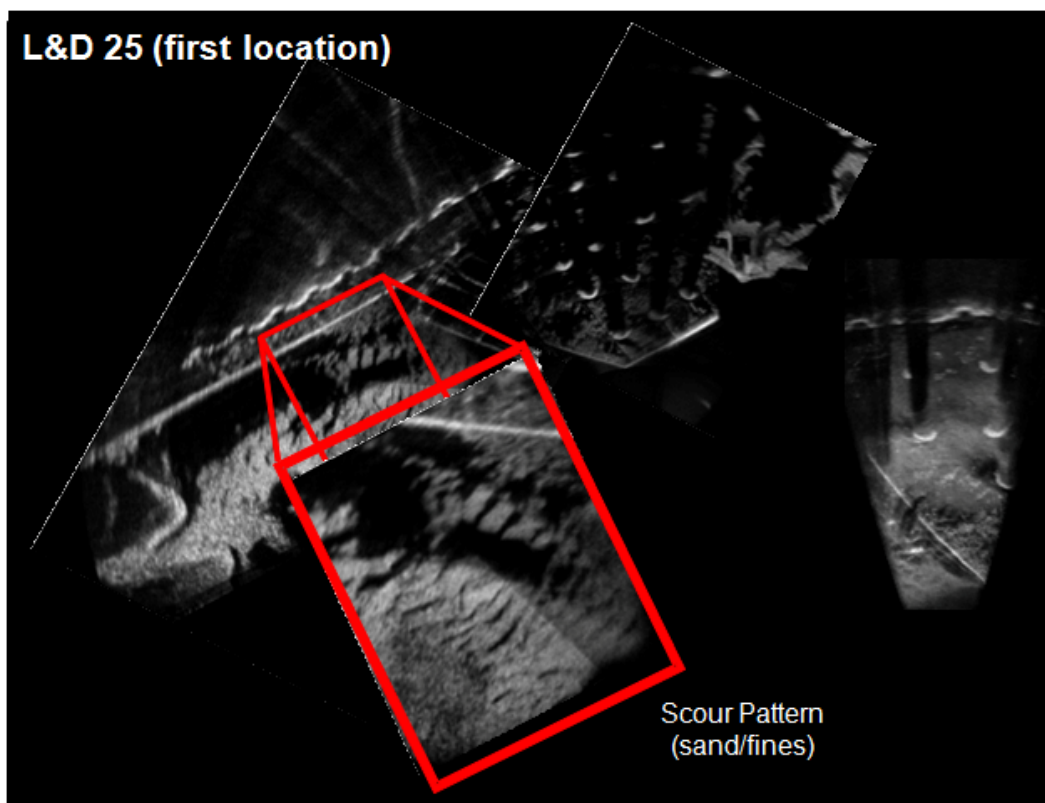


Figure 4-25. Mosaic image of scour patterns.

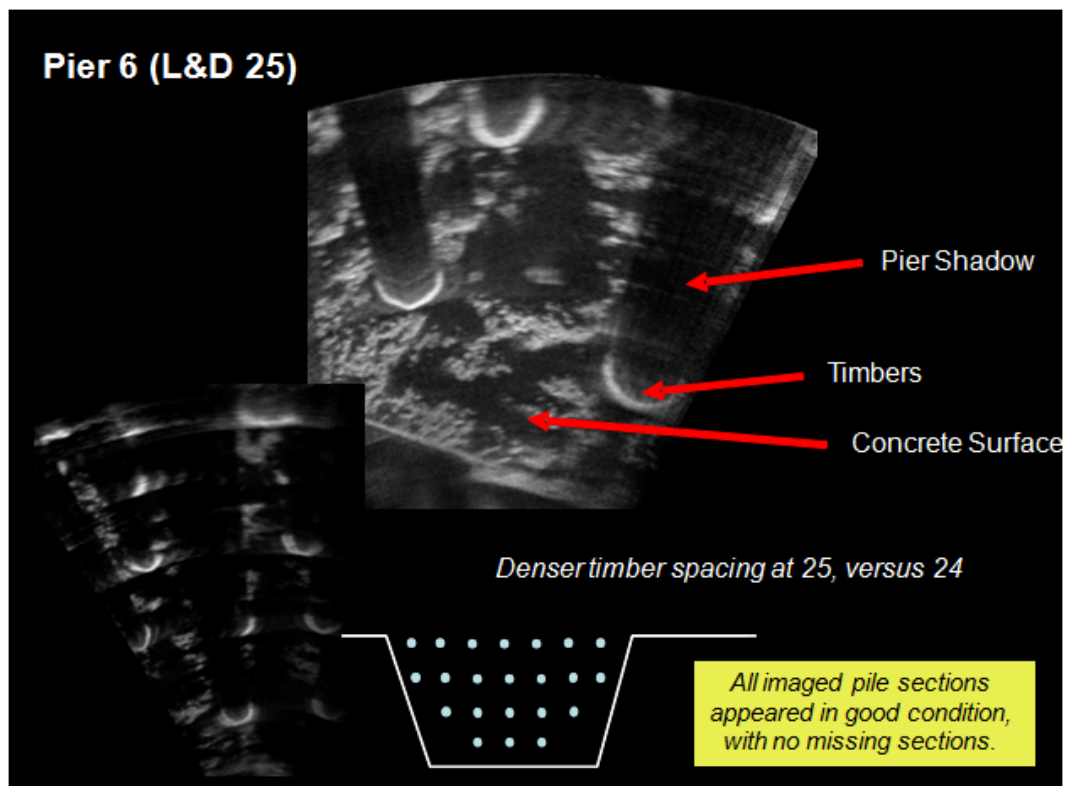


Figure 4-26. Mosaic image of timber piles.

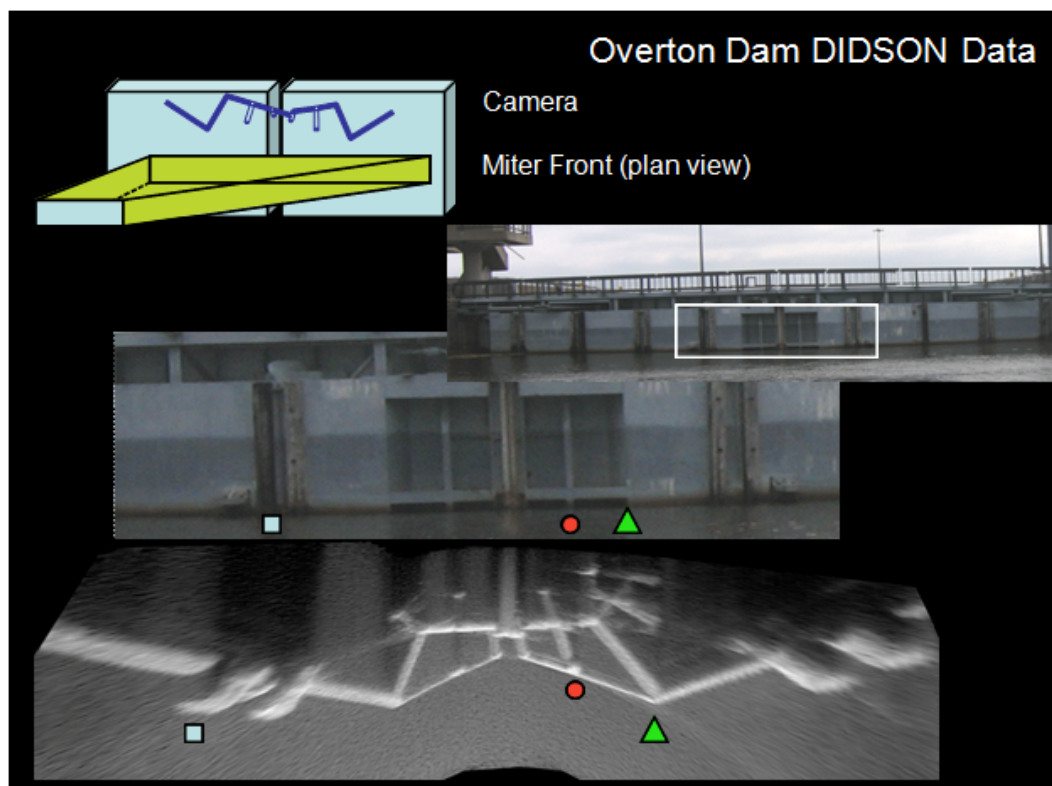


Figure 4-27. Upstream face of a miter gate.

The inside of the same miter gate is shown in Figure 4-28. The images below show the gate structure scanned at various incidence angles. Depending on angle of sound beam incidence with the gate structure, the shallow, the deep, or a combination of the two can be obtained. The inset shows the hinge or pentel section.

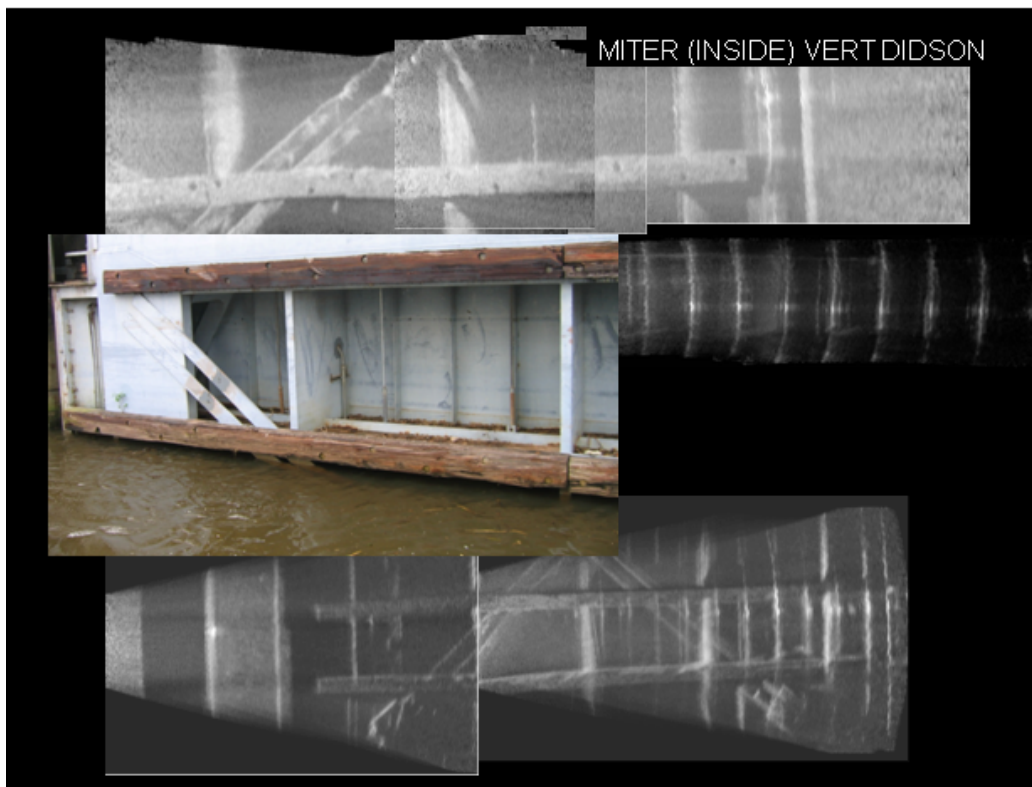


Figure 4-28. Downstream side of the miter gate.

Lock chamber objects are captured in the mosaiced images in Figure 4-29.

One inspection request was to image the object in Figure 4-30, which was a chamber retrofit to relieve lifting of the chamber floor.

Figure 4-31 shows the front of a tainter gate and its passive cathodic protection components.

Images of the space under an elevated (flexible) lock wall indicated trapped debris. Figure 4-32 shows the orientation and location of the acoustic camera during the image acquisition. Figure 4-33 illustrates that the debris tended to be trapped near the lower (on the riverbed), not the upper, elevations. The representative image in Figure 4-34 shows interlocking of the debris with itself and the support timbers.

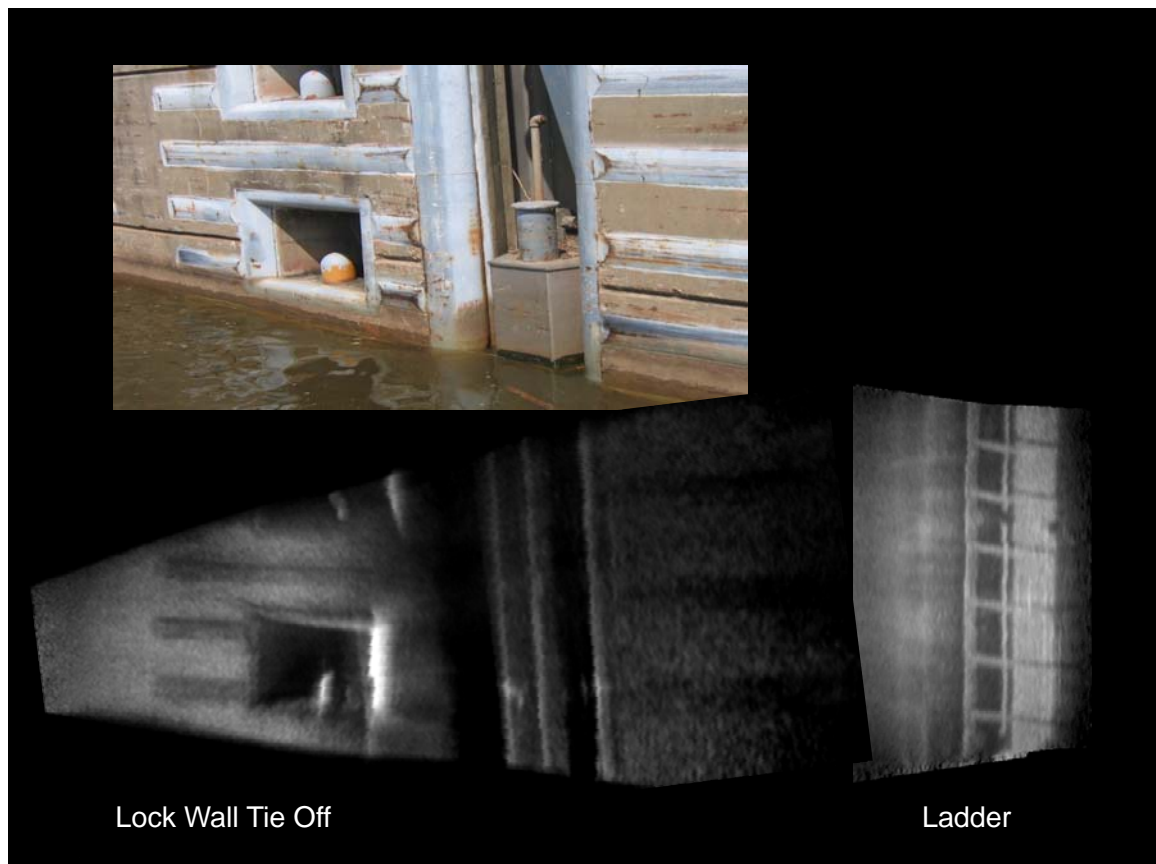


Figure 4-29. Acoustic camera mosaics of underwater lock components and a corresponding visible image.

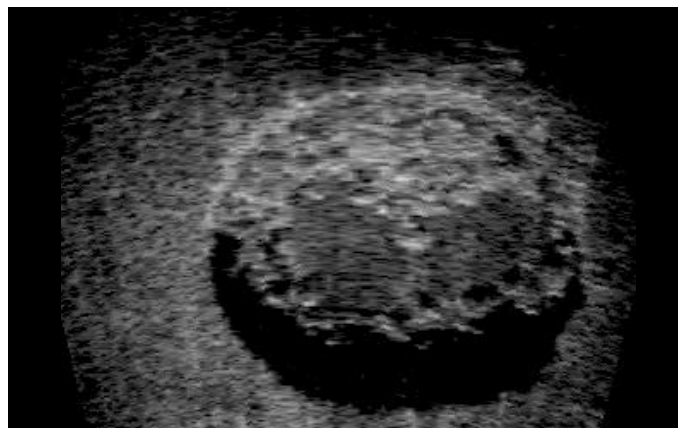


Figure 4-30. Lock chamber retrofit of a vent.

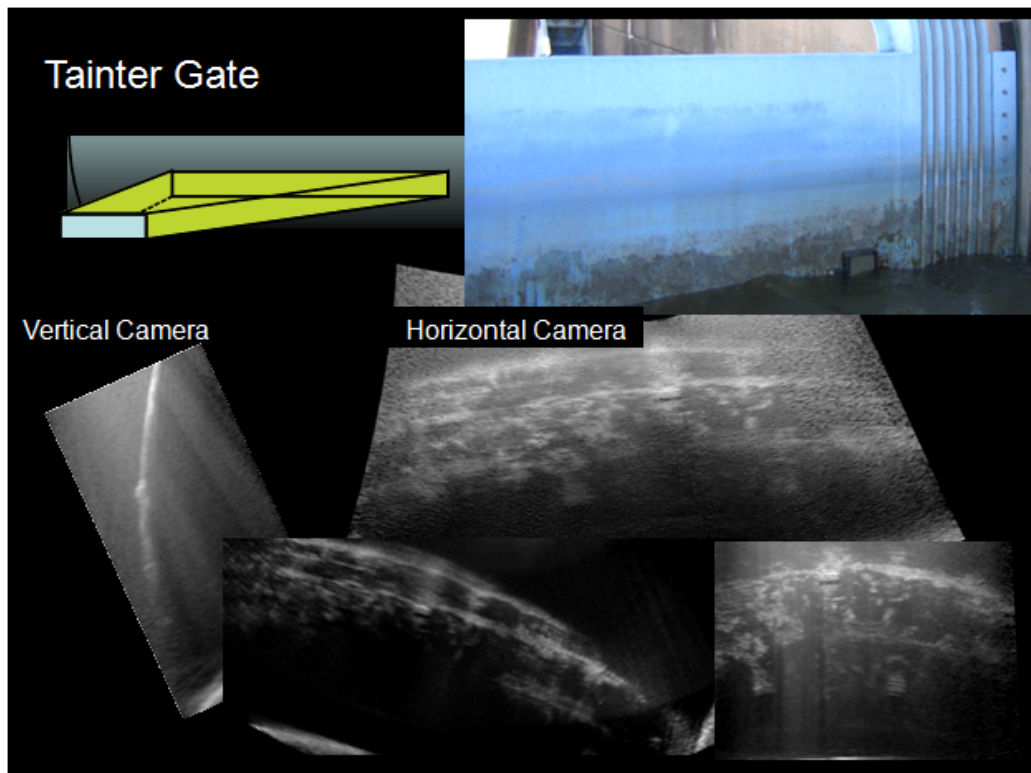


Figure 4-31. Acoustical images of a tainter gate.

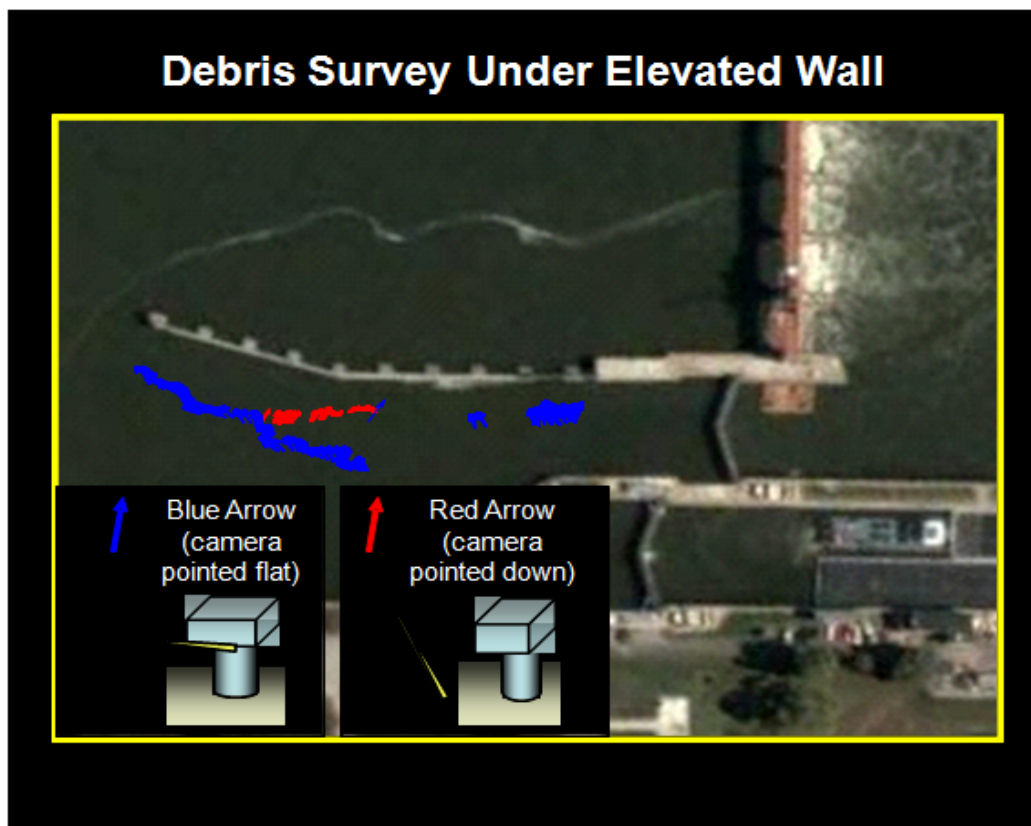


Figure 4-32. Acoustic camera image acquisition information.

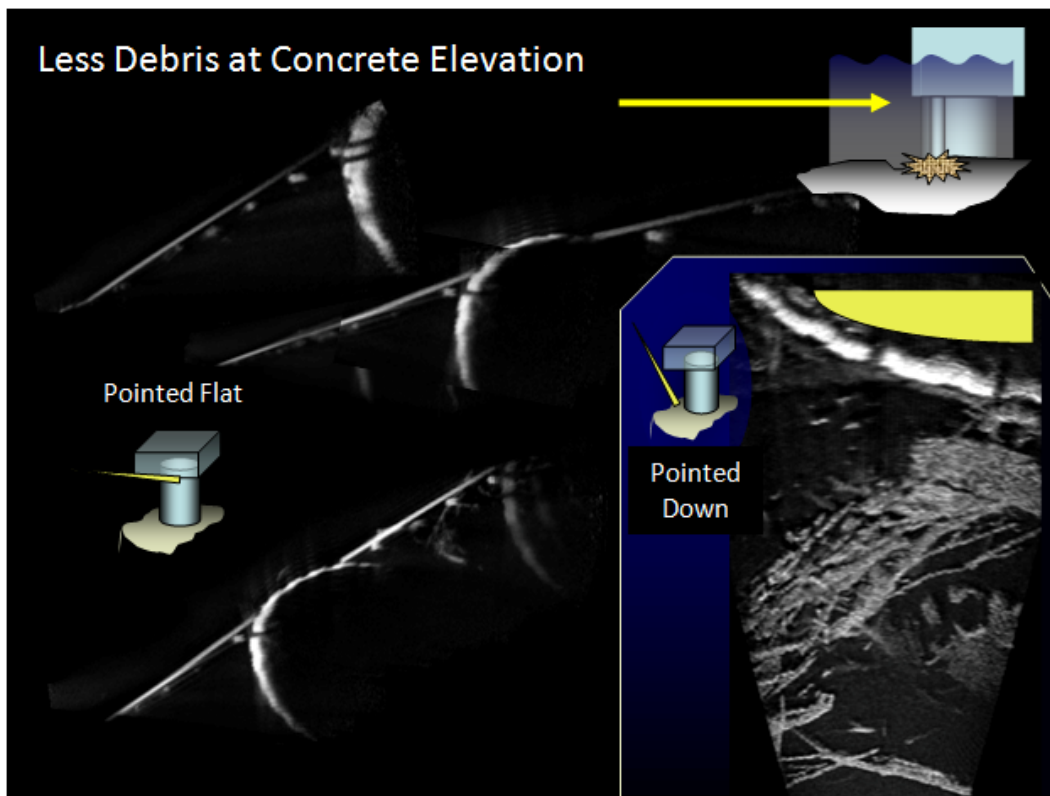


Figure 4-33. Images that indicate the location of debris.

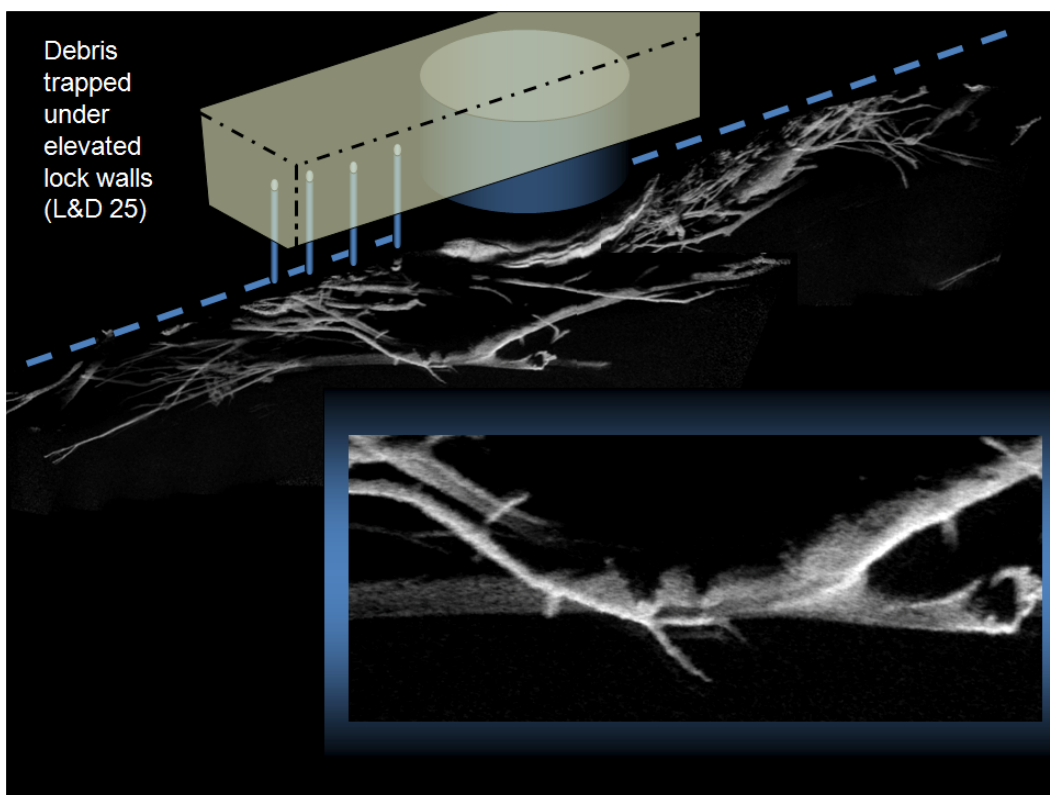


Figure 4-34. Images showing intertwined debris and lock wall pilings.

Figure 4-35 shows a steel service gate that was experiencing binding issues in a narrow concrete guide.

Figure 4-36 shows a number of views of the gate, the gate channel, and concrete at the Delaware Dam. A few concrete pop outs or spalls were detected, and those were on the outside of the guide surface. Boat deployment was employed, while overhead cranes lowered and raised the gate. Video showed gate motion within the track and track condition during translation.

Figure 4-37 shows normal beam incidence (i.e., not a glancing blow). Track groove and concrete surface conditions were verified for sections of the structure.

A unique deployment was undertaken in scanning partially submerged conduits of varying lengths, cross sections, and diameters. The 3- to 4-ft-diameter tubes were the most challenging, partly due to the more acute grazing surface and multipath reflections downrange. The square culverts were extremely challenging because all four surfaces were acoustic mirrors. Angle and ranging were most critical in this setup. In hindsight, the cable guide system implemented required too much time to set up in each pipe. A push-rod with a self-centering pig would have hastened the deployment time drastically. On the plus side, the two-cable system was extremely stable with smooth motion and precise setting of rotation angles. As the cables were moved toward the top airspace, sediment did not interfere with system motion.

ClearSight was used to mosaic the high-frame-count mosaics in Figure 4-39. The concrete walls, joints, and sediments were the main features. The bottom figure was taken with a man-carried camera, through the large-diameter (5-ft) culvert.

Figure 4-40 shows miscellaneous objects. Note that shadows, even those from moving fish, have been used to estimate surface depth or position (bottom right).



Figure 4-35. Steel service gate with binding issues.

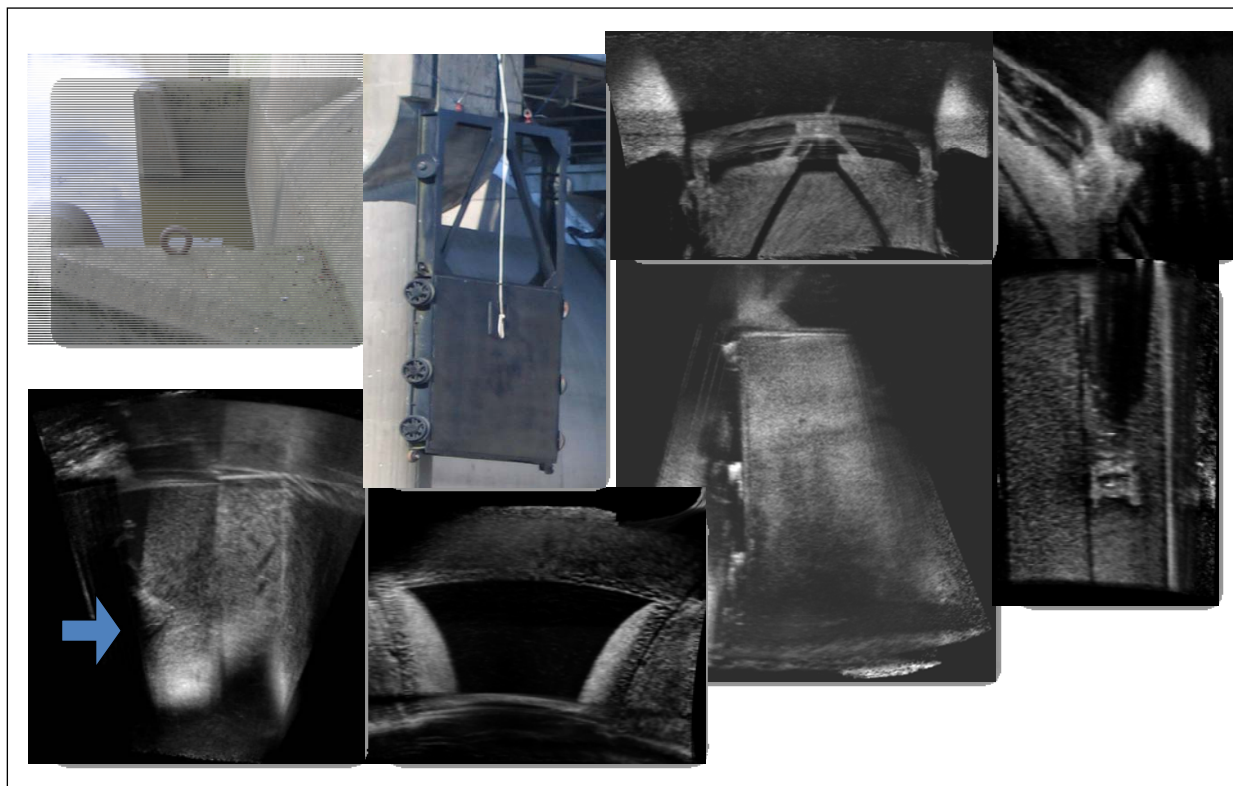


Figure 4-36. Acoustical images of service gate and guideway at Delaware Lake.

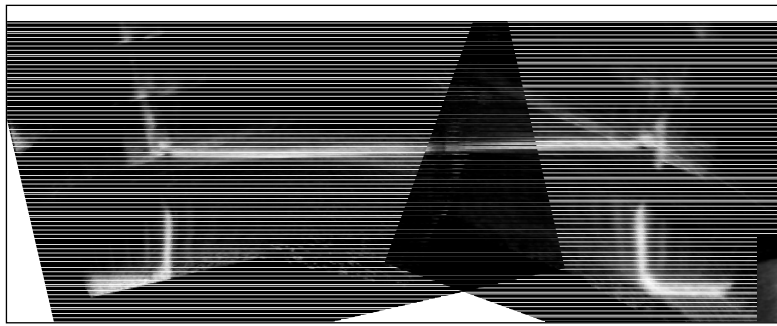


Figure 4-37. Image of track groove and surrounding concrete taken with acoustic camera pointed normal to the surfaces.

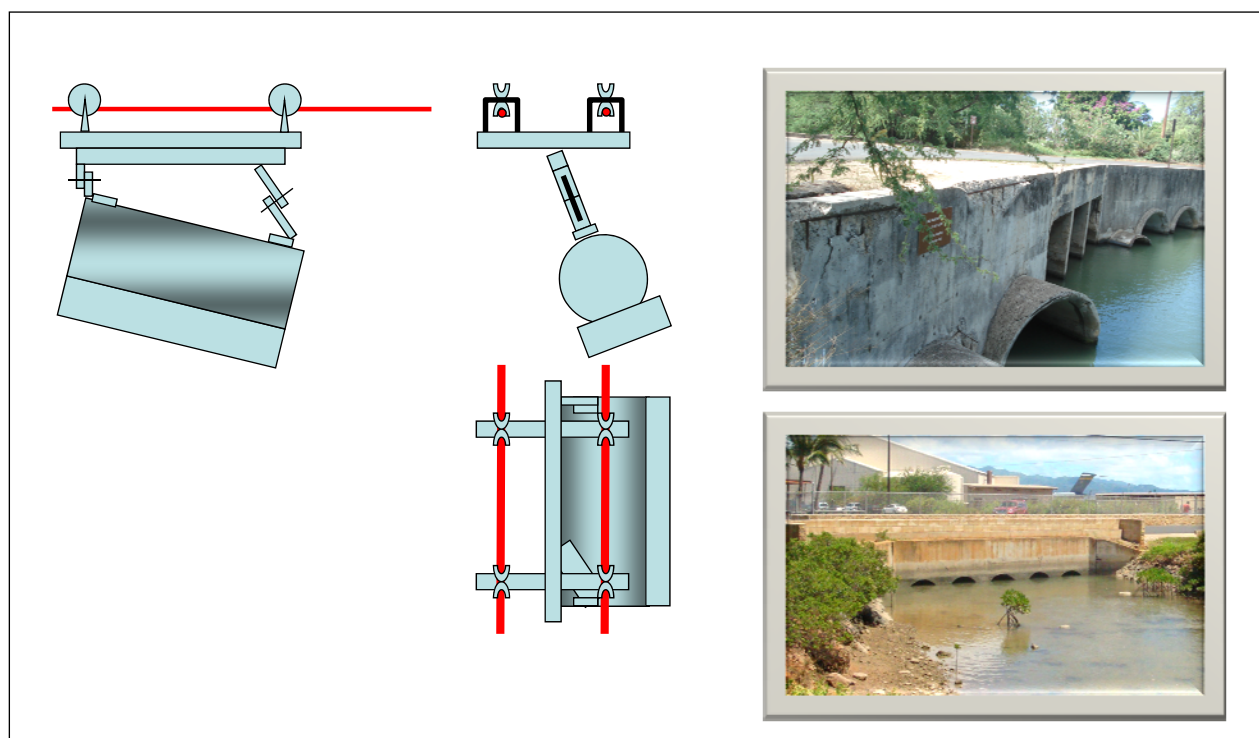


Figure 4-38. Deployment mechanism for conduit inspections.

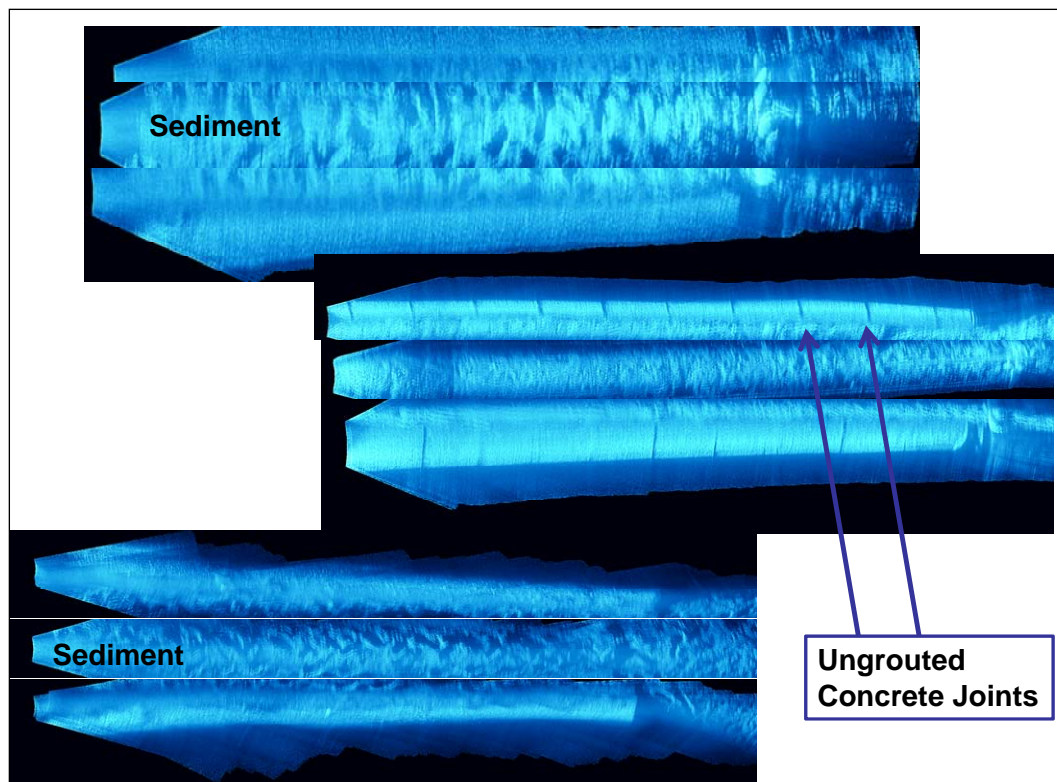


Figure 4-39. Mosaics from acoustic camera culvert scans.

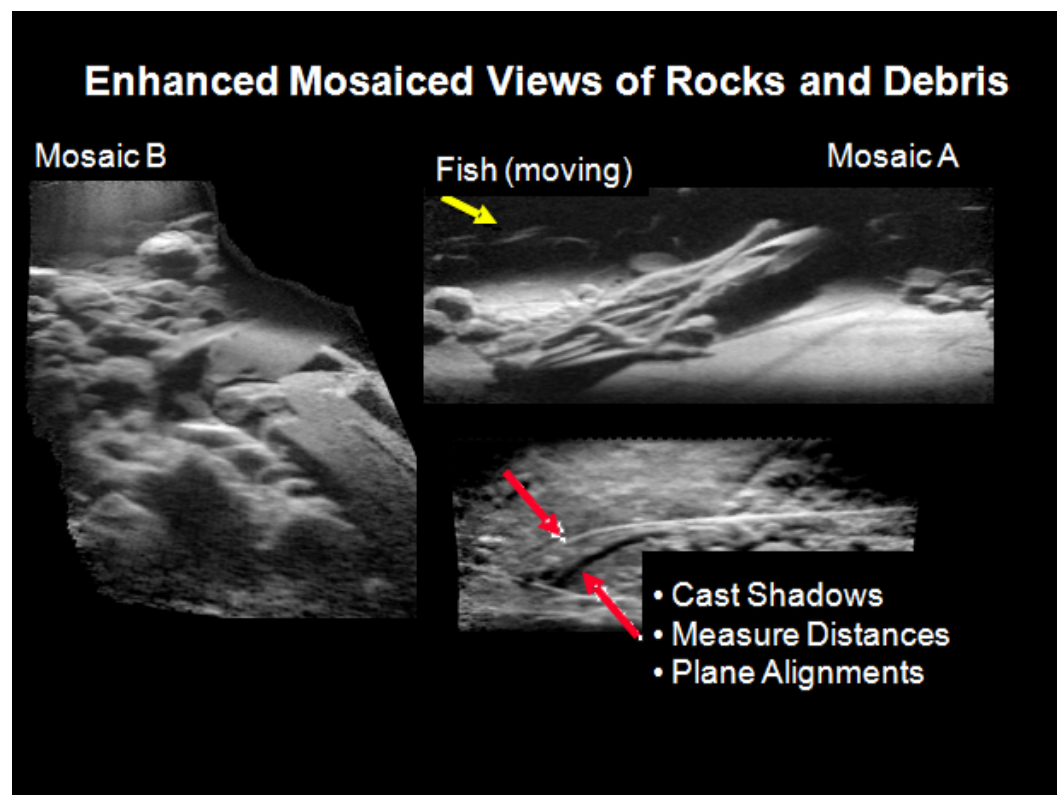


Figure 4-40. Miscellaneous objects encountered during scans.

5 Guidelines for Acoustic Camera Inspections

To conduct a successful acoustic camera inspection:

1. Decide the best means of deploying the acoustic camera (boat-mounted pole, diver, etc.)
2. Determine the best camera orientation (vertical or horizontal). For vertical faces, orient the camera so the sensor array is vertical. Use horizontal orientation for horizontal faces.
3. For imaging scans, align the camera with an incidence angle of approximately 20° . For surface mapping, align the camera with an angle of 90° to the surface.
4. Slowly move the camera (fewer than 2 fps) along the surface using the DIDSON software to record the image data. Or start panning the camera with a slow angular speed while recording the images.
5. After the scanning has been performed, review recorded data to determine the frames to use to create mosaic images.
6. Use the DDF Parser software to create data files ready for input to mosaic software.
7. For best mosaic results, use ClearSight software for scans performed in the push-broom method. SIFT algorithm software works best for images obtained with a fixed-reference panning method.
8. To generate a surface plot, use EdgeDetect software to generate an *xyz* coordinate file from the selected frames in the DIDSON files. Load the coordinate file into a 3D plotting software package (commercial packages are available).

6 Conclusions

Acoustic cameras can create, using high-frequency sound waves, images of underwater environments, providing clarity in turbid water. They are useful for inspecting features of underwater structures, and software tools that enhance the clarity of those images and expand the field of view have been developed.

In this study, an acoustic camera was used to inspect and provide condition assessments for specific portions of navigation structures where abnormalities were suspected or had been detected by other means. The camera provided visual information and dimensions of scale so structural features and/or damage could be quantified. Particularly useful was its ability to inspect scour areas, as well as to perform general condition assessments.

This study found the sharpest details are obtained at close ranges (4 to 20 ft) because the camera can be operated at higher frequencies. Also, the beam spread for each element increases as a function of distance from the camera. For broader views of an area, lower frequency operation is useful to approximately 100 ft.

Deployment issues must be considered when planning for an inspection because camera position and orientation are critical to success. Operating the camera from the boat-based deployment platform proved versatile, and diver deployments provided successful results. Special circumstances called for creative camera positioning.

The researchers recommend that acoustic camera imaging be expanded to include surveying guidance so entire structures can be scanned systematically, generating an image of the total structure. Also, techniques could be developed to create 3D models of navigation structures from the data obtained.

References

- Belcher, E., H. Q. Dinh, D. C. Lynn, and T. J. Laughlin. 1999. Beamforming and imaging with acoustic lenses in small high-frequency sonars. In *Proceedings, Oceans '99, Riding the Crest into the 21st Century, MTS/IEEE Conference, 13-16 September, Seattle, WA*.
- Belcher, E., W. Hanot, and J. Burch. 2002. Dual Frequency Identification Sonar (DIDSON). In *Proceedings, International Symposium of Underwater Technology, 19 April, Tokyo, Japan*.
- Kim, K., N. Neretti, and N. Intrator. 2004. Acoustic camera image mosaicing and super-resolution. In *Proceedings, Oceans '04, MTS/IEEE Conference, 9-12 November, Kobe, Japan*.
- Sound Metrics Corp. 2005. Dual Frequency Identification Sonar (DIDSON) operations manual, V4.51.02.

Appendix A: AcousticView User Guide, ClearSight Software

(Included with written permission of AcousticView software)

System requirements

Hardware requirements

- Q9550 (2.83GHz Core 2 Quad-Core x86) or newer
- 2GB RAM
- 120GB disc space

Operating system requirements

- Windows XP, Vista, Windows 7, 32/64 bit

Java requirements

- Sun Java JDK, Version 1.6, Update 16 or newer, for installation

Limitations and tips for proper scanning

- Best results are achieved when scanning in straight lines and at a fixed speed.
- The DIDSON should be tilted relative to the scanned objects, in accordance with Sound Metrics scanning guidelines.
- The algorithm does not support mosaicing of zigzag sequences. To do so, the file should be split into ranges that scan in a single direction.
- When the camera does not move at all with respect to the target, no resolution improvement can be achieved.
- Mosaicing of flat surfaces without any anchor points might fail.
- Mosaicing of fast scans might fail due to the large difference between consecutive frames. Optimal scanning speed should leave 60 to 70% of the picture in consecutive frames.

Installation instructions

To install ClearSight:

Currently, the installation directory should be C:\acousticview. Any attempt to install in another directory results in an error. This will be corrected in the next version.

1. Close all open windows.
2. Insert the AcousticView USB Flash Memory.
3. Change directory to AView_USB\ClearSightDIDSON_Installation on the USB Flash Memory.
4. Click on ClearSightSetup.exe.
5. Windows Vista users will be asked to OK the installation.
6. Read the Software License Agreement.
7. If you accept the terms, press accept.
8. The software should be installed in directory C:\acousticview.
9. OK the rest of the installation.
10. A shortcut icon will appear on the desktop, enabling access to the ClearSight software.
11. When installation is finished, click on the jre-6u16-windows-i586-s.exe; this will install a Java runtime environment.
12. When both installations are done, please insert the dongle provided with the software. If you do not have one, contact the company to purchase one.
13. Wait until installation of the dongle is done. It takes a few minutes.
14. When the red light of the dongle is on, the dongle has been installed and you are ready to start the software.
15. Keeping the dongle connected at all times, click on the AcousticView shortcut to start the program.
16. Click on the first button (directories and files) to choose a directory where the DIDSON files exist.
17. A list of available files will appear; choose the file you want to mosaic by clicking on it.
18. Click on the rounded arrow (second button) to choose the frames from which mosaic should be created.
19. A small monitor window will present processing progress.
20. When mosaic is read, it will appear on the left files list under the file that was chosen.
21. Double click on the subpart that contains the processed mosaic frames you want to view.
22. You then can increase or reduce resolution by clicking on the + or – buttons, then clicking on the picture itself.
23. You also can move the image on the screen and measure distances.

24. Please provide comments to info@acousticview.com.
25. Should you encounter a problem, provide information about software version and the full details of the problem to info@acousticview.com.

Before you run the program, make sure to insert in a USB slot the dongle. It should stay in the USB slot while you run the software.

Using ClearSight

Main window

To get started, double click on the ClearSight icon that was created during installation. The main application window is shown in Figure A-1. It is organized in two panes: Project and Viewer.

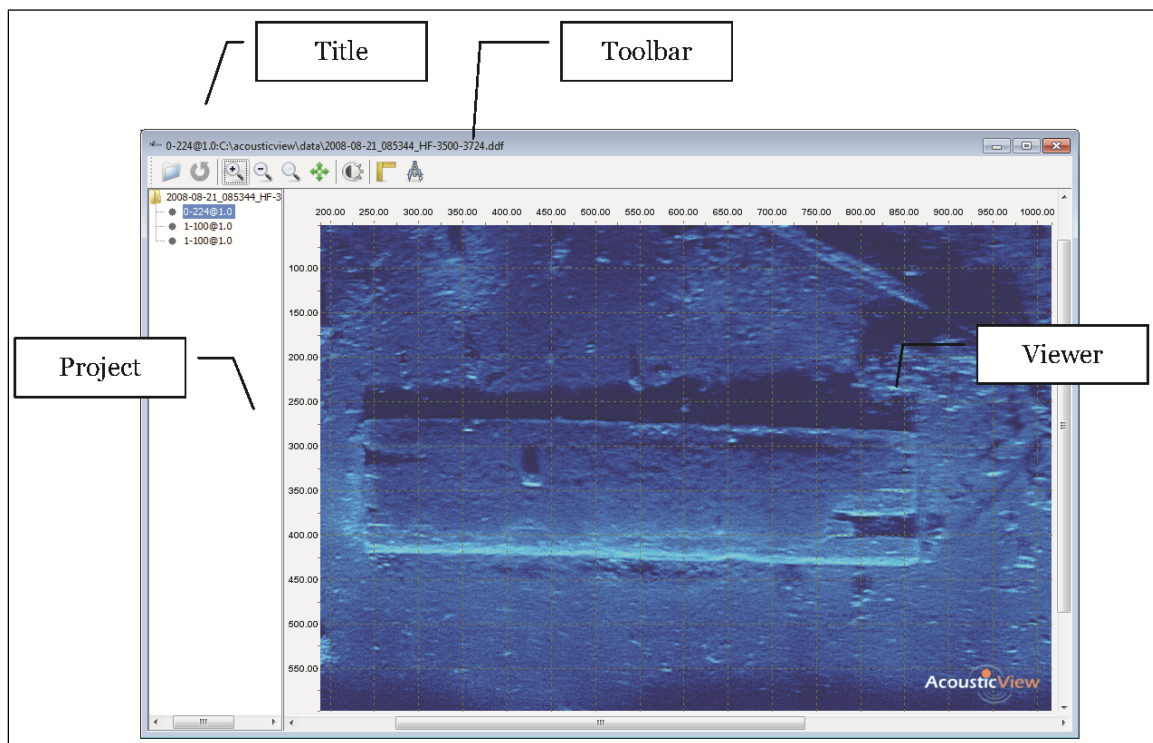


Figure A-1. ClearSight console.

Project pane

To view a mosaic already created, click on one of the mosaic elements in the Project pane on the left. This might take a few seconds.

Each of the elements in the Project management pane is described below.

As show in Figure A-2, two types of Project pane objects are available:

- **Sonar Scan:** represents a single sonar movie scan file. The name of the scan is shown next to the icon.
- **Mosaic:** represents a single mosaic with a range a frames from the sonar file which appears above. The name of the mosaic shown next to the icon contains the range of frames and resolution (from-to@resolution).

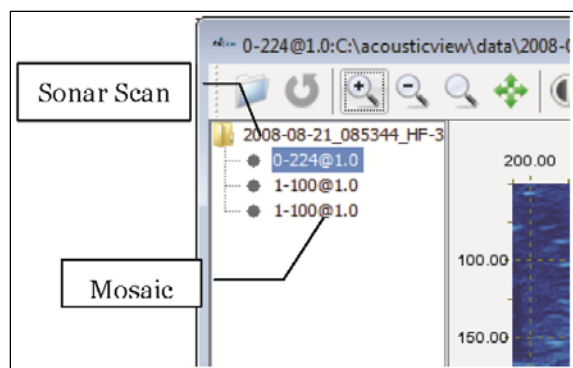


Figure A-2. Project pane objects.

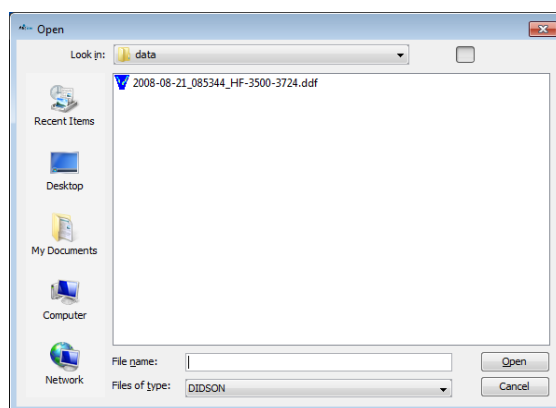
Adding a new Sonar Scan

To add a new Sonar Scan, press

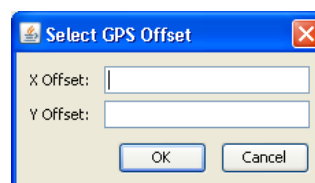


Pressing the button will open a file browser dialog box (see figure at right). Browse to the location of the Sonar Scan and press Open. A new Sonar Scan will be added to the Project pane.

Another option for adding new Sonar Scan is by clicking on Right Mouse when in Project pane. After clicking on Right Mouse in Project pane, a pop-up menu appears that allows adding a Sonar Scan.



After the new Sonar Scan is added to the Project pane, a dialog box (see figure at right) pops up. This dialog box allows adding GPS offset from the pole. The values should be entered in meters.



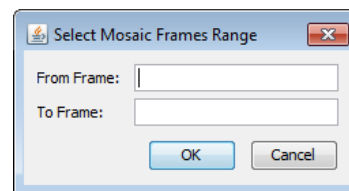
Removing a Sonar Scan

To remove Sonar Scan from the project, click on Right Mouse after selecting Sonar Scan in the Project pane. After clicking on the Right Mouse, a pop-up menu appears that allows removing Sonar Scan from the project. When removing Sonar Scan, only Project view is affected; the file remains in the file system.

Creating a new Mosaic

To create a new Mosaic, select the desired Sonar Scan and press .

Pressing the button will open a range selection dialog box (see figure at right). Select the frame range, and press OK. Make sure to choose and upper range that is smaller or equal to the number of frames in the file. In older versions, choosing a frame range that is outside the range of frames caused the program to freeze. After a range is chosen, a progress bar will appear on the screen. Wait until processing completion. A new Mosaic should appear under the chosen Sonar Scan. You need to click on that mosaic to see it in the Viewer pane.



Viewing a Mosaic

To view a Mosaic, double click on the desired Mosaic in Project pane. The chosen Mosaic will be opened in the Viewer pane.

Removing a Mosaic

To remove a Mosaic from the project, click on Right Mouse after selecting Mosaic in the Project pane. After clicking on the Right Mouse, a pop-up menu appears that allows removing Mosaic from the project.

Removing all Mosaics from Sonar Scan

To remove all Mosaics created for sonar scan from the project, click on Right Mouse after selecting Sonar Scan in the Project pane. After clicking on the Right Mouse, a pop-up menu appears that allows removing mosaics created for Sonar Scan from the project.

Viewer pane

Clicking a Mosaic in the Project pane on the left reveals Mosaics in the Viewer pane on the right. When Mosaic is shown in the Viewer pane, the following tools are available (Figure A-3):

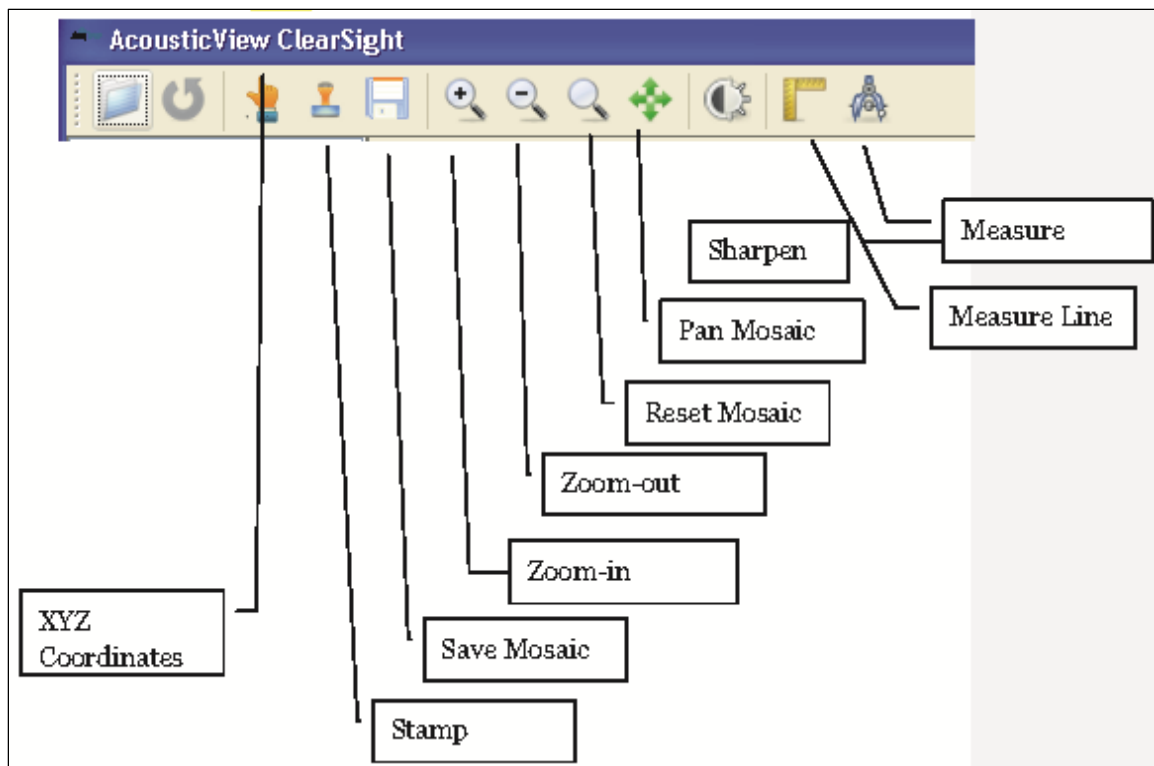


Figure A-3. Mosaic tools available in the Viewer pane.

File formats

Mosaic file

The Mosaic file is stored in a BMP file, also known as Bitmap Image File. BMP image file format is used to store bitmap digital images. Complete description of the file format can be found at http://en.wikipedia.org/wiki/BMP_file_format.

GEO file

The GEO files are stored in a binary file that has three consecutive maps, each showing latitude, longitude, and depth.

The width and the height of each map are equal to the width and height of the Mosaic file. Each pixel in the map holds a float value.

Figure A-4 shows the binary file structure.

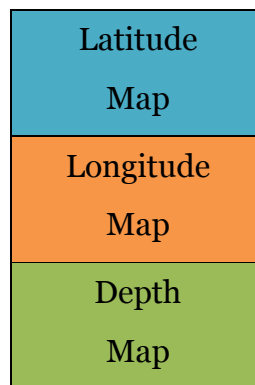


Figure A-4. Binary file structure.

Transformation

The geometric model that transforms between coordinates measured by the GPS to the pixels on a single sonar image is shown in Figure A-5. In addition to values measured by the GPS, the transformation model considers the offset of the GPS from the pole and sonar tilt-and-pan coordinates. The results of the transformation model applied are used with the image registration process to produce a pseudo-3D model (also called 2½D) for each of the pixels of the mosaic.

The four steps of image registration are: feature detection, feature matching, transformation estimation, and image resampling and transformation. Feature detection is the process of finding objects such as corners, edges, and line intersections manually or automatically. The features from the sensed image are paired with the corresponding features in the reference image in the second step. In the third step, the transformation is estimated based on the displacement vector of each feature. Once the mapping is established, the multiple images are combined to generate a mosaic image in which each pixel is geo-referenced.

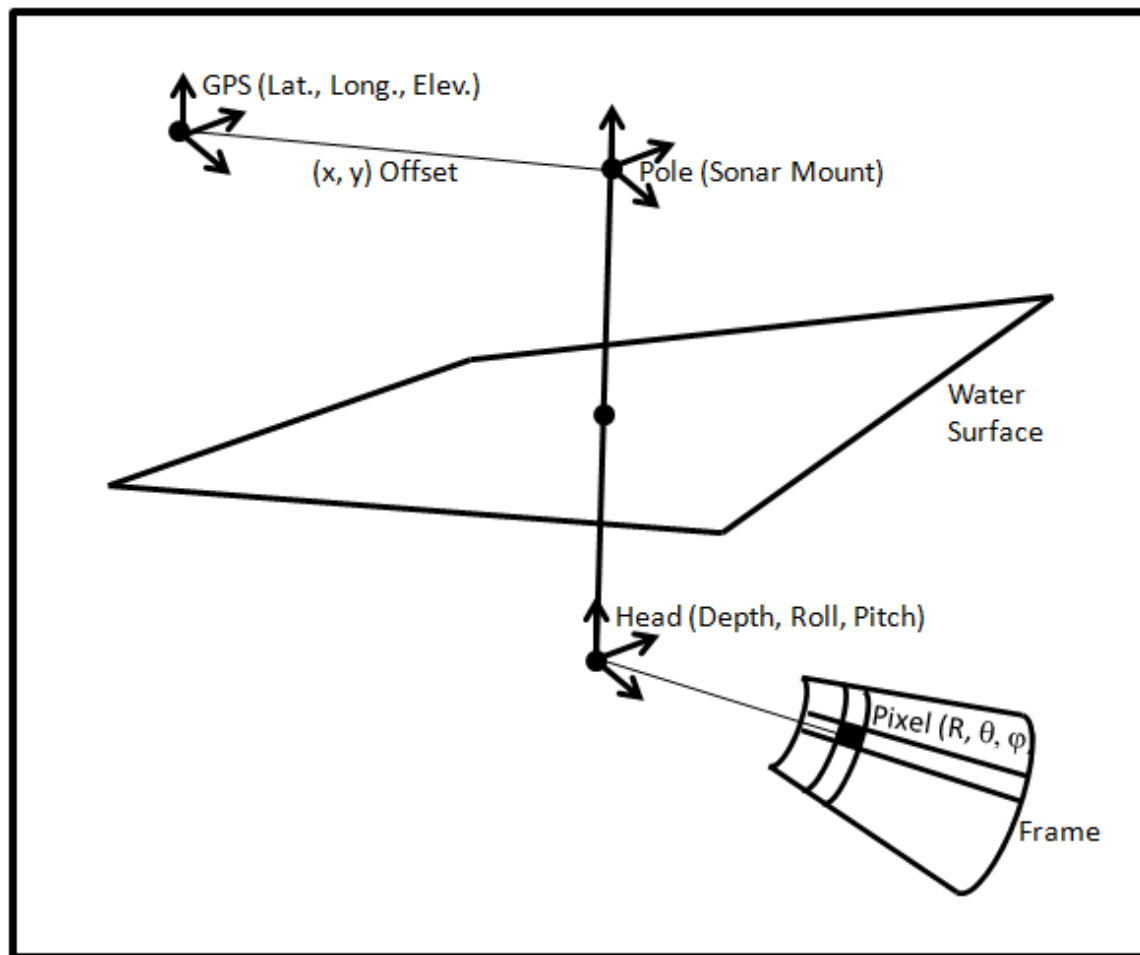


Figure A-5. The transition from GPS coordinates to pixels.

Data acquisition

Data with the DIDSON forward-looking sonar is scanned as shown in Figure A-6. The camera is pointing toward the target at an angle, and the picture frame that is scanned can be seen on the right.

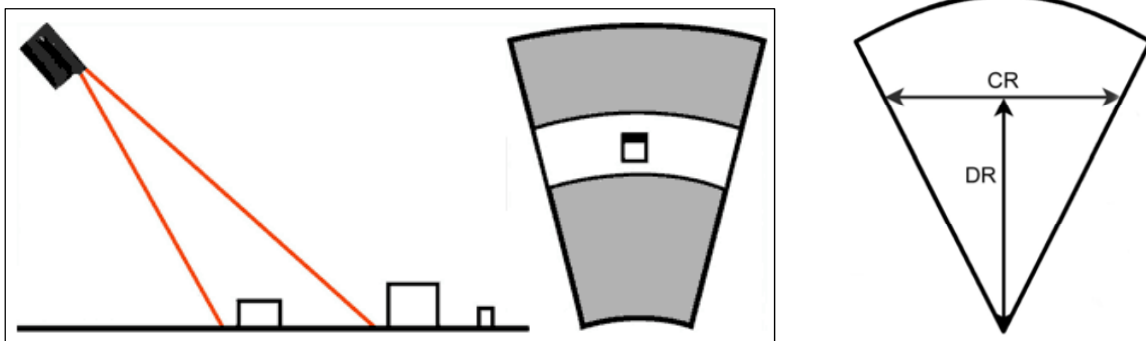


Figure A-6. Scanning data with the DIDSON forward-looking sonar.

The cross range (CR) insonified by DIDSON is half the downrange (DR).

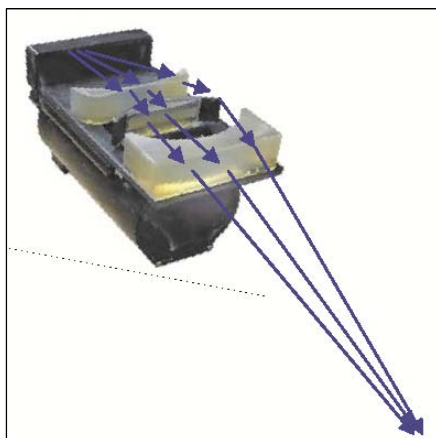


Figure A-7. The DIDSON scans over a range of depth using a moving acoustic lens that changes the focus of the ultrasonic sound to cover the full downrange.

Imaging geometry

The transformation between two acoustic camera images can be calculated by putting one image into the coordinate system so the image is on the xy plane with the positive y axis along the center line of the image and the center of the arc at the origin (see Figure A-8).

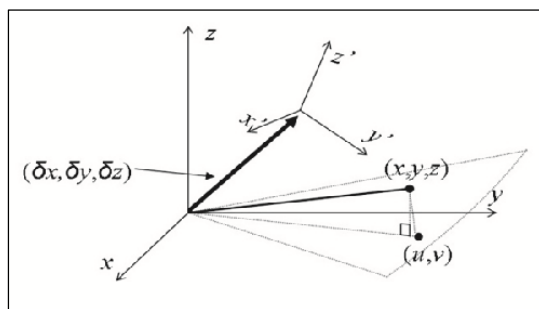


Figure A-8. The imaging geometry of an acoustic camera. The camera is located at the origin of the xyz coordinate system with the pitch, yaw, and roll $(0, 0, 0)$. In the next frame $(x'y'z')$ coordinate), the camera is displaced by $\delta\mathbf{x} = (\delta x, \delta y, \delta z)^T$ and rotated by (ϕ, θ, ψ) .

During the imaging process, a point denoted by a position vector $\mathbf{x} = (x, y, z)^T$ is projected to the polar coordinates (r, α) as:

$$\begin{aligned} u &= r \sin \alpha = x \sqrt{1 + \tan^2 \beta}, \\ v &= r \cos \alpha = y \sqrt{1 + \tan^2 \beta}, \end{aligned} \quad (\text{A.1})$$

where

$r_{xy} \equiv (x^2 + y^2)^{1/2}$, or to the Cartesian coordinates (u, v) ,

$$\begin{aligned} r &= |\mathbf{x}|, \\ \alpha &= \sin^{-1} x / r_{xy}, \end{aligned} \quad (\text{A.2})$$

where

β = the angle between \mathbf{x} and the imaging plane.

When the camera is translated by $\delta \mathbf{x} = (\delta x, \delta y, \delta z)^T$ and rotated by (φ, θ, ψ) , the new coordinates of \mathbf{x} are:

$$\mathbf{x}' = (x', y', z')^T = \mathbf{R}_{\varphi\theta\psi} (\mathbf{x} - \delta \mathbf{x}), \quad (\text{A.3})$$

where

$\mathbf{R}_{\varphi\theta\psi}$ = a 3-by-3 rotation matrix. The linear transformation \mathbf{T} between two images should satisfy:

$$\begin{pmatrix} u' \\ v' \\ 1 \end{pmatrix} = \begin{pmatrix} x' \sqrt{1 + \tan^2 \beta'} \\ y' \sqrt{1 + \tan^2 \beta'} \\ 1 \end{pmatrix} = \mathbf{T} \begin{pmatrix} x \sqrt{1 + \tan^2 \beta} \\ y \sqrt{1 + \tan^2 \beta} \\ 1 \end{pmatrix} = \mathbf{T} \begin{pmatrix} u \\ v \\ 1 \end{pmatrix}, \quad (\text{A.4})$$

where

$$\beta' = \tan^{-1} z' / (x'^2 + y'^2)^{1/2}.$$

When the reflecting points of the target object are located roughly on a plane such as the sea floor, z can be approximated by:

$$z = ax + by + z_0. \quad (\text{A.5})$$

For a, b, β , and β' , which are sufficiently small so that their squares are negligible, we have:

$$\mathbf{T} = \begin{pmatrix} R_{11} + R_{13}a & R_{12} + R_{13}b & -(R_{11}\delta x + R_{12}\delta y + R_{13}(\delta z - z_0)) \\ R_{21} + R_{23}a & R_{22} + R_{23}b & -(R_{21}\delta x + R_{22}\delta y + R_{23}(\delta z - z_0)) \\ 0 & 0 & 1 \end{pmatrix}. \quad (\text{A.6})$$

This serves as a first-order approximation of the transformation between two acoustic camera images. The error due to the second- and higher-order terms might appear as blurriness in the resulting images.

The six unknown parameters of the affine transform can be obtained by matching features in two images. However, other parameters such as R_{ij} , a , b , or $\delta \mathbf{x}$ in (A.6) cannot be figured separately because those parameters are coupled and under-constrained. Consequently, under the above approximation, it is impossible to reconstruct the precise motion of the acoustic camera merely based on image registration parameters.

Mosaicing details

Using the above geometry modeling, two sonar frames are mapped between each other to obtain the same coordinate system between them. Then anchor points are found in both images so registration can take place and the two frames can be combined, as illustrated in Figure A-9.

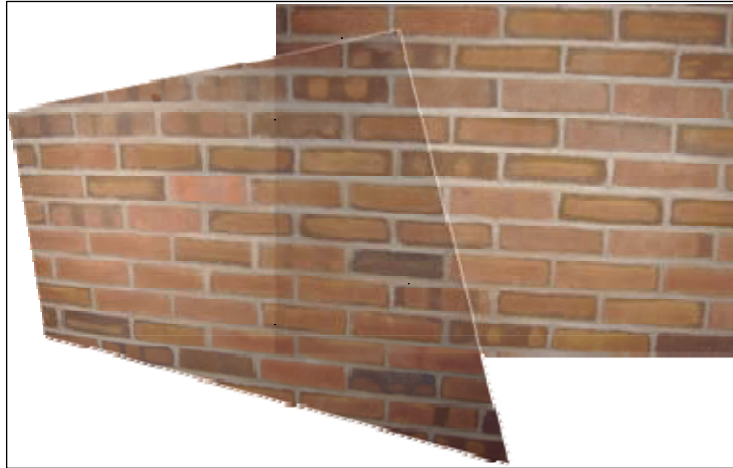


Figure A-9. Mosaic created by applying a coordinate system transformation to align images.

Appendix B: DDF Parser User Manual

DDF Parser

Overview

DDF Parser offers a streamlined approach to preparing DIDSON Data Files (.ddf) for panoramic software such as Kolor autopano giga and AcousticView synesthesia ClearSight.

Capabilities

- Selectable and intelligent frame extraction.
- Single- and multi-threaded .png extraction and ddf reconstruction.
- Lens correction and image fill ratio.
- Static and dynamic alpha channel for upper and lower values based on a threshold.
- Dynamic contrast scaling based on user-set threshold values.

Installation and requirements

No installation or application program interface (API) is necessary to run this program. It was written in C# on a 64-bit Windows 7 machine and has not been tested on other operating systems. The program requires 40KB of free hard-drive space. The files created by the program might vary.

This version can accurately parse only DDF3 files. To avoid crashes, don't use other file types.

Getting started

The program locks the interface until the user selects a file to parse with the Load DDF button. When the file is selected, the program first will determine if the file is valid (DDF3). Then, it will configure its controls to reflect the file. The header information then will be displayed to the user.

Before the file can be parsed, the user must select a folder in which to store the parsed files by using the Select Folder button. If the user is not rebuilding a .ddf and multiple frames are selected, it is recommended the user creates and selects an empty folder for this step.

By default, the Parse DDF button will create a single frame representing the first frame in the file. This behavior was chosen because it is fast and clean, and Windows 7 can update the file while it is being viewed. This allows the user to configure the controls to the data before a large batch is created.

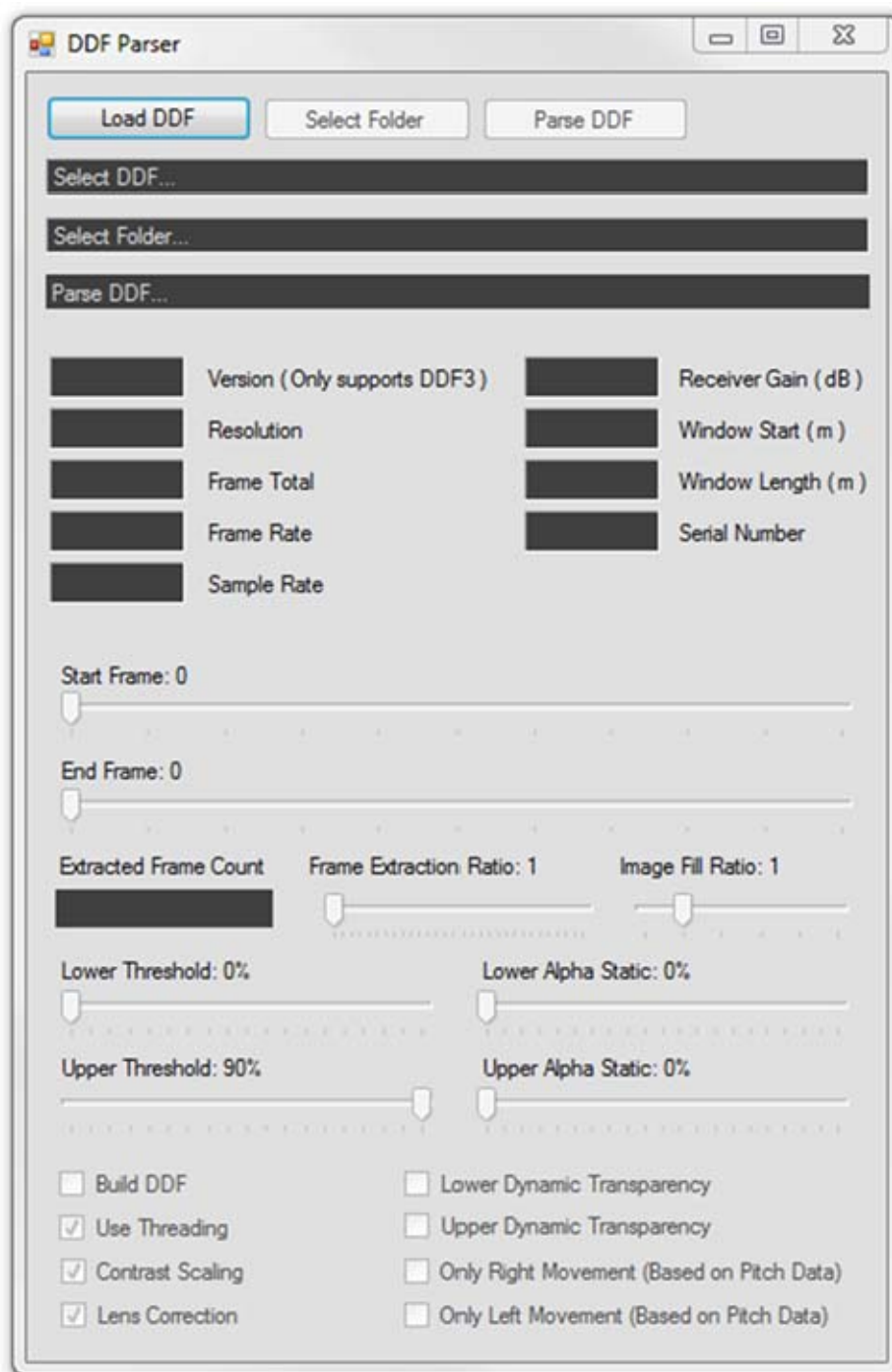


Figure B-1. DDF Parser (no file selected).

Graphical user interface – controls

Load DDF button

This allows the user to browse the file structure for a ddf file. The program will show the directory and file name in the Select DDF field and the header information in the appropriate field. The program, by highlighting the version field, will warn the user if the file selected is not the correct version.

Select Folder button

This allows the user to browse the file structure for a folder in which to store the parsed files. New folders can be created from this window, if necessary.

Parse DDF button

This creates a batch of .png files or a new .ddf file, depending on the user's selected configuration.

Build DDF check box

If this box is checked, the program will create .ddf instead of .png files. This capability can be used to segment files into manageable chunks. This feature is compatible with all the frame selection features. Threshold, transparency, threading, contrast scaling, and lens correction features will have no effect on the .ddf created by this process.

Use Threading check box

This feature decreases drastically the time required to create batches of .png files, but it will max out your processor.

Contrast Scaling check box

This feature will rescale the contrast in each frame to a full 0-to-255 ratio. It also will work with the upper and lower threshold controls to ensure that the contrast ratio is maintained.

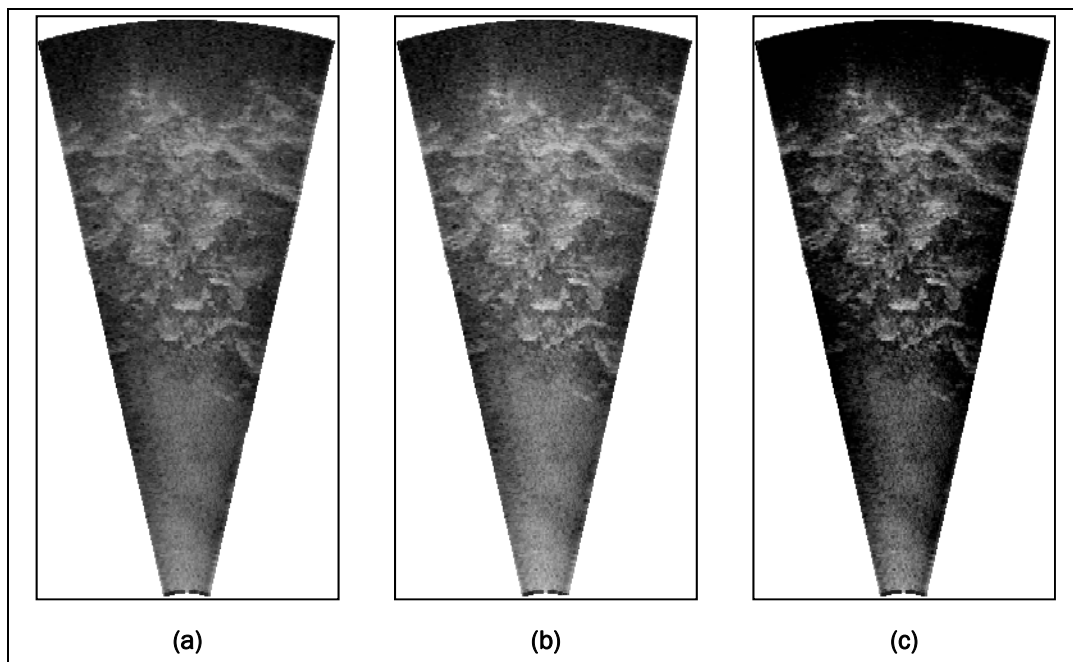


Figure B-2. (a) Original image; (b) contrast scaled image; (c) contrast scaled image with low threshold: 20% and lower alpha static: 100%.

Lens Correction check box

This feature produces the cone-shaped images that more accurately represent the sonar path through the water, based as the window start and window length values stored in the header of each frame. By deactivating this feature, the original rectangle image will be produced.

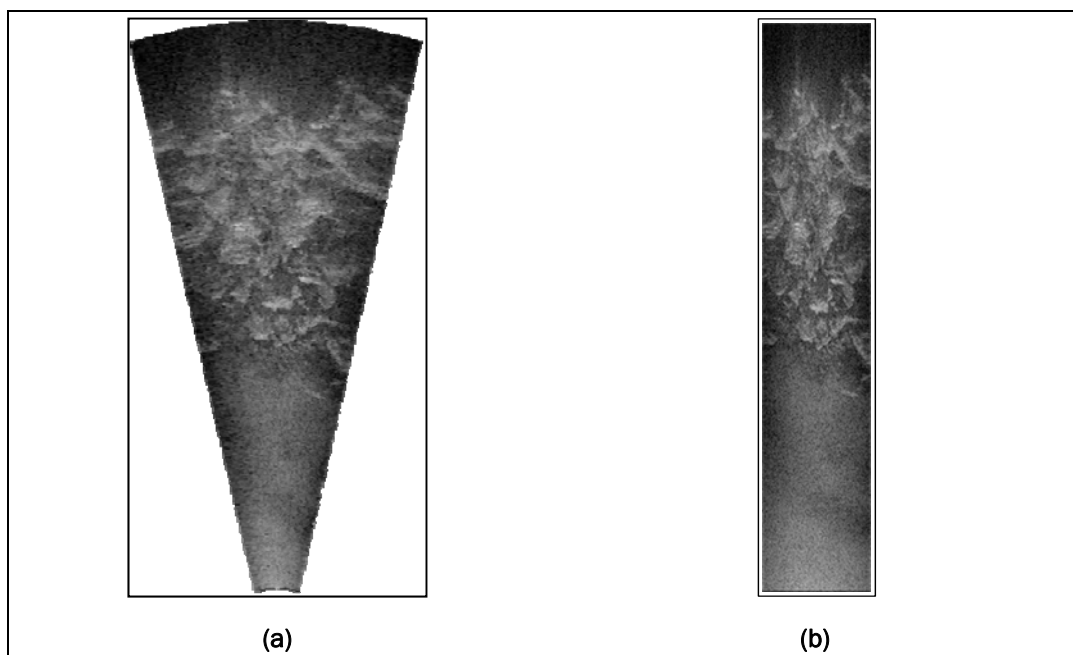


Figure B-3. (a) Using lens correction; (b) original image stored in .ddf.

Lower Dynamic Transparency check box

This feature changes the way the pixels below the lower threshold value set by the user are handled by the program. If unchecked, pixels below the threshold will be converted to black with a percentage alpha equal to the Lower Alpha Static track bar. If checked, pixels below the threshold will be given a scaled alpha channel, with the Lower Transparency Dynamic track bar as the lower scale and the Lower Threshold track bar as the upper threshold. All pixels below the Lower Transparency Dynamic track bar value will be transparent.

Upper Dynamic Transparency check box

This feature changes the way the pixels above the upper threshold value set by the user are handled by the program. If unchecked, pixels above the threshold will be converted to white, with a percentage alpha equal to the Upper Alpha Static track bar. If checked, pixels above the threshold will be given a scaled alpha channel, with the Upper Transparency Dynamic track bar as the upper scale and the Upper Threshold track bar as the upper threshold. All pixels above the Upper Transparency Dynamic track bar value will be transparent.

Only Right Movement check box

This feature uses the Pitch data taken from the frame headers to determine direction of movement. If this box is checked, frames will be extracted only if the program determines the camera angle has been rotated farther right than the previously extracted image.

Only Left Movement check box

This feature uses the Pitch data taken from the frame headers to determine direction of movement. If this box is checked, frames will be extracted only if the program determines the camera angle has been rotated farther left than the previously extracted image.

Start Frame track bar

This value defines the first frame that will be batch extracted from the .ddf. It cannot exceed the End Frame value. If the Start and End Frame values are equal, one frame will be extracted. The Extracted Frame Count field tracks the number of frames that will be extracted by the program before it is run.

End Frame track bar

This value defines the last frame that will be batch extracted from the .ddf. It cannot drop below the Start Frame value. If the Start and End Frame values are equal, one frame will be extracted. The Extracted Frame Count field tracks the number of frames that will be extracted by the program before it is run.

Frame Extraction Ratio track bar

The Frame Extraction Ratio defines the ratio frames that will be extracted from the .ddf. For example: a value of 1 will extract every frame, a value of 2 will extract every other frame, a value of 3 will extract every third frame, etc. The Extracted Frame Count field tracks the number of frames that will be extracted by the program before it is run.

Image Fill Ratio track bar

The Image Fill Ratio is sometimes necessary when using lens correction. This feature adds a number of pixels to the right and left of each pixel in the image. This value is defaulted to 1.

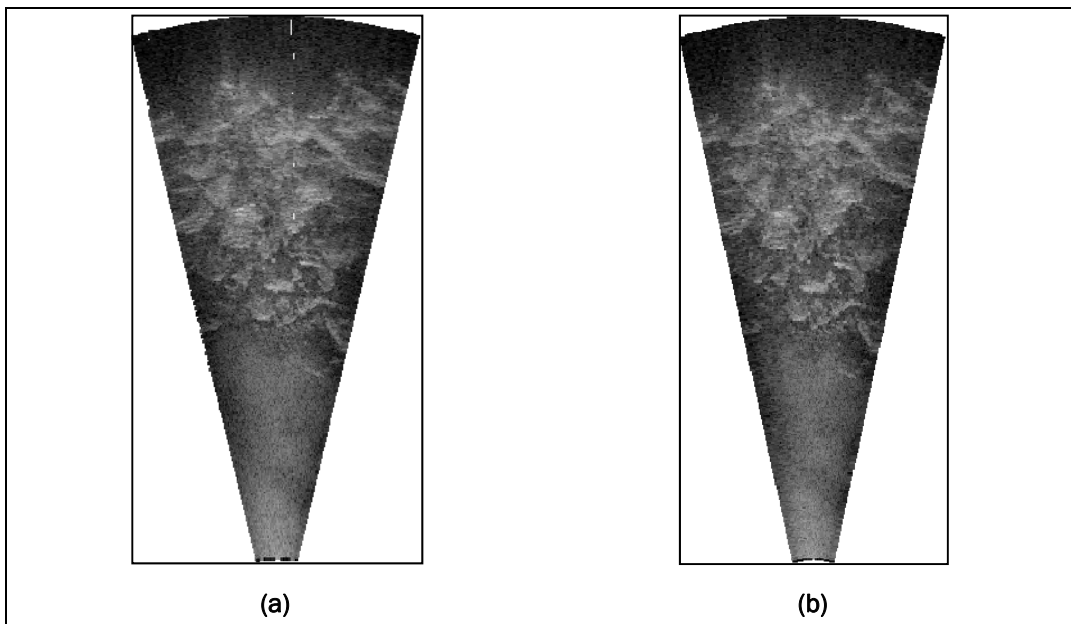


Figure B-4. (a) Image fill ratio: 0; (b) image fill ratio = 1.

Lower Threshold track bar

This feature removes pixel values from the image that are below the user-set threshold level. What is done with the removed pixels depend on other controls.

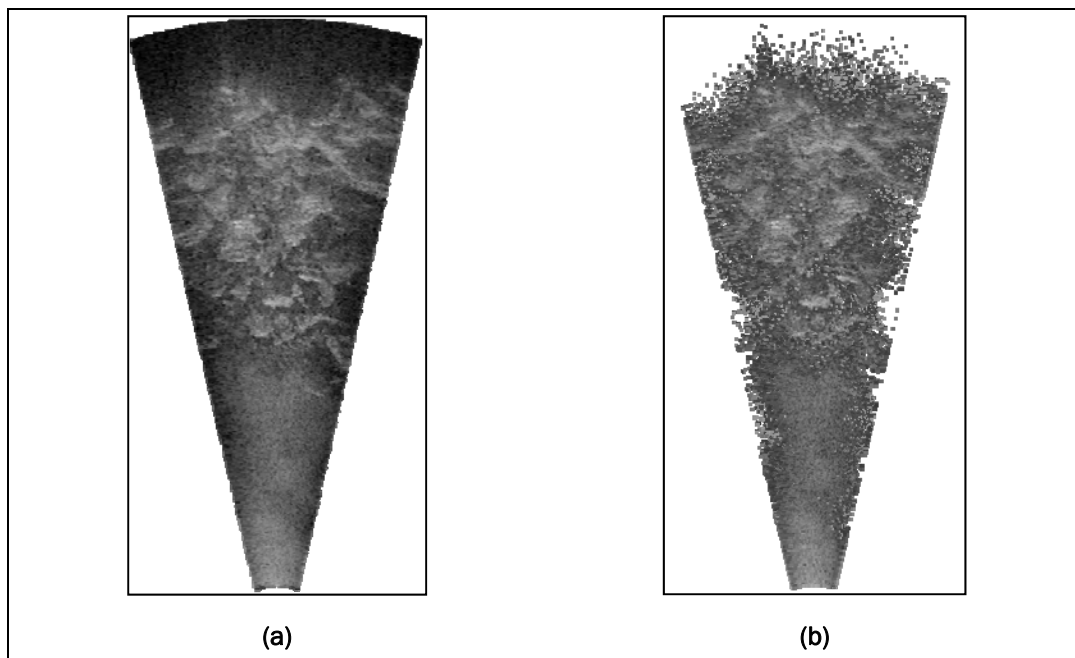


Figure B-5. (a) Low threshold: 0%; (b) low threshold: 20%.

Lower Alpha Static track bar

This value is used to set the alpha channel associated with any pixel below the user-set threshold level. This control requires the Lower Dynamic Transparency check box be unselected.

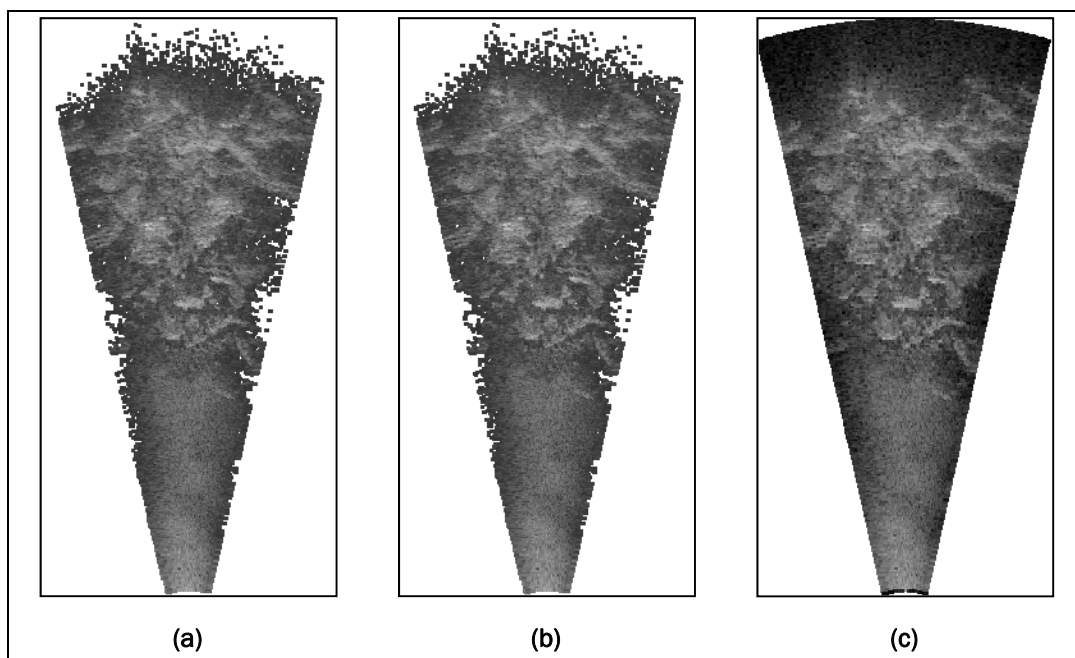


Figure B-6. Each image has a low threshold value of 20%; (a) lower alpha static: 0%; (b) lower alpha static: 50%; (c) lower alpha static: 100%.

Lower Transparency Dynamic track bar

This value refers to a second threshold value that defines a ratio of transparent pixels to translucent pixels. The translucent pixels will have a gradient scaled alpha channel.

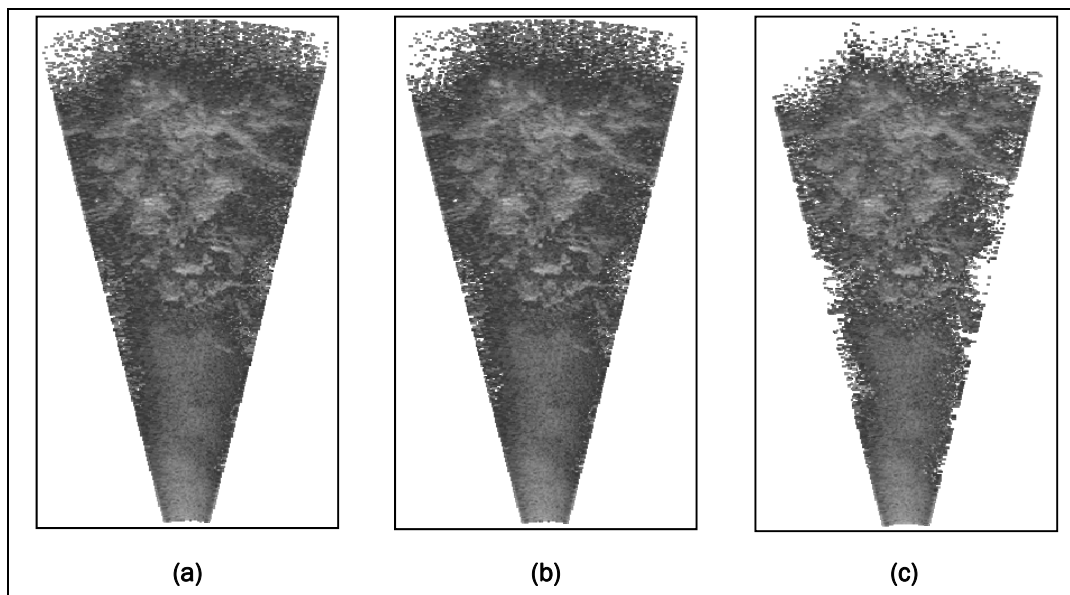


Figure B-7. Each image has a low threshold value of 20%; (a) low transparency dynamic: 0%; (b) low transparency dynamic: 50%; (c) low transparency dynamic: 100%.

High Threshold track bar

This feature removes pixel values from the image that are above the user-set threshold level. What is done with the removed pixels depends on other controls.

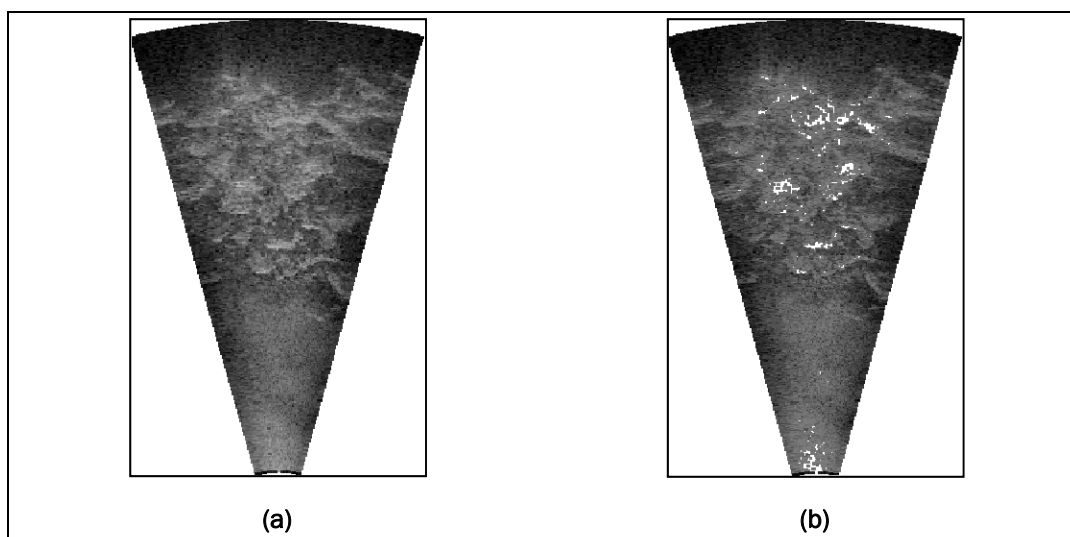


Figure B-8. (a) High threshold: 90%; (b) high threshold: 50%.

Upper Alpha Static track bar

This value is used to set the alpha channel associated with any pixel above the user-set threshold level. This control requires that the Upper Dynamic Transparency check box not be selected.

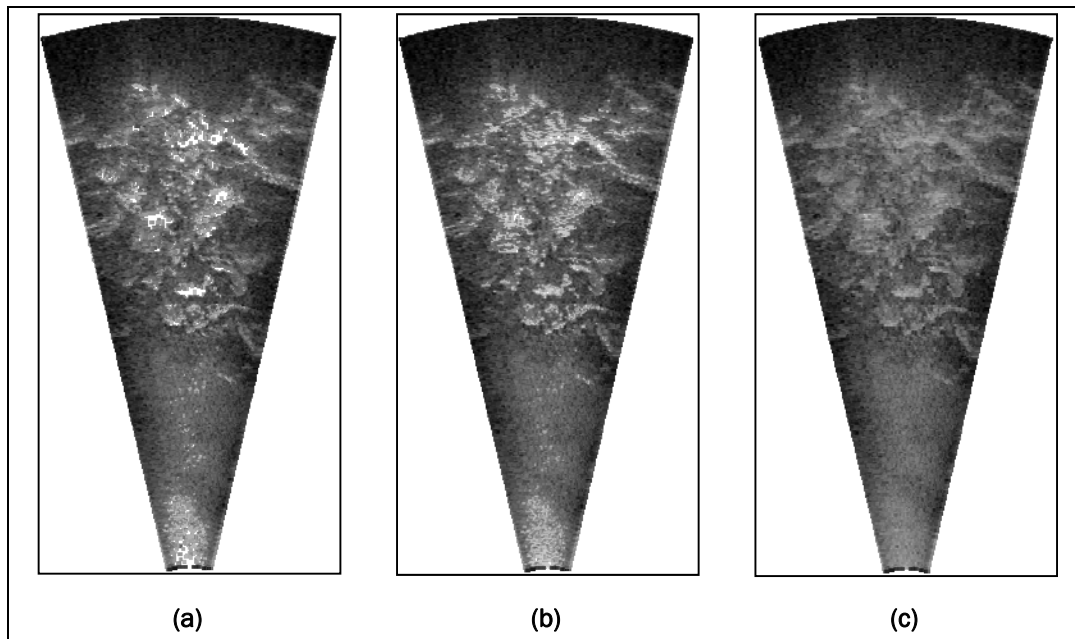


Figure B-9. Each image has a high threshold value of 50%; (a) upper alpha static: 0%; (b) upper alpha static: 50%; (c) upper alpha static: 100%.

Lower Transparency Dynamic track bar

This value refers to a second threshold value that defines a ratio of transparent pixels to translucent pixels. The translucent pixels will include a gradient scaled alpha channel.

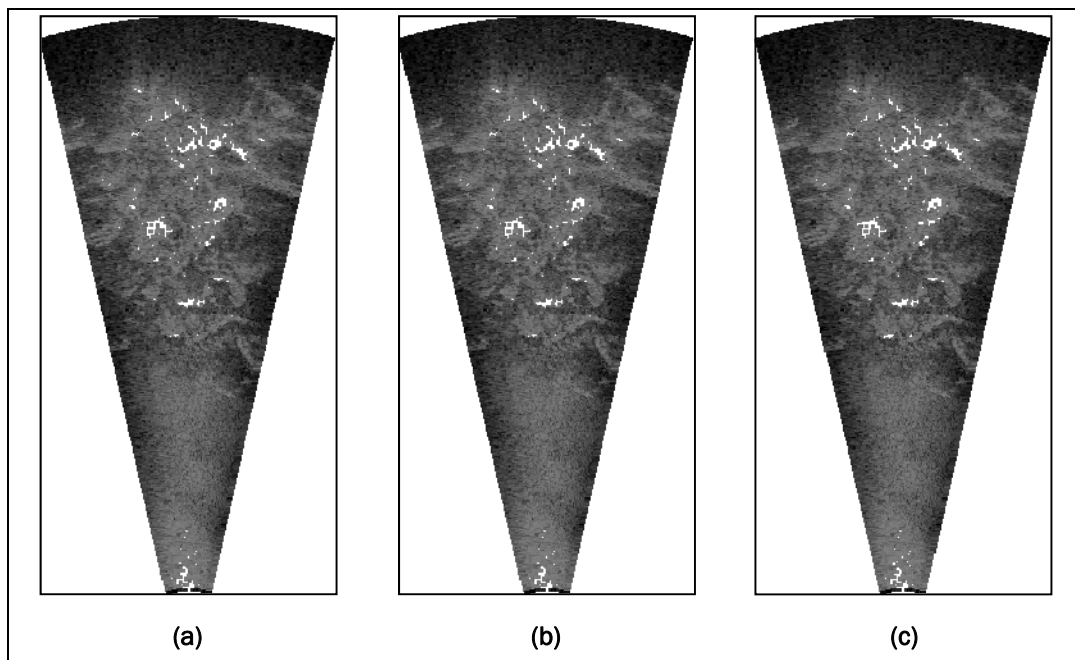


Figure B-10. Each image has a high threshold value of 50%; (a) upper transparency dynamic: 0%; (b) upper transparency dynamic: 50%; (c) upper transparency dynamic: 100%.

Appendix C: DIDSON Acoustic Camera Specifications

General information about the DIDSON acoustic camera used during this program:

DIDSON-S (Standard Version)

DETECTION MODE	
Operating frequency	1.1 MHz (1.0 MHz < SN16)
Beam width (two-way)	0.4 H by 14 V
Number of beams	48
Source level (average)	202 dB re 1 Pa at 1 m
Standard Range Settings	
Window start	0.75m to 23.25m in 0.75m intervals
Window length	4.5m, 9m, 18m, 36m
Range bin size relative to window length	8mm, 17mm, 35mm, 70mm
Pulse length relative to window length	16us, 32us, 64us, 128us
Extended Range Settings	
Window start	0.84m to 26.04m in 0.84m intervals
Window length	5m, 10m, 20m, 40m
Range bin size relative to window length	10mm, 20mm, 40mm, 80mm
Pulse length relative to window length	18us, 36us, 72us, 144us
IDENTIFICATION MODE	
Operating frequency	1.8 MHz
Beam width (two-way)	0.3 H by 14 V
Number of beams	96
Source level (average)	206 dB re 1 uPa at 1 m
Standard Range Settings	
Window start	0.38m to 11.63m in 0.38m steps
Window length	1.13m, 2.25m, 4.5m, 9m
Range bin size relative to window length	2.2mm 4.4mm, 9mm, 18mm
Pulse length relative to window length	4us, 8us, 16us, 32us
Extended Range Settings	
Window start	0.42m to 13.02m in 0.42m steps
Window length	1.25 m, 2. 5 m, 5 m, 10 m
Range bin size relative to window length	2.5mm, 5mm, 10mm, 20mm
Pulse length relative to window length	4.5us, 9us, 18us, 36us
BOTH MODES	
Frame rate	4-21 frames/s
Field-of-view	29°
Remote focus	1 m to max range
Power consumption	30 W typical

Weight in air (DC option)	7.0 kg (15.4 lb)
Weight in water (DC option)	0.61 kg neg. (1.33 lb)
Dimensions	30.7 cm by 20.6 cm by 17.1 cm
Depth rating	152 m (500 ft)
Control	Ethernet or switches
Display up-link	Ethernet or NTSC video
Maximum cable length (100BaseT option)	61 m (200 ft)
Maximum cable length (Thinnet option)	152 m (500 ft)
Maximum cable length (Patton option)	1220 m (4000 ft) (with local power)

Topside requirements: Windows (95, 98, Me, NT, 2000, XP), Ethernet card, video monitor (optional)

Appendix D: EdgeDetect User Manual

To use EdgeDetect, first open a DIDSON .ddf by selecting File on the menu bar and Open from the drop-down selection. Use the File Open dialog box to select the desired .ddf.

When you have selected the file, the first frame in the file will show in the Original Image control (left picture box). The first frame with the detected edge will be shown in the Edge Image control (right picture box); the text boxes on the left of the screen will update, as well. The frame indication text box located under Original Image should indicate frame zero.

Figure D-1 shows the EdgeDetect user interface window.

There are two ways to select another frame. One is to enter the frame number you wish to see in the Frame Number text box and hit the Enter key. The screen will update to this frame and its corresponding detected edge. The user also can click the Next Frame command button labeled with the right arrow head found to the right of the Frame Number text box to advance to the next frame. That is, if the frame number is 20, clicking the Next Frame command button will advance to 21.

There is a Save Profiles check box under Edge Image. If that box is checked, then the *xyz* coordinates of the edge pixels relative to the camera will be saved in a file. The file will have the same name as the input file, with the .ddf extension replaced with .xyz.

Three text boxes are located below Edge Image. The Threshold Value text box specifies the signal strength value used to determine if an edge has been detected. This is necessary because the signal level of the background environment can vary, depending on the structure and location.

The Start Distance and End Distance text boxes are used to specify the distance from the camera to search for the edge. This is useful because at times there can be obstructions not of interest such as large rocks, debris, fish, etc. By specifying the distance of interest, those elements can be removed from consideration in searching for the edge.

The program can be terminated by clicking File in the menu bar, then clicking Exit in the drop-down list.

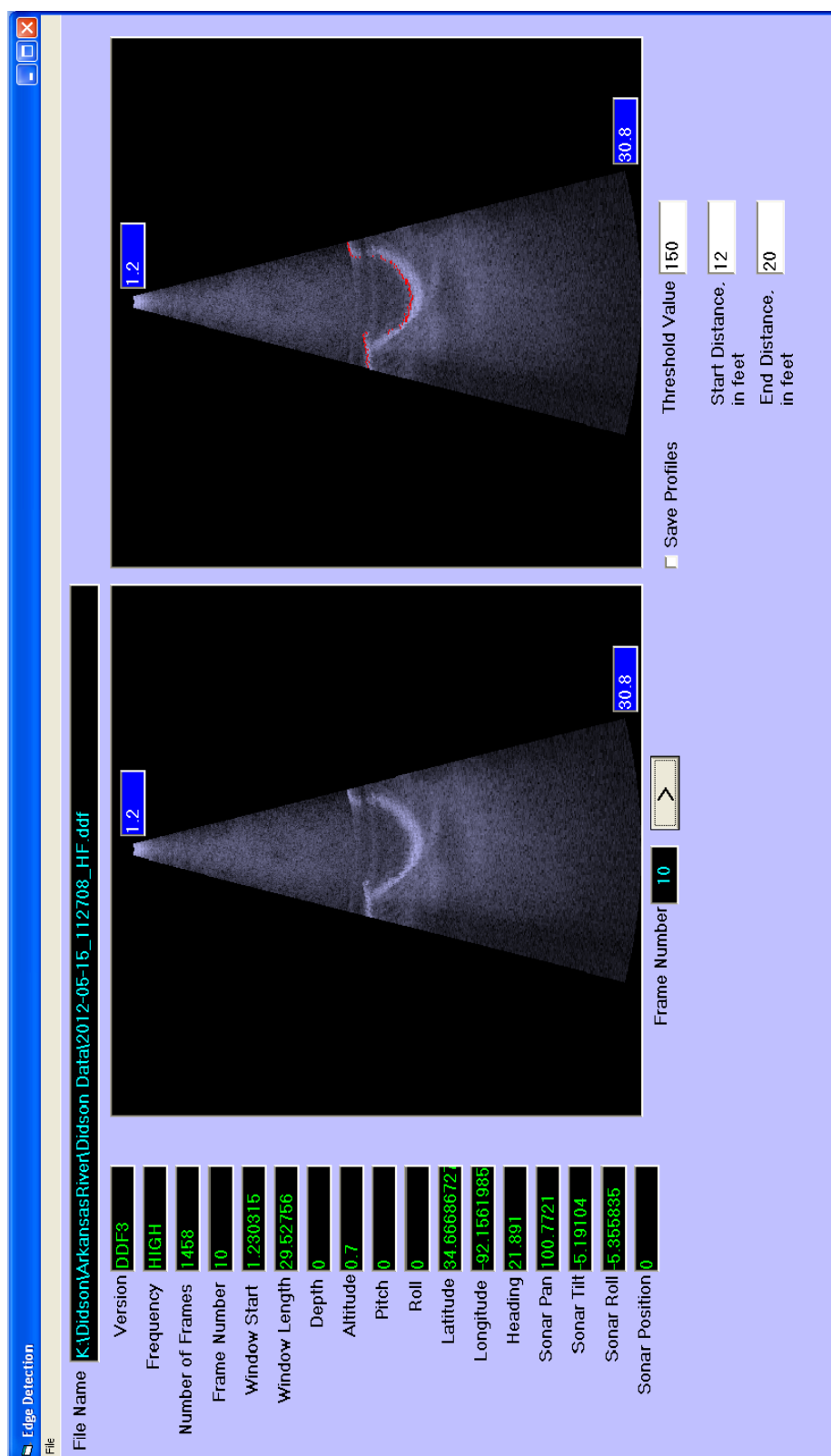


Figure D-1. EdgeDetect user interface window.

REPORT DOCUMENTATION PAGE				Form Approved OMB No. 0704-0188	
Public reporting burden for this collection of information is estimated to average 1 hour per response, including the time for reviewing instructions, searching existing data sources, gathering and maintaining the data needed, and completing and reviewing this collection of information. Send comments regarding this burden estimate or any other aspect of this collection of information, including suggestions for reducing this burden to Department of Defense, Washington Headquarters Services, Directorate for Information Operations and Reports (0704-0188), 1215 Jefferson Davis Highway, Suite 1204, Arlington, VA 22202-4302. Respondents should be aware that notwithstanding any other provision of law, no person shall be subject to any penalty for failing to comply with a collection of information if it does not display a currently valid OMB control number. PLEASE DO NOT RETURN YOUR FORM TO THE ABOVE ADDRESS.					
1. REPORT DATE (DD-MM-YYYY) August 2013		2. REPORT TYPE Final		3. DATES COVERED (From - To)	
4. TITLE AND SUBTITLE Underwater Inspection of Navigation Structures with an Acoustic Camera				5a. CONTRACT NUMBER	
				5b. GRANT NUMBER	
				5c. PROGRAM ELEMENT NUMBER	
6. AUTHOR(S) James A. Evans, Terry W. Warren, and Richard W. Haskins				5d. PROJECT NUMBER	
				5e. TASK NUMBER	
				5f. WORK UNIT NUMBER	
7. PERFORMING ORGANIZATION NAME(S) AND ADDRESS(ES) Information Technology Laboratory US Army Corps of Engineers 3909 Halls Ferry Road Vicksburg, MS 39180-6199				8. PERFORMING ORGANIZATION REPORT NUMBER ERDC/ITL TR-13-3	
9. SPONSORING / MONITORING AGENCY NAME(S) AND ADDRESS(ES) Headquarters, US Army Corps of Engineers Washington, DC 20314-1000				10. SPONSOR/MONITOR'S ACRONYM(S) HQUSACE	
				11. SPONSOR/MONITOR'S REPORT NUMBER(S)	
12. DISTRIBUTION / AVAILABILITY STATEMENT Approved for public release; distribution is unlimited.					
13. SUPPLEMENTARY NOTES					
14. ABSTRACT The US Army Corps of Engineers' (USACE) operations within turbid waters creates a need for better ways to inspect, quantify, monitor, and locate infrastructure in a difficult environment. Inspection methods have included dewatering, tactile diver inspection, and side-scan or multi-beam sonars. These older approaches can have high cost, inherent danger, and/or limited output quality. Newer technologies that use highly focused acoustic beams could greatly improve underwater observation. The research described in this report addresses the limitations and expands the capabilities of an underwater, high-resolution acoustical imaging system for USACE. These efforts have produced new hardware and software and associated methods that address specific needs in system deployment, data collection, and analysis. During this research, continuous leveraging of reimbursable needs within USACE districts has produced an invaluable view of performance, capabilities, and limitations. It is believed that acoustical imaging technology will be a catalyst for the development of other advanced inspection capabilities within the Corps' navigation system.					
15. SUBJECT TERMS Acoustical imaging system DIDSON		Scour Turbid Underwater inspection system		Water inspection	
16. SECURITY CLASSIFICATION OF:			17. LIMITATION OF ABSTRACT	18. NUMBER OF PAGES 94	19a. NAME OF RESPONSIBLE PERSON
a. REPORT Unclassified	b. ABSTRACT Unclassified	c. THIS PAGE Unclassified			19b. TELEPHONE NUMBER (include area code)